INVESTIGATION OF THE ACTIVITY AND SELECTIVITY OF THE MoO_3/Al_2O_3 CATALYST AND THE STRUCTURAL INVESTIGATION USING IN-SITU RAMAN

by

Kelvin Stephen Jacobs

Thesis presented for the Degree of

MASTERS IN APPLICATION SCIENCE

In the Department of Chemical Engineering

UNIVERSITY OF CAPE TOWN

December 2002

TABLE OF CONTENTS: **Page**

Synopsis

Metathesis is a very versatile reaction, which allows the conversion of simple, relatively inexpensive olefins into specialty, high-purity olefins which are useful intermediates in the fragrance, agricultural and many other specialty chemical industries. Supported molybdenum on alumina is an active heterogeneous catalyst for the metathesis of olefins. Its activity, as a function of time, passes a maximum. It is known that the activity of molybdenum-based catalyst increases up to monolayer capacity.

Catalysts with various Mo-loadings were prepared by controlled adsorption method using ammonium heptamolybdate as a precursor. A catalyst using a new slurry impregnation method was also prepared for comparative reasons. Before the metathesis process, the molybdenum catalysts are activated at 550 °C under N_2 in a fixed bed reactor. The loading of the prepared catalysts was below and above monolayer capacity. It was observed that up to a loading 0.3 g MoO_3 per g Al_2O_3 the initial conversion increases more than proportional to the MoO_3-loading. The catalysts with a MoO_3-loading higher than 0.3 g MoO_3 per gram Al_2O_3 show initially a lower activity, ie. The activity per molybdenum atom in the catalyst decreases. With increasing time-on-stream the activity of the catalysts declines. The decline is much stronger over the catalysts with a higher initial activity.

The selectivity for the primary metathesis products, ethene and 7-tetradecene, is thought to be governed by the acidic properties of the catalyst, which catalyse double bond isomerization. The catalyst with the lowest loading (controlled adsorption), 0.1 g MoO_3/gAl_2O_3, showed the highest selectivity for the primary metathesis products, ethene and 7-tetradecene. This is attributed to the lowest Lewis/Brønsted acidity ratio. The catalyst prepared via the new slurry impregnation (NSI) method had a lower primary metathesis selectivity than the catalyst prepared via the controlled adsorption (CA) method. The activity of these

catalysts is comparable. Hence, the observed difference in the selectivity for the primary products cannot be attributed to the difference in catalytic activity. The selectivity for the primary products is much lower for the catalysts with a higher MoO_3-loading. This might be partially attributed to the different level of conversion, since at high conversion secondary reactions become noticeable.

These catalysts were tested by different spectroscopic analysis, which includes XRD, FTIR-pyridine adsorption and TEM. It was found that the spectroscopic results compliment the results obtained using Raman spectroscopy.

During catalysts preparation different phases of molybdenum are present as the catalysts loading increases. This was confirmed by doing Raman mapping experiments. To have a better understanding of the changes taking place on the catalyst during reaction conditions, in-situ Raman studies were performed on the catalysts. The important molecular bond at which the active carbene site would form is (M=O) bond. During the mapping experiment this bond was monitored. The mapping experiments revealed that as the catalyst loading increases there tends to be different molybdate phases present on the surface of the catalyst, especially with the 0.4 g MoO_3/gAl_2O_3 and 0.5 g MoO_3/gAl_2O_3 catalysts.

From the mapping experiments that were performed it can be concluded that the peak area and intensity of the M=O band increases with increasing catalyst loading, but starts to decrease above 0.3 g MoO_3/gAl_2O_3, possibly due to multiphases forming above the monolayer capacity.

ACKNOWLEDGEMENTS

I would like to extend my gratitude to Sasol for granting me the opportunity to further my studies.

Many thanks to my family who has always been around for me by God's grace, especially during the time I spend at UCT. I am also grateful to Professor Eric van Steen for his guidance and assistance in compiling this thesis.

I would like to acknowledge the assistance of Dr.Alta Spamer during the practical side of this degree and thank her for bearing with me. I extend my appreciation to those at Sasol Library that assisted me in obtaining the necessary literature and all those involved in spectroscopic analysis at Sasol's Material Characterization group.

1 INTRODUCTION

Olefin metathesis is a conversion process that can adapt the availability of olefins to the demand. In addition, it offers a unique path for producing important intermediates and end products from olefins, for example in the field of specialty chemicals and polymers (Ivin and Mol, 1997). From normal olefins, this catalytic reaction can be represented by reaction (**1**)

$$2\ R_1\text{-}CH{=}CH\text{-}R_2 \rightleftharpoons R_1\text{-}CH{=}CH\text{-}R_1 + R_2\text{-}CH{=}CH\text{-}R_2 \qquad (\mathbf{1})$$

Where R_1 and R_2 are alkyl groups or hydrogen. A simple example is the metathesis of propene into ethene and but-2-ene. This was the first industrial application of olefin metathesis as a means of converting surplus propene into products. In fact many olefin substrates can undergo metathesis in the presence of a suitable catalyst, resulting in a wide variety of possible products (Ivin and Mol, 1997). For acyclic olefins the metathesis process is essentially thermo-neutral and a statistical distribution of reactant and product molecules will eventually be obtained. This means that in the case of reaction (**1**), the equilibrium mixture consists of reactant and products in the approximate molar ratio of 2:1:1 if both metathesis products remain in the same reaction medium.

The first heterogeneous, oxidic catalyst for alkene metathesis was $MoO_3/CoO/Al_2O_3$ (Banks and Bailey, 1964). The presence of CoO resulted in a higher initial metathesis activity, but also in a faster deactivation of the catalyst (Engelhardt, 1982). Later generations of the heterogeneous molybdenum-based catalysts did generally no longer contain cobalt.

In this study the metathesis of 1-octene is investigated over heterogeneous molybdenum-based catalysts. The primary products of this reaction are expected to be ethene and 7-tetradecene. The latter can be used for the production of detergent-type alcohols.

1.1 Commercial Processes

1.1.1 Phillips Triolefin Process

The metathesis reaction was discovered at a time when the market was oversupplied with propene, but the demand for ethene was high. Thus, metathesis of propene became the first industrialized metathesis process (Philips Triolefin Process) when propene was cheap and readily available (Mol and Moulijn, 1987, see Figure 1.1). Due to the increasing demand for propene, the process was shutdown in 1973. The reaction is carried out at 370-450 °C over WO_3/SiO_2 catalyst with an equilibrium conversion of 40-43%. The feed of the reactor contains major amounts propane so that propene/propane mixtures from the refinery can be used. The products were used for the production of polyethylene and polybutadiene. This process combined with an isomerization unit, can produce high purity 1-butene.

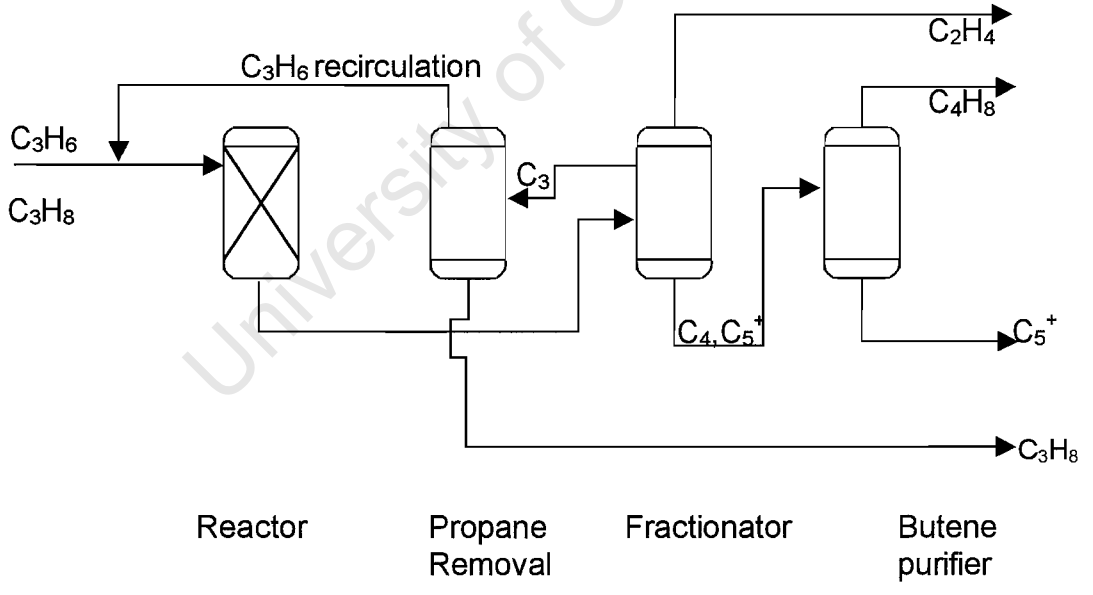

Figure 1.1: Schematic representation of the Phillips Triolefin Process (Mol and Moulijn, 1987).

Due to the increase of the demand for propene, alternative routes to increase the propylene output of the naphtha cracker are being investigated (N.N., 2002) Metathesis represents one route to enhance the propene production by reacting

some of the ethene with C_4 streams. The basis for the metathesis technology is the reaction of ethylene and 2-butene to produce polymer grade propylene:

$$CH_2{=}CH_2 + CH_3{-}CH{=}CH{-}CH_3 \longrightarrow 2{-}CH_3{-}CH{=}CH_2 \qquad (2)$$

This metathesis technology is offered by two companies, Lummus and Axens (formerly IFP before its merger with Procatalyse) and is close to commercial use. The Lummus process is a gaseous phase process at low pressures and elevated temperatures (330-400 °C) utilising a tungsten-based catalyst, while the Axens process uses a liquid phase reaction at moderate temperature (20-50 °C) and relatively high pressure, over a rhenium catalyst.

In ABB Lummus Global's *Olefin Conversion Technology (OCT)*, the ethylene stream can vary from dilute ethylene, typical from a FCC, to polymer grade ethylene. 1-butene in the feedstock is isomerised to 2-butene, as the original 2-butene is consumed in the metathesis reaction. Butanes pass through the system as inerts. The reactor is a fixed-bed reactor. This technology can be used with a variety of C_4 streams, including the mixed C_4s produced in steamcracking, raffinate C_4s from MTBE or butadiene extraction, and C_4s produced in the FCC units. The Phillips/Lummus technology, marketed as *Triolefins or Olefins Conversion*, is already in use at Lyondell (Texas, USA). It will make a major debut when a metathesis unit added to the new world scale cracker brought on stream recently. The cracker is rated at 920 000 tonne/year of ethene and 550 000 tonne/year of propene, but when the metathesis unit is added, sometime in 2003-04, it will adjust the output to 830 000 tonne/year of propene. The metathesis unit will take additional C_4's from the Sabena C_4-splitter. The unit, to be operated by BASF on the Port Arthur site, will take C_4's from the Port Arthur cracker, bolstered by a C_4 stream from Shell's Deer Park, Texas, complex. The unit will deliver 400 000 tonne/year of butadiene and 300 000 tonne/year of branched alkylates for octane enhancement, based on the isobutene stream. The

remaining n-butenes stream will be fed to the metathesis unit to react with ethylene to make the additional propylene.

In the Axens '*Meta-4* process, FCC or C_4's from a steamcracker are selectively hydrogenated to convert butadiene. 1-Butene, and isobutene are removed either in a MTBE unit or by fractionation. The resulting 2-butene-rich stream is fed to the metathesis unit with ethylene, where the materials pass through a moving catalyst bed to give polymer-grade propylene. Axens has demonstrated the use of its technology over two years (1988-90) at Chinese Petroleum in Kaohsiung, Taiwan, with which it has jointly developed the process. It markets its technology under *Meta-4* brand name and has worked recently with Linde and Technip to develop the case for metathesis units in steamcrackers. Three years ago, Axens was selected over Lummus to provide technology for a metathesis unit in Europe, when DSM and Veba were looking to boost propylene at Gelsenkirchen, Germany. However, the project did not go ahead after an alternative solution to propylene supply was found. Axens is now in talks with prospective customers in Asia.

1.1.2 Phillips Neohexene Process:

The Phillips Neohexene Process (Banks et al., 1982) is used in the synthesis of neohexene (3,3-dimethyl-1-butene), which is an intermediate in the production of synthetic musk (see Scheme 1.1). The reaction is performed over WO_3/SiO_2-MgO at a temperature of 370 °C and pressure of 30 bar. The conversion for the reaction is ca 65-75%.

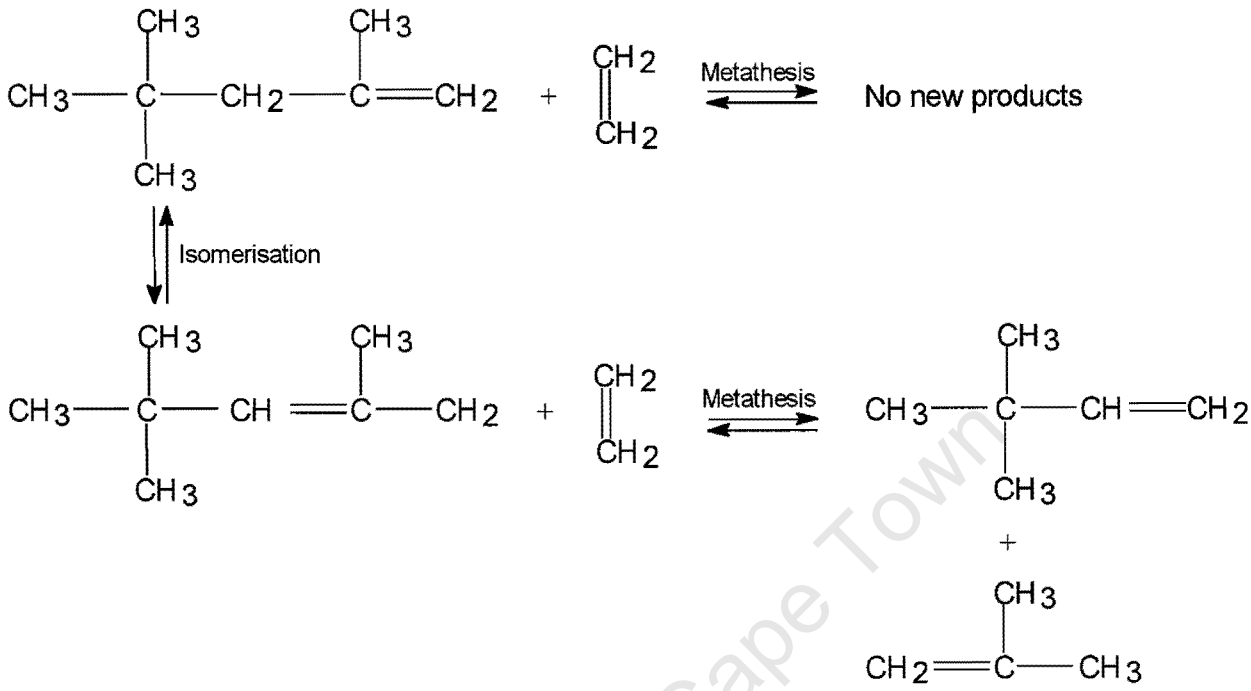

Scheme 1.1: Synthesis of 3,3-dimethyl-1-butene (neohexene) via metathesis

1.1.3 Shell Higher Olefin Process (SHOP)

Another important large-scale industrial process is **SHOP** (Mol and Moulijn, 1987) for converting ethene to detergent-range (C_{11}-C_{14}) alkenes (see Figure 1.2). In the first step of this three-stage process ethene is catalytically oligomerized yielding a mixture of linear α-alkenes ranging from C_4-C_{40}, all containing even numbers of carbon atoms. The valuable C_{10}-C_{20} α-alkenes are separated from the mixture and can be converted into products such as detergents, fatty acids, *etc.* The remaining lighter ($<C_{10}$) and heavier ($>C_{20}$) alkenes go to purification beds, which remove catalyst and solvent residues. In the second step these alkenes undergo double bond isomerization over a solid catalyst to a thermodynamic mixture of internal alkenes. The mixture is then passed over a solid catalyst in the third step, resulting in linear internal alkenes with both odd and even numbers of carbon

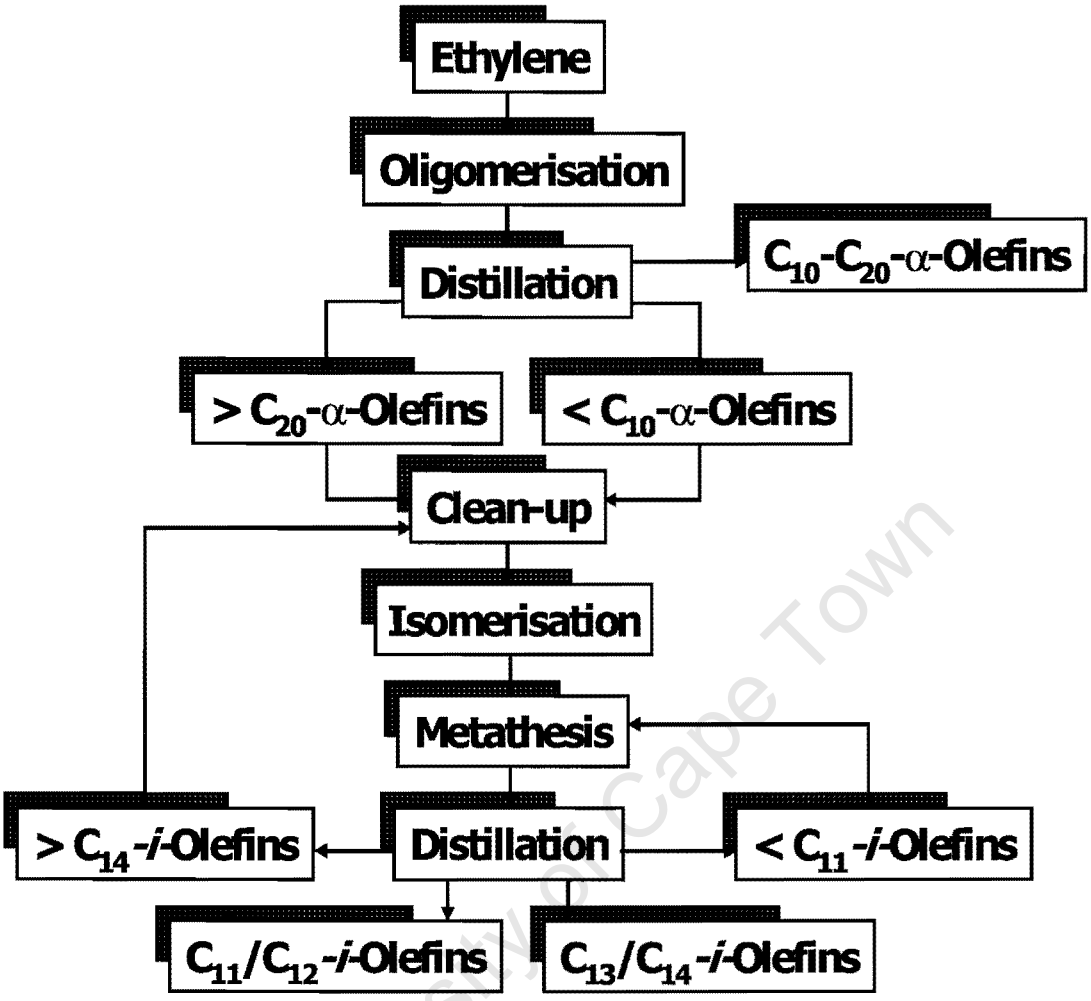

Figure 1.2: Schematic representation of the Shell Higher Olefin Process

numbers, in a thermodynamic distribution. This yields about 10-15wt% of the desired detergent-range (C_{11}-C_{14}) alkenes per pass, which are separated by normal distillation. The isomerization and metathesis catalyst operate at 80-140 °C and 3-17 bar, suggesting that a MoO_3/Al_2O_3 metathesis catalyst is used. The remaining lower (<C_{11}) and higher (>C_{14}) alkenes are recycled. The C_{11}-C_{14} alkenes with linear content of 96% are hydroformylated to detergent-range alcohol.

Shell Chemicals began commercial applications of the process in 1979 in Geismar, Louisiana (USA) with a production capacity of 200 000 ton per annum, which has increased in 1982 to 270 000 ton per year. A second plant came on stream in 1982 in Stanlow (UK) to produce 170 000 ton per year of higher alkenes.

While metathesis is part of a large-scale process in the SHOP technology, the FEAST project is an example of the application of the metathesis in the production of specialty chemicals (FEAST-Further Exploitation of Advanced Shell Technology). This project started with the preparation of various olefins in the multi-kg scale by ethenolysis or isobutenolysis of cyclic butadiene and isoprene oligomers (Grünert, 1992a). It has been continued with the construction of a 3000 t/a plant for the production of hexadiene-1,5 and decadiene-1,9 from cyclooctadiene-1,5 over Re_2O_7/Al_2O_3 catalyst.

1.1.4 Polymerisation processes based on metathesis

The commercialisation of metathetic polymerization has been handicapped by the competition of a large number of inexpensive and versatile polymerization processes. Thus polymers produced by metathesis have only found niche markets as specialty polymers. Examples of polymers obtained in commercial-scale processes are polyoctenamer and polynorbornene.

1.2 THERMODYNAMIC CONSIDERATIONS IN METATHESIS OF 1-OCTENE

The metathesis of light olefins (e.g. for the production of propene) is thermodynamically limited. Hence, it is of importance to consider possible thermodynamic limitations on the metathesis of 1-octene. The metathesis of 1-octene yields as primary products ethene and 7-tetradecene.

$CH_3\text{-}(CH_2)_5\text{-}CH_2\text{=}CH_2 \rightleftharpoons ½\ CH_2\text{=}CH_2 + ½\ CH_3\text{-}(CH_2)_5CH\text{=}CH\text{-}(CH_2)_5CH_3$ **(3)**

The reaction can be carried out at moderate conditions (T = 50-100 °C, atmospheric pressure, over MoO_3/Al_2O_3 catalyst). Under these conditions the reactant, 1-octene, and the product, 7-tetradecene, will be present in the liquid phase, whereas the product ethene will be present in the gas phase.

Figure 1.3 shows the Gibbs free energy of reaction as a function of temperature (the thermodynamic data used are given in Table 1.1). The reaction is highly favoured and equilibrium conversions in excess of 99.9% can be achieved. The reaction is quite strong endothermic (ΔH^{rxn}(80 °C)=184.82 kJ/mol 1-octene converted) and hence the reaction is favoured by an increase reaction temperature. The high equilibrium conversion and the strong endothermicity of the reaction can be ascribed to the formation of a product in a different phase.

Table 1.1: Data of used to evaluate thermodynamic constraints on 1-Octene metathesis (Daubert and Danner, 1987)

	ΔG_f^{liquid} (kJ/mol)	ΔH_f^{liquid} (kJ/mol)	ΔG_f^{gas} (kJ/mol)	ΔH_f^{gas} (kJ/mol)
Ethylene	-	-	68.12	52.28
7-tetradecene	-153.08	-207.31	-	-
1-Octene	1.04	-82.90	-	-

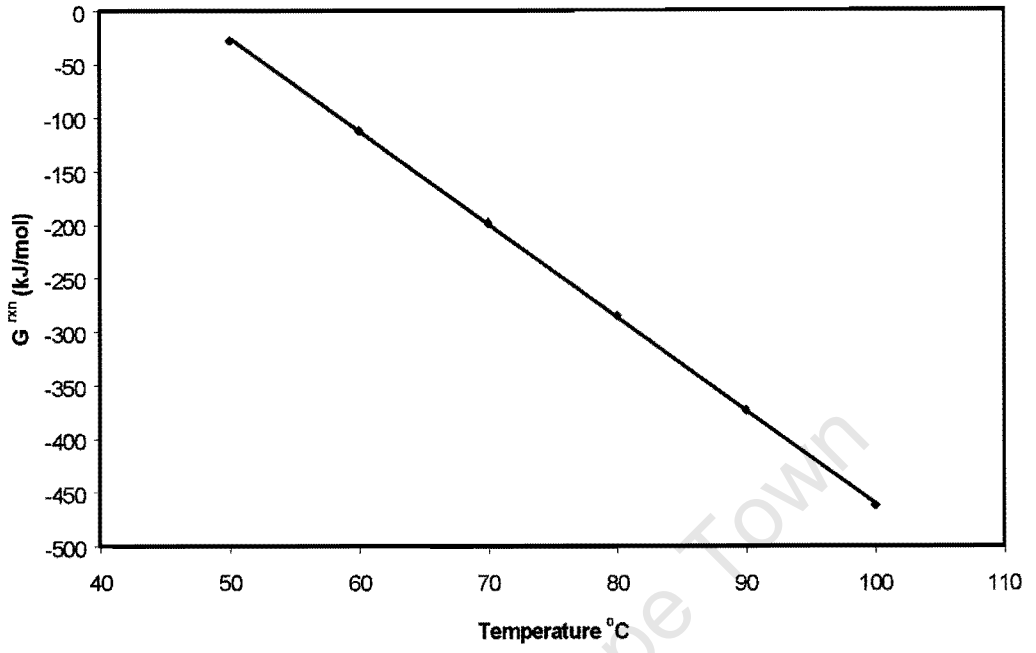

Figure 1.3 Gibbs free energy of reaction for 1-octene metathesis (per mole of 1-octene converted)

1.3 MECHANISM OF METATHESIS

The state of knowledge about the molecular aspects of the metathesis reaction is characterized by a widely accepted reaction mechanism and an understanding of the essential features of the active sites (Grünert, 1992a). In heterogeneous catalysis, however, there is considerable debate about the origin of active sites. In particular, the nature of the active site precursors and the mechanisms by which they are converted into active sites during interaction with the reactant olefins are unclear. The non-pairwise carbene mechanism (see Scheme 1.2) of the metathesis reaction was first proposed by Herisson and Chauvin (1971), and a large body of evidence has supported it since then (Taube et al., 1986; Mol and Moulijn, 1987).

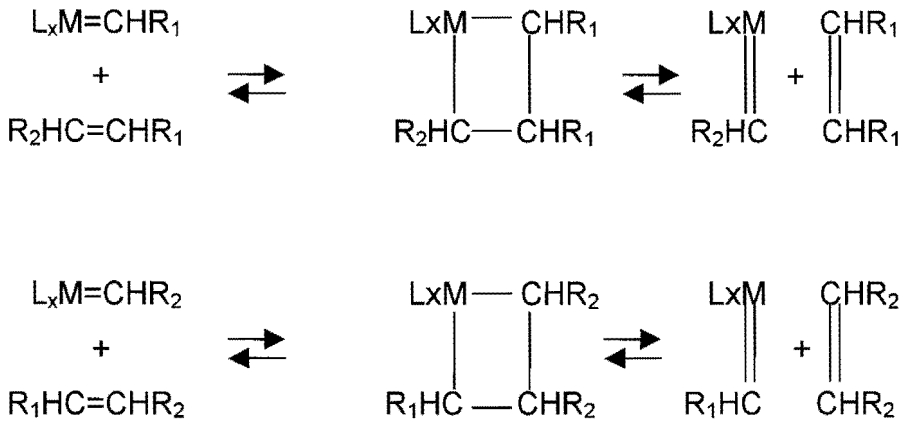

(**4**)

Scheme 1.2: Non-pairwise carbene mechanism of the metathesis reaction (Herisson and Chauvin, 1971)

Deuterium and ^{13}C isotopic studies with both homogeneous and heterogeneous catalysts proved the exchange of alkylidene moieties during the metathesis reaction. This is, however, still compatible with a pair-wise mechanism involving the formation of a cyclobutane intermediate. Conclusive arguments in favour of the non-pairwise carbene mechanism (see Scheme 1.2) were provided by the synthesis and structural characterization of stable, catalytically active carbene complexes (Katz and Hersch, 1977) and the isolation of a stable metallocyclobutane complex from the reaction between titanium methylidene complex active in the metathesis and an alkene (Howard et al., 1980).

An indirect proof of the non-pairwise carbene mechanism was provided by a study of the intramolecular metathesis of a mixture of d_0- and d_6-decadiene-2,8 over a $CoO/MoO_3/Al_2O_3$ catalyst (Grubbs and Swetnick, 1980).

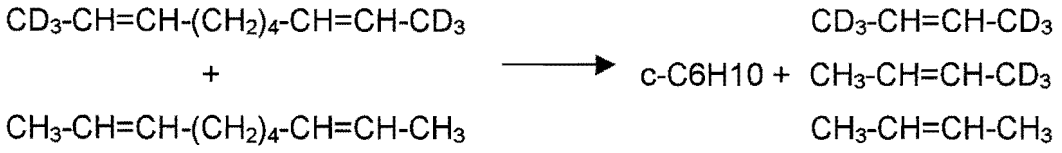

(**5**)

The existence of the d_3-butenes among the reaction products at low conversions allowed to exclude a reaction pathway via a cyclobutane intermediate, which would have combined the ethylidene groups of the d_0-and d_6-decadiene yielding exclusively to d_0-and d_6-butenes.

The first direct observation of a carbene species on a support surface was claimed by Shelimov et al (1988). The carbene, which was suggested to arise from the reaction of Mo^{4+}/SiO_2 (MoO_3/SiO_2, photoreduced in CO) with cyclopropane at 20 °C, was characterized by UV-Vis spectroscopy. However, the band ascribed to this species was not detected during propene metathesis under the same conditions while, on the other hand, independent evidence was presented that ≈70% of the Mo^{4+} ions on the surface were able to form carbenes. Nevertheless, the non-pairwise carbene mechanism is also generally accepted for metathesis over heterogeneous catalysts.

1.4 CATALYST USED IN HETEROGENEOUS METATHESIS

Metathesis is typically carried out over supported rhenium, tungsten and molybdenum catalysts. The typical support, method of preparation and reaction temperature of the metathesis is shown in Table 1.2. The support materials used for catalysts for metathesis are commonly used support materials. Sometimes a co-catalyst is added to the reaction system. The most common technique used for the preparation of these catalysts is incipient wetness impregnation. Rhenium and molybdenum are typically applied at conditions close to ambient conditions. Tungsten typically requires high reaction temperature.

1.4.1 Catalyst preparation

It is sometimes encountered that nominal performance of a catalyst in literature or even the same laboratory cannot be reproduced despite the "identical" preparation procedures. A main part of the difficulties is considered to result from

Table 1.2: Overview of heterogeneous Catalysts used in metathesis of alkenes (Grünert, 1992a)

Active component	Support	Co-catalyst/promoter	Method of preparation	Applied T^{rxn}, K
Re_2O_7	Al_2O_3		Impregnation	Ambient
			Impregnation	270-410
Re_2O_7	Al_2O_3	SnR_4	Impregnation	Ambient
Re_2O_7	Al_2O_3	(SnR_4) M_xO_y[a]	Impregnation	293-473
Re_2O_7	Al_2O_3	SnR_4 B_2O_3	Impregnation	Ambient
Re_2O_7	SiO_2·Al_2O_3	SnR_4	Impregnation	Ambient
Re_2O_7	Al_2O_3	$CsNO_3$		
Re_2O_7	Al_2O_3		Ex. $Re_2(CO)_{10}$	393
WO_3	SiO_2		Impregnation	680-870
WO_3	SiO_2 + MgO		Impregnation	520-670
WO_3	Al_2O_3		Impregnation	470-670
WO_3	SiO_2·Al_2O_3		Impregnation	670
WO_3	TiO_2		Impregnation	470-670
WO_3	SiO_2		Ex. W(η^3-metalallyl)$_4$	680-870
MoO_3	SiO_2[1]		Impregnation	300
MoO_3	Al_2O_3		Impregnation	370-620
MoO_3	TiO_2	SnR_4	Impregnation	300
MoO_3	SnO_2	$SnMe_4$	Impregnation	300
MoO_3	SiO_2[1]		Impregnation	300
MoO_3	SiO_2		Ex. Mo(η^3-allyl)$_4$	363
MoO_3	SiO_2 or Al_2O_3		Ex. Mo(η^3-allyl)$_4$ or Mo_2(η^3-allyl)$_4$	273

[1] catalyst photo-reduced

"subtle" differences in the preparation details (Okamoto et al., 1998). Although it is generally perceived that the preparation method of a catalyst strongly affects the catalytic properties, precise and systematic studies have rarely been

conducted on what and how preparation variables modify the outcomes of the catalyst. This may be owing to the fact that there are too many preparation variables for researchers in a group to cover: For instance with a simple technique such as impregnation following factors may affect the final performance of the catalyst: surface area, pore volume, pore size distribution, crystal structure, impurity, size and shape of the support materials, solvent, concentration or amount and pH of the impregnation solution, duration and temperature of the impregnation solution, numerous parameters during the drying and calcination processes and many others. It maybe hard to figure out what variables are predominant with a particular catalyst system, since impregnation processes depend on microscopic processes, such as the chemical or physiochemical interactions between the ions or molecules in the impregnation solution and support surface.

The preparation of a 13 wt.-% molybdena-alumina catalyst was investigated in a practical and unique manner to find predominant preparation variables (Okamoto, 1998). In this study, Al_2O_3 powder or small particle form was used as a support. This study led to the following conclusions:

1. The surface area of the support is the most predominant parameter for the dispersion of Mo oxide and sulfide species and their dispersion increases as the surface area of the support increases.
2. Formation of crystalline MoO_3 is observed at the surface Mo concentration higher than 3.2 Mo atoms per nm^2
3. A homogeneous distribution of the Mo oxide species is attained by an equilibrium adsorption method.
4. Other preparation variables such as drying processes influence the distribution of Mo oxide species in MoO_3/Al_2O_3 as well as the surface area of the catalyst.

The use of Al_2O_3 extrudates or pellets as a support would exacerbate the effects of the preparation variables on the dispersion of Mo species. However, catalyst preparations using these types of Al_2O_3 as a support are of industrial importance.

1.4.1.1 Incipient wetness impregnation

Impregnation methods are commonly used to add catalytically active components to pre-formed support materials. They are also more specially used to add promoters to catalysts prepared by other methods, since they represent the simplest procedure by which this can be achieved. For example, catalysts used for the hydro-treatment of hydrocarbons for the removal of S, N and O containing molecules are typically sulphided molybdenum or tungstate catalysts supported on γ-alumina and promoted by cobalt or nickel. The catalysts are prepared by impregnation (Maitra et al., 1986).

The incipient wetness technique involves a pore filling of the porous support with a solution containing the catalyst (precursor). This technique is suitable for low loading of additives. In addition, it is a very facile method and requires very little time. However, it can be difficult to control dispersion and may give non-uniform deposition of the impregnated material on the support. In particular, on drying, the material can migrate to the pore mouth and this can accentuates the non-uniformity of the final product. Notwithstanding this severe disadvantage, the method is widely used. Uniform filling of the pores can be achieved using the incipient wetness technique, using concentrated solutions at pH values that minimize adsorption. The pH is adjusted taking into account the isoelectric point of the support used. To overcome the problem of aggregation during the drying step and non-uniformity of the adsorption using the incipient wetness technique, greater quantities of liquid can be used and, in the extreme, this involves the use of a large excess of dilute solution. This has been used by Wang and Hall (1982) to prepare monolayer molybdenum/alumina catalysts.

1.4.1.2 Controlled adsorption

Controlled adsorption from solution uses highly diluted solutions of the additive. The pH is adjusted to control the rate of adsorption. The method has been optimised for MoO_3/γ-Al_2O_3 and WO_3/Al_2O_3 catalysts (Maitra et al., 1986). The pH is used to control (a) the surface charge of the support and (b) the size of oxy-anions of molybdenum and tungsten.

The solution chemistry of the oxy-anions of tungsten and molybdenum is complex. For tungsten, a variety of species containing one, six and twelve tungsten atoms can be present in aqueous solution which, at present, can be controlled to some extent by the selection of the solution pH (Maitra et al., 1986).

1.4.1.3 New slurry impregnation method

Recently, Zdrazil (2001) described a novel method for the preparation of supported MoO_3 catalysts, which is easier and cleaner. A slurry of MoO_3 in water is used instead of the conventional impregnation solution containing $(NH_4)_6Mo_7O_{24}$. Although these catalysts were used for the hydrodesulferization reaction, it is well known that the oxide form of the catalyst shows activity for metathesis (Haber, 1994).

The new slurry impregnation and the conventional method for the preparation of MoO_3/support solids are schematically described in Figure 1.4. In the conventional method the support is impregnated with solution of soluble molybdenum compound, ammonium heptamolybdate. In the new slurry impregnation the porous support is impregnated with a slurry of finely ground MoO_3. Various shapes of alumina (powder, extrudates, etc.) can be impregnated using the new slurry impregnation. The impregnation time depends on particle size of the support, loading and temperature. For higher loading (ca. 70-100% of the amount needed to form a monolayer), the required impregnation time is about 3-5 d for extrudates (1.5mm) at room temperature, whereas the time

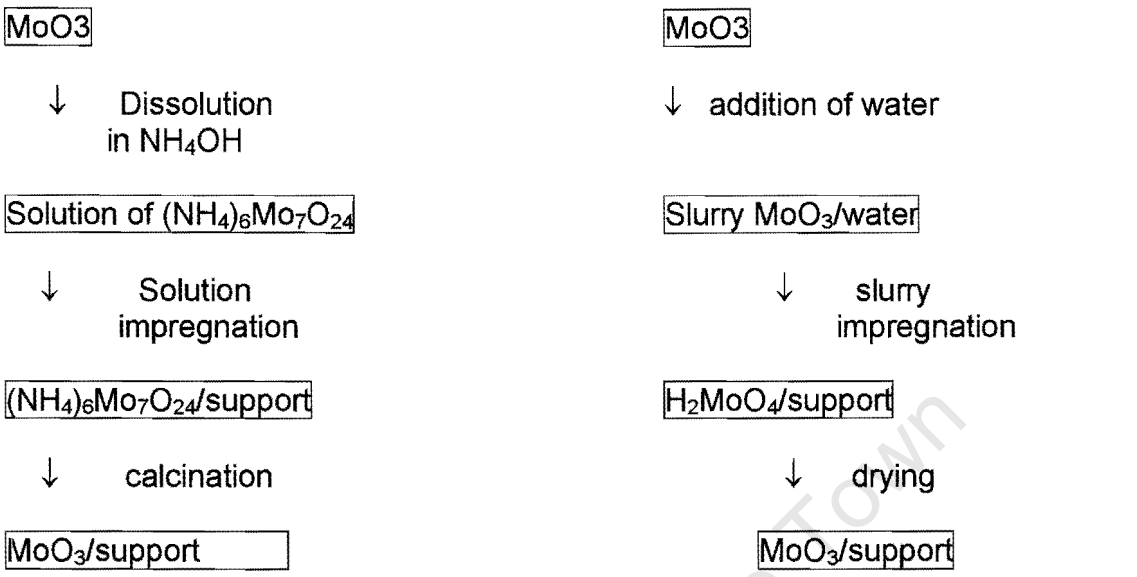

Figure 1.4: Comparisson between conventional incipient wetness impregnation and the new slurry impregnation (Zdrazil, 2001)

needed is ca. 2-3 h for the impregnation of the aqueous paste of finely ground MoO_3 in Al_2O_3 at 95-100 ^{o}C. The impregnation is shorter for lower loading. It was found that the highest amount of MoO_3 deposited by slurry impregnation corresponds well to the formation of saturated monolayer.

1.4.1.4 Solid/Solid wetting

Xie and co-workers (1984) have demonstrated that dispersed supported molybdena/alumina catalysts can also be obtained from simple physical mixtures by the spreading of MoO_3 on the surface of the Al_2O_3 support. On the basis of X-ray diffraction (XRD) and X-ray photoelectron spectroscopic (XPS) measurements they have proved that MoO_3 spontaneously spreads over the surface of Al_2O_3 in physical mixtures of the two oxides when these are subjected to thermal treatments at temperatures around 400-500 ^{o}C in air for 24 h.

Fransen et al. (1976) reported a similar phenomenon of the spreading of MoO_3 on the surface of Al_2O_3 support by a different method. In this method, MoO_3 and Al_2O_3 were taken in two separate beds and MoO_3 (maintained at 600°C) was transported to the Al_2O_3 support in the form of $MoO_2(OH)_2$ by steam.

Leyer et al. (1988) have extended this study and reported supporting evidence for this spreading phenomenon by the application of ion scattering spectroscopy (ISS). Based on laser Raman spectroscopy (LRS) studies, Leyer et al. (1986) have also demonstrated the significance of gas atmosphere on the resulting dispersed molybdenum species during thermal treatments in the case of simple physical mixtures. Under an absolute dry O_2 atmosphere only MoO_3 phase was observed, whereas under an O_2 atmosphere saturated with water vapour, formation of the surface heptamolybdate phase was observed (Knözinger, 1988). Catalysts obtained via the latter method were also found to show comparable catalytic properties with that of a conventional impregnated catalyst for HDS of thiophene (Koranyi et al., 1990). The spreading process was phenomenological termed as solid/solid wetting and the driving force for this phenomenon was proved to be due to the decrease in surface free energy (Leyer et al., 1990).

1.4.2 Molybdenum species in MoO_3/Al_2O_3

A supported catalyst usually consists of an active component dispersed on a support with a highly specific surface. The forms of active components present in heterogeneous catalysts are of importance in catalysis (Xie and Tang, 1990). An active component dispersed on a support may end up in one of three forms (Pott and Stork, 1976):(1) it may retain its chemical identity as a separate crystalline or amorphous phase, (2) it may form a new stoichiometric compound with the support or additive, or (3) it may dissolve in the support to give a solid solution. In investigations of a few catalysts, some authors have suggested that the active components may be present as a monolayer. For example, Russell and Stokes (1946) have concluded that the catalyst MoO_3/Al_2O_3 may form a monomolecular layer of MoO_3 on the surface of alumina, because the catalytic activity is linearly

related to the molybdenum content up to a limit corresponding to full coverage. A great many oxides and salts can disperse spontaneously onto the surface of supports to form a monolayer or submonolayer, because in these cases the monolayer is a thermodynamically stable form.

In order to assess the nature and distribution of the surface species formed, mechanical mixtures of MoO_3/Al_2O_3 have been prepared with MoO_3 loading ranging from 0.1 to 2 monolayers and calcined at 770K for 8 h and 24 h, in the presence of water vapour (Del Arco et al., 1993; see Figure 1.5). On increasing the calcination time, MoO_3 transforms to polymolybdate species, increasing the surface coverage. When these catalysts are calcined for 24 h, the surface of the support is completely covered when the molybdena loading is equivalent to 0.7-0.8 monolayers; the remaining molybdena exceeding this quantity remains on the polymolybdate monolayer, both in the crystalline and dispersed state, leading to

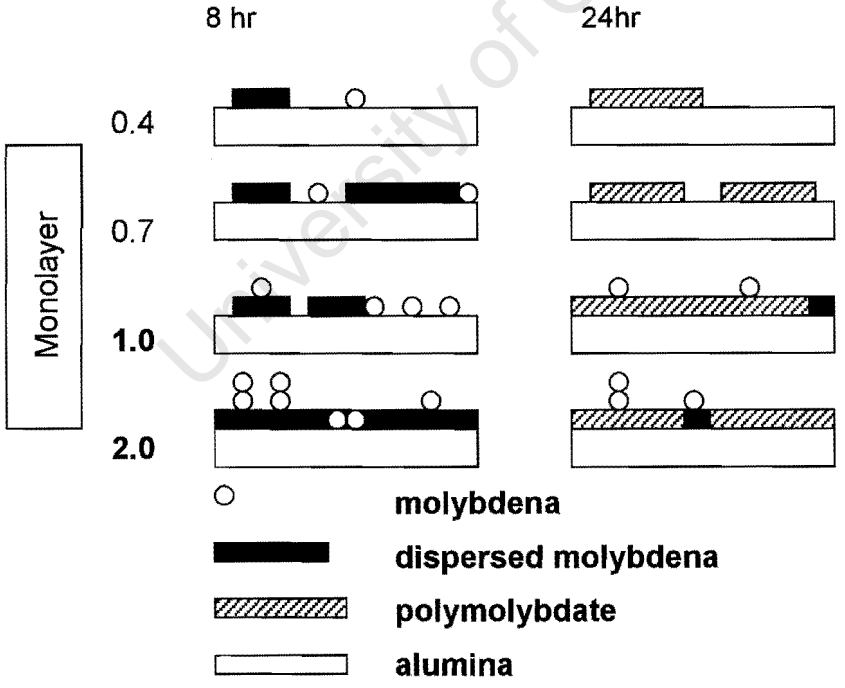

Figure 1.5: Dispersion of molybdenum-containing species on the surface of alumina (Redrawn from Del Arco et al., 1993).

multilayer formation. If calcination is carried out only during 8 h the transformation to polymolybdate does not take place, but the alumina surface is progressively covered by crystalline and dispersed alumina on increasing the molybdena loading, covering being complete for a loading equivalent to 2 monolayers.

Beside the formation of the monolayer, two other molybdenum compounds have to be considered: $Al_2(MoO_4)_3$ and bulk MoO_3. Alumina molybdate seems to be present either for high molybdenum contents (Medema et al., 1978) or if the calcination temperature of the catalyst is higher than 535 °C. When the MoO_3 content in the mixture exceeds this critical dispersion capacity, there will be a residual crystalline phase of MoO_3. The interaction between molybdenum oxide with the alumina support has been discussed by many authors (see e.g. Grange, 1980) and (Fransen et.al., 1976)

The following interaction complex was proposed (Medema et.al., 1978):

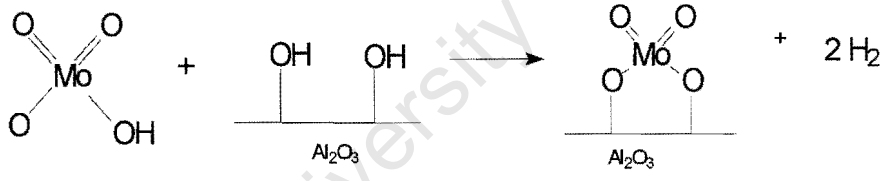

After the drying (110 °C for 12h) and calcination steps (600 °C in air for 2 h), following surface species may be obtained (Medema et.al., 1978):

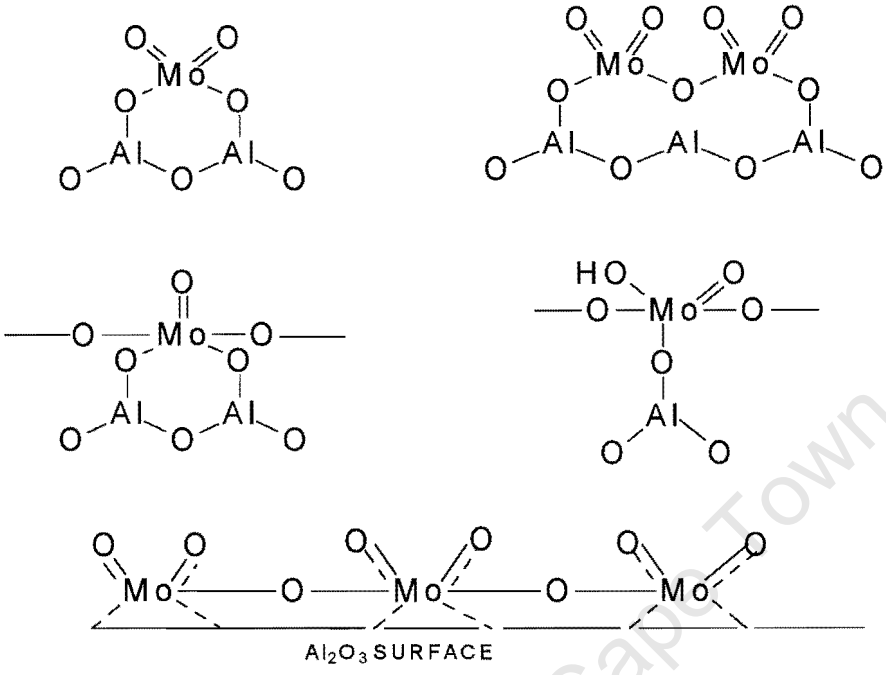

The concentration of these species is highly dependent on the pH of the impregnation solution. As has been mentioned before, the activity of the MoO_3/Al_2O_3 is directly related to the molybdenum content up to a limit corresponding to full coverage.

1.4.3 Nature of the Active Site in MoO_3/Al_2O_3 catalysts in metathesis

Although two types of symmetry are observed for molybdenum deposited on γ-alumina, the active species for metathesis seems to be the Mo^{6+} ion situated in an octahedral cavity of symmetry C_{4v} (Ismayel-Milanovic et al., 1973). This active Mo^{6+}-centre is probably located inside the lattice of the alumina since at high Mo-content, when the formation of MoO_3 is very likely to occur the catalytic activity is greatly lowered. Such a site would be produced after dehydration of the alumina carrier at high temperature. If we assume that the (100) face of the alumina is the most exposed one, the surface of the solid may be represented in the following way:

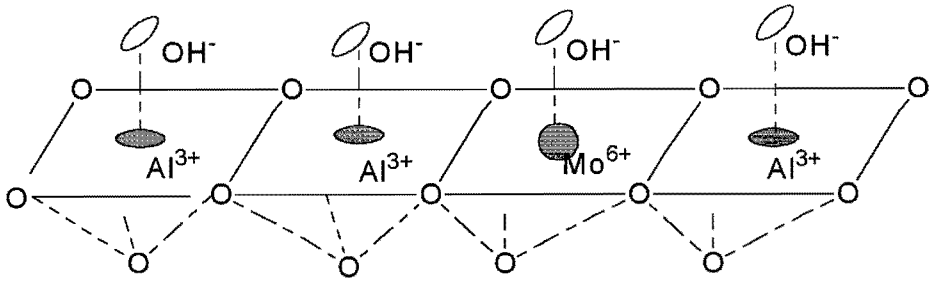

Figure 1.6: Solid surface showing the Mo^{6+} covered with OH-groups prior to dehydration (Redrawn from Ismayel-Milanovic et al., 1973).

Mo^{6+} is covered with OH groups when the alumina is evacuated at low temperature. Upon dehydration at high temperature (600°C) the solid takes a new surface composition due to the condensation of adjacent OH groups with formation of gaseous water:

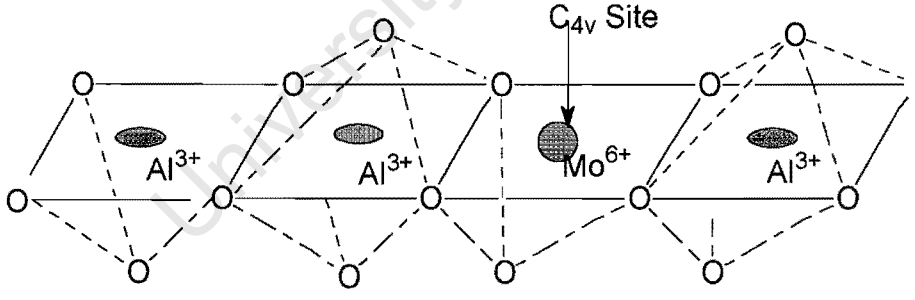

Figure 1.7: New surface composition due to condensation of OH groups at 600°C. (Redrawn sketch from Ismayel-Milanovic et al., 1973)

The development of the metathesis activity of supported molybdena and tungsten oxide catalyst has been ascribed to the active sites originating from surface compounds in which the metal is in the 6+ oxidation state (Figure 1.7)

and 4+ oxidation state. The existence of the 4+ oxidation state has been drawn most convincingly from investigations with model catalysts prepared via fixation of organometallic complexes (Startsev et al., 1976) and with photoreduced Mo/SiO_2 (Shelimov et al., 1986). Several possible pathways for the formation of the active carbene sites from Mo(IV), W(IV) precursor species have been proposed (Iwasawa et al., 1985). With the organometallic complexes a route involving the abstraction of a vinyl hydrogen by the central Mo ion has been substantiated by isotopic methods.

For more conventional catalysts the situation is less clear. Certainly, reduction of the catalyst (with subsequent removal of adsorbed hydrogen) has been frequently found to favour the metathesis reaction (Engelhardt, 1980), and a relation between the reducibility of the hexa-valent Mo (or W) ion on a support surface and the metathesis activity of the corresponding catalyst has been established (Thomas et al., 1985). This relation is largely based on the observation that alumina-supported catalysts with a small metal oxide content, whose reducibility is very low, exhibited inferior metathesis activities (Thomas and Moulijn, 1982). On the other hand some metathesis activity is also often found with unreduced catalysts (Engelhardt, 1980). There is a report on a situation where no influence of the reduction degree on the metathesis activity was detected (Lombardo et al., 1980). For Mo/TiO_2 systems, the average oxidation number of the most active surfaces was found to be considerably higher than 4+; more extensive reduction caused a drastic loss of activity (Miyahara, 1980). This evidence may suggest the existence of a second active site precursor. The oxidation state of this site must then be higher than the 4+ oxidation state. In the past, Mo(V) species were repeatedly considered to be involved in the metathesis sites (Giordano et al., 1973). Mo(VI) was proposed to be the active precursor in the activation process where the metathesis reaction is initiated by the treatment of an oxidized MoO_3/Al_2O_3 catalyst with olefin at room temperature (Goldwasser et al., 1981). However, in a subsequent paper the same authors considered a slight reduction of the surface, which is indicated by

the emergence of a Mo(V) EPR signal, to be also essential for the activation (Engelhardt et al., 1982).

For reasons that have not yet been fully elucidated, the reproducibility of the metathesis activities measured with MoO_3/Al_2O_3 catalysts after activation in an inert atmosphere was much lower than that with WO_3/Al_2O_3 catalysts. Sometimes series were obtained differing from each other in the activity level by 30-40%, but having the same graduation between the different catalysts. It is believed (Grünert et al, 1992b) that this is due to ease of poisoning of molybdena-based metathesis catalysts by oxygen traces in the gases or mobile oxygen on the surface than WO_3/Al_2O_3 catalyst (Grünert et al, 1989). The reason why highly loaded MoO_3/Al_2O_3 catalysts are more easily poisoned may be an indication that the species capable of forming active sites constitute only a small fraction of the total molybdenum in these catalysts.

1.5 Effect of reaction conditions on the metathesis reaction

Only a few studies have dealt in depth with the effect of reaction conditions on the metathesis of olefins. The effect of temperature on this type of reaction is mostly dominated by the effect of the temperature on the position of thermodynamic equilibrium. The effect of pressure has not yet been investigated in depth, but a study at Sasol indicated that pressure does not affect the reaction significantly.

1.5.1 Space Velocity

The effect of space velocity on metathesis of 1-butene has been investigated at 160 °C over $CoO\text{-}MoO_3/Al_2O_3$ (Bradshaw et al., 1967). The results are shown in Table 1.3. With increasing space velocity, the residence time of 1-butene in the catalyst bed becomes shorter. At low space velocity it is expected that the C_3 and C_5 selectivity should be high because the contact time between feed and catalyst is high leading to secondary reactions (isomerization and subsequent

metathesis). As the space velocity increases, less 2-butene will be formed, hence C_2 and C_6 selectivity rises as expected. These results show clearly how the product selectivity is affected by the double bond isomerization of reactant molecule.

Table 1.3: Effect of space velocity on metathesis of 1-butene at 160 °C over $CoO\text{-}MoO_3/Al_2O_3$ (Bradshaw et al., 1967)

GHSV	500	2000	5000	10000
%Metathesis	54.5	31.9	9.0	1.7
%Butene-2 in product butene	64.9	52.3	21.3	8.0
Products(mole%)				
C_2H_4	12.3	15	22.4	21
C_3H_6	43.6	36.8	21.4	11
C_5H_{10}	28.2	31.5	26.2	25
C_6H_{12}	11.9	12.7	26.6	40
C_7H_{14}	3.0	1.8	1.0	1
C_8H_{16}	1.0	1.4	2.8	2
C_9H_{18}	tr	0.8	tr	tr
Selectivity(C_2+C_6)	24.2	27.7	49.0	61

1.6 Problem Statement

It is evident from this review that the metathesis reaction is very valuable to convert olefins into important intermediates, which can further be used to produce products for the detergent market. This opens a door for relatively low value Sasol feed to be converted into high valued products. Various MoO_3/Al_2O_3 catalysts with varying MoO_3 loading catalyst will be prepared. The trend in activity and selectivity is to be monitored. Detailed Raman spectroscopy analysis will be done on these catalysts, which will not only give structural information but also more about the activation and deactivation of the MoO_3/Al_2O_3 catalyst.

2 EXPERIMENTAL

2.1 Catalyst Preparation

Supported MoO_3/Al_2O_3 catalysts with variable loadings (9.1 wt.-%, 16.7 wt.-%, 23.1 wt.-%, 28.6 wt.-% and 33.3 wt.-%) were prepared using the controlled adsorption technique and the new slurry impregnation (Zdrazil, 2001).

γ-Alumina (150 m^2/g) obtained from Sasol Chemie (Sasol Germany GmbH) was used as a support. The γ-alumina used, was a fine white powder with a single point adsorption pore volume of 0.461cm^3/g. The γ-alumina was calcined in a furnace at 550 °C overnight, before use, to remove any adsorbed impurities and moisture.

The amount of MoO_3 to form a monolayer is of importance in the distribution of the various Mo-species present on the catalyst. When the area taken by 1 MoO_3-species can be taken to be 1.50 $\times 10^{-19}$ m^2 (Fransen et al., 1975), 0.24 g MoO_3 per gram of Al_2O_3 or 19.4 wt.-% MoO_3/Al_2O_3 will yield monolayer coverage.

2.1.1 Catalyst preparation by controlled adsorption

Supported MoO_3 on γ-Al_2O_3 catalysts (Sasol Germany GmbH, S_{BET}= 150 m^2/g; V_{pore}= 0.461 cm^3/g) with a MoO_3-loading of 9.1 wt.-%, 16.7 wt.-%, 23.1 wt.-%, 28.6 wt.-% and 33.3 wt.-% were prepared by controlled adsorption.

A known mass of precursor, ammonium heptamolybdate (AHM: $(NH_4)_6Mo_7O_{24}$) 99% purity, Merck, batch no,1182), which is the source of MoO_3, was added to 100 ml of bi-distilled water under constant stirring at 200 rpm using a magnetic stirrer. Within 10 min ammonium heptamolybdate was totally dissolved. The appropriate amount of the γ-alumina support was added to the stirred solution after 30 min. The initial pH of this solution was 6.1 at a temperature of 20 °C. This is below the point of zero charge (PZC=7-9) of the support. After 17 h the pH was at 7.2. To lower the pH of the solution, 15 drops of HNO_3 (Rochelle Chemicals,

55% chemically pure, batch no 1353) was added. The pH was consequently brought down to 6.1. After 28 h the impregnation was stopped and left to age overnight. The wet catalyst was placed on a rota-evaporator to dry at 120 °C without applying any vacuum. The rate of rotation was set at 100 rpm. After 5 h on the rota-evaporator the catalyst was dry. In order to get the catalysts in the oxidic form, MoO_3, the catalyst was placed in a static calcination oven to decompose the ammonium heptamolybdate precursor. No gases were passed over the catalysts except the air from the atmosphere. The temperature was raised with 3 °C/min to 550 °C, at which it was kept for 12 h.

2.1.2 Catalyst preparation by new slurry impregnation

Recently, Zdrazil (2001) described a novel technique to prepare supported MoO_3-catalysts. The advantages of this method over the conventional impregnation methods are the simplicity, cleanliness of the method and the fact that no decomposition of a precursor is necessary because MoO_3 is used directly. A MoO_3/γ-Al_2O_3 catalyst with 9.1 wt.-% MoO_3 was prepared using this technique.

The appropriate amount of MoO_3 (99+% purity, Aldrich Chemical Company Inc. catalog nr.22, 181-3) was dissolved in 150 ml of bi-distilled water and stirred for 20 min till all the MoO_3 was dissolved. The support, γ-alumina (Sasol Germany GmbH, S_{BET}= 150 m^2/g; V_{pore}= 0.461 cm^3/g) was then added to the stirred solution and a further 150 ml of bi-distilled water was added. The impregnation temperature was taken up to 90 °C. After 14 h of impregnation the stirring of the solution was stopped and the catalyst left to age overnight. The wet catalyst was then dried at 120 °C for 5 h. No calcination was needed.

2.2 Catalyst characterization

2.2.1 Elemental analysis

The molybdenum loading of the synthesized catalysts were determined using Inductive Coupled Plasma atomic adsorption spectroscopy (ICP-AAS). The sample was digested at 80 °C for a period of 40 min in a Milestone Ethos Plus microwave oven. A mixture of HCl (6 M), HNO_3(2 M)and HBF_4(1 M) was used for the digestion. After digestion the sample was analyzed on the Vista CCD simultaneous ICP.

2.2.2 BET surface area determination

Approximately 0.25 g of a sample was pre-dried, by heating it in a nitrogen flow at 200 °C overnight. Contaminants, which may have adsorbed onto the surface or in the pores of the sample, were removed in this step. After cooling down to room temperature, the sample was weighed again and transferred to the instrument (Tristar, Micromeritics) for analysis. Nitrogen was adsorbed onto the sample at -196 °C. The pressure range for adsorption of nitrogen was fixed: data points were selected to cover the BET equation range, up to saturation pressure.

2.2.3 Transmission Electron Microscopy (TEM)

The catalysts were viewed in a Philips CM200 TEM operating at a high voltage of 200 kV. Images were digitally recorded with a Gatan Image Filter (GIF) fitted to the microscope. Samples were prepared by dipping a copper TEM grid covered with a lacey carbon film into the catalyst powder.

2.2.4 X-ray diffraction (XRD)

The samples were analysed with the Siemens XRD. The experimental conditions are given in Table 2.1.

Table 2.1: Operating conditions for XRD-analysis

V	40 kV
A	25 mA
Divergence slit	1°
Receiver slit	0.15°
Scanning range:	2θ = 5° to 105°
Step size	2θ = 0.05°
Counting time	2 s

2.2.5 CO-chemisorption

The active surface area and % metal dispersion can be obtained by applying measured doses of a reactant gas to a reduced sample. The gas chemically reacts with each active site, until all the available sites have reacted.

Approximately 0.25 g of a sample was weighed down and pre-reduced in-situ, by heating (2 °C/min) it in a hydrogen flow to the reduction temperature (425 °C) for a period of time (7 h). After reduction the sample was evacuated, removing the reduction gas from the surface of the sample. The evacuation process was continued by cooling the sample down to the analysis temperature (35 °C) under vacuum.

To differentiate the chemisorption from the physisorption contribution, the sample was evacuated after the completion of the initial analysis, which removes only the reversibly adsorbed gas. Then the analysis was repeated under the same conditions as the original analysis, except during the second analysis the active area of the sample was already saturated with chemisorbed molecules.

2.2.6 Temperature Programmed Reduction

The reducibility of supported MoO_3-catalysts on γ-Al_2O_3 was investigated using temperature programmed reduction (TPR). These experiments were performed

on an Autochem 2910 (Micrometrics) instrument. Approximately 0.05g of sample was dried, by heating it in an argon flow from room temperature to 120 °C with a heating rate 5 °C/min, at which temperature the sample was kept for 10 min. After cooling to ambient temperature, the catalyst was exposed to a 10% H_2/Ar mixture, at a flow rate of 50 ml(STP)/min. The sample was heated up to 950 °C using a linear heating rate of 10 °C/min. The concentration of hydrogen in the effluent was monitored with a thermal conductivity detector (TCD).

2.2.7 Infrared Spectroscopy

The amount of Brønsted and Lewis acid sites present on the catalysts were characterised by pyridine adsorption, which was determined using FT-IR (Perkin Elmer FT-IR spectrometer). A 13 mm diameter disk was prepared from 10 mg sample and 40 mg potassium bromide (KBr). Bruker Vector 22 with a DTGS detector was used for the analysis. The instrument was operated with Opus NT software. A resolution of 4 cm^{-1} was used and 128 Scans per spectrum were collected. Initially the sample was dried at 365 °C for an hour under argon flow (flow rate = 60 ml/min. The sample was then cooled down to 200 °C before the background spectrum was collected. Pyridine was used as the probe molecule and it was adsorbed at 200 °C for 15 min. Excess pyridine vapour was purged out of the cell with argon for 1 h before the first spectrum was collected. Further purging was done for 4 h with the spectra being collected at 1 h intervals. The spectrum collected after 4 h was used for the analysis because of the minimal effect of the vapour after this time.

The intensities of the peaks around 1449 cm^{-1} and 1541 cm^{-1} were integrated using the baseline as the straight line that connects the frequency limits and the peak envelope. These peaks correspond to the Lewis and Brønsted acid sites respectively.

2.2.8 Raman Spectroscopy

The Raman process is an *inelastic scattering process*, which produces secondary light quanta with different energies to that of the excitation frequency. During the interaction of the primary light quantum with a molecule or crystal, the energy of vibrational states may be exchanged and a secondary light quantum of lower or higher energy is emitted. The energy difference is equal to the generated or destroyed *vibrational energy* E_{vib}. The inelastic interaction of a primary light quantum with a crystal in its vibrational ground state produces the Stokes Raman spectrum. If a molecule or crystal is not in their vibrational ground state, the interaction of the primary light may produce the *anti-Stokes Raman spectrum* (see Figure 2.1).

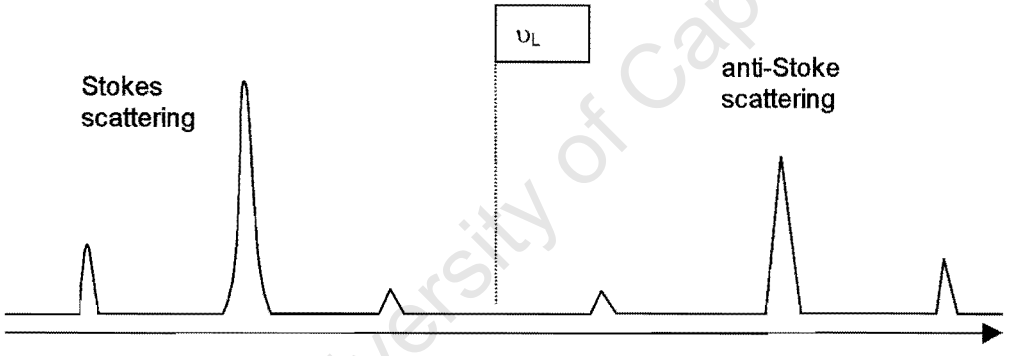

Figure 2.1: Scheme of Stokes and anti-Stokes scattering relative to the excitation frequency.

Atomic movements in crystals are only allowed with defined phase relations giving rise to the vibrational modes of a crystal. These collective atomic movements are termed acoustic or optical photons depending on the generation of a dipole moment during the vibration. Optical photons take part in inelastic light scattering processes due to their induced dipole moment.

The interaction of electromagnetic radiation with matter leads to absorption and reflection and light-scattering processes. In Rayleigh scattering most scattered photons have the frequency identical to the incident ones. But a small part of the scattered light may have a higher or smaller energy than that of the incident light. This process is known as the Raman effect: the incoming photon excites the scattering matter from its electronic ground state into a virtual state, from which it relaxes under the emission of a Raman scattered photon of smaller or higher energy (Stokes or anti-Stokes scattering), depending on the initial and final vibrational levels. These light scattering processes can be understood within a classical model of the scattering process. Such a classical model can describe the observed Raman Shifts. The intensity or line shape of Raman bands, however, can only be determined via quantum mechanical ab-initio calculation of the Raman-scattering transition moment.

In a quantum mechanical picture of the Raman scattering, the incoming photon either generates an excited phonon and therefore has a lower energy after the scattering process or it annihilates an excited phonon in the solid and thus has a higher energy after the scattering event. This process can be understood as a series of three elementary steps:

1. The incident photon is annihilated (absorbed) under the generation of the virtual electron hole- pair 1.
2. The virtual electron hole - pair 1 generates or annihilates a phonon under the formation of the virtual electron hole - pair 2.
3. The virtual electron hole - pair 2 recombines under the emission of the Raman scattered photon.

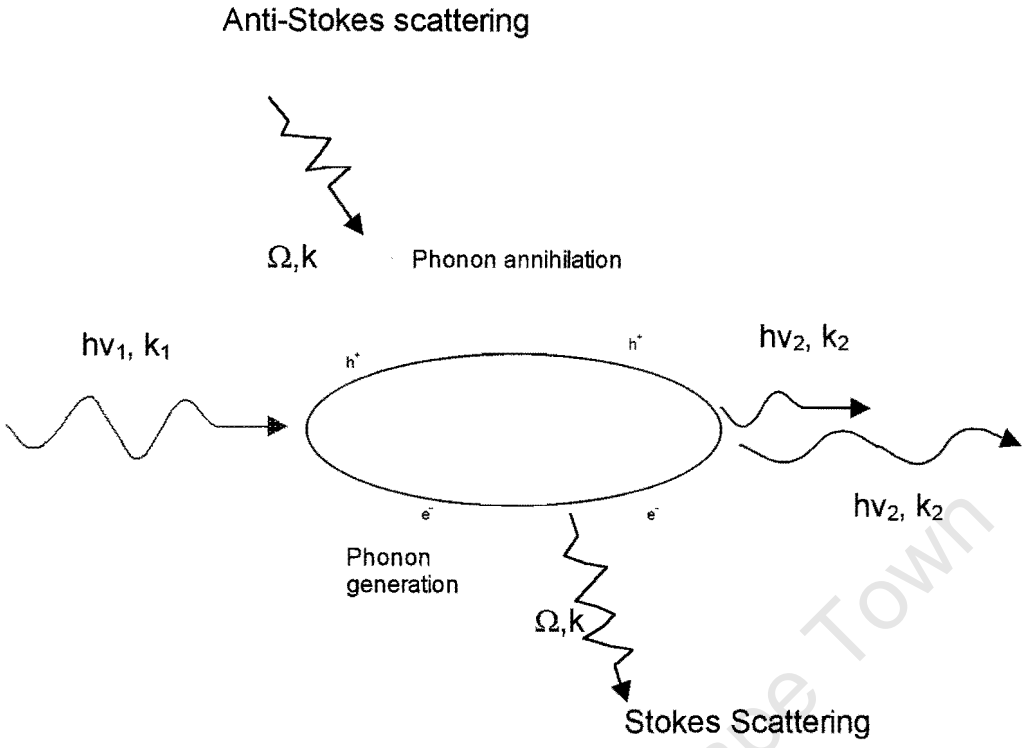

Figure 2.2: Scheme of the Raman scattering process in solid material.

As in infrared spectroscopy, not all vibrations are observable in Raman spectroscopy. A vibration is Raman active if it changes the polarizability of the molecule. This requires in general a change in the shape of the molecule. The selection rule for infrared spectroscopy was that a dipole moment must change during the vibration. As a consequence the stretch vibrations for example of H_2 (4160.2 cm^{-1}), N_2 (2330.7 cm^{-1}) and O_2 (1554.7 cm^{-1}) are observed in Raman spectroscopy but not in Infrared. The two techniques thus compliment each other, in particular for highly symmetrical molecules.

A strong point of Raman spectroscopy for research in catalysis is that the technique is highly suitable for *in situ* studies. The spectra of adsorbed species interfere weakly with signals from the gas phase, enabling studies under reaction conditions. A second advantage is that typical supports such as silica and alumina are weak Raman scatterers, with the consequence that adsorbed

species can be measured at wavenumbers as low as $50cm^{-1}$. This makes Raman spectroscopy a powerful tool to study catalytically active phases on a support.

Some major problems may arise when recording Raman spectra of catalysts. Laser heating could lead to loss of hydration water, phase transition, partial reduction or even complete decomposition and, thus, to artificially change samples. Heating by the laser beam can be reduced by applying low laser powers (<10 mW). Cooling with an inert gas of high thermal conductivity is another alternative to avoid overheating of the sample.

Fluorescence can overwhelm the Raman spectrum, which may be due to organic impurities, basic surface OH groups, proton superpolarizability or reduced transition metal ions when resonant excited. Fluorescence problems can be often solved by simply burning-off the organic contaminants or dehydroxylating the surface, if the sample tolerates these treatments.

The Raman scattering has an inherently low sensitivity due to the small Raman scattering cross-sections as compared to IR absorption coefficients. A technical solution to the problem of low sensitivity was found in the highly sensitive CCD cameras and in high performance, holographic notch filters to cut off the very intense Rayleigh scattering. These two inventions considerably improved the spectrometer technology: triple stage spectrometers, necessary for stray light reductions, with low light throughput now can be avoided. This led to an increase in measured intensity by a factor of ca. 10^2. The new generation Raman spectrometers also allow for time-resolved experiments due to their high sensitivity and long-time stability.

2.2.8.1 Raman spectrophotometer

All Raman spectra were recorded with Renishaw spectrometer equipped with a confocal microscope (Leica microscope) and a motorized XYZ-table (see Figure 2.3).

Figure 2.3: Representation of the Raman instrument used for analysis.

Laser

The light for illuminating the sample and exciting the Raman scattering and fluorescence is provided by the laser. The laser is ideally suited to Raman spectroscopy, as it provides a beam of monochromatic radiation at a known and stable frequency. Any type of continuous wave (CW) laser with emission from between 400 to 800 nm could be used. The laser used in the experiments was an Argon ion (Ar^+) green (514.532 nm) laser.

CCD camera

A *charged coupled device* (CCD) *array detector* is employed to detect the optical signals produced by the sample after analysis by the Grating, Filter or Etalon light path. The camera is very sensitive but can be damaged by optical overload. The

CCD head needs an unobstructed flow of air in order to dissipate heat generated by the thermoelectric coolers.

Microscope

The microscope (see Figure 2.3) provides a convenient means of mounting the sample, focussing the laser beam onto it, and passing the returning beam into the system unit for analysis and detection. It is based on a standard research-grade metallurgical microscope with several optical adapters to allow laser light and/or the microscope illumination to fall on the sample. The microscope is fitted with a trinocular head with a camera.

2.2.8.2 In-situ Raman experiments

Renishaw spectrometer is equipped with a reactor chamber (see Figure 2.5). The reactor unit consists of a gas inlet, outlet and a water circulation system. The water circulation pump is switched on for cooling purposes. A small quantity of catalyst sample was placed in the reactor. This reactor unit is then placed inside the microscope onto the XYZ-motorized stage and the necessary connections are made. Gases can flow over the catalyst (but not through a catalyst bed).

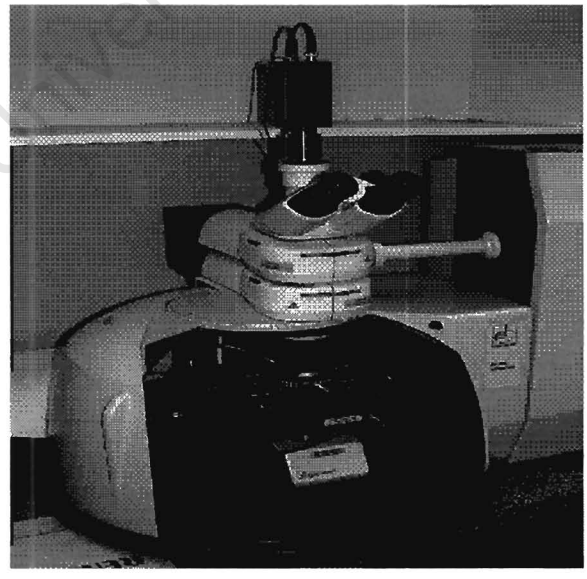

Figure 2.4: Representation of the microscope used to focus on the catalysts.

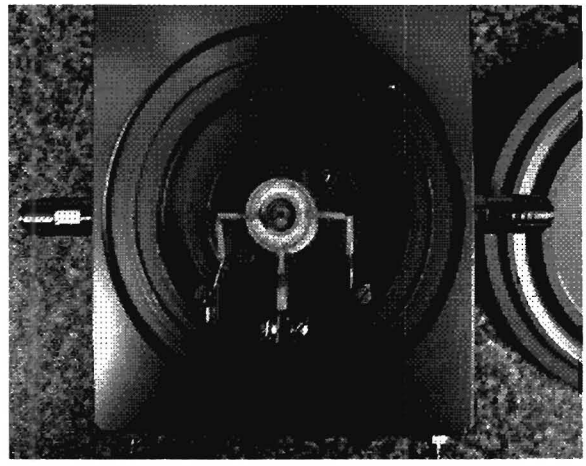

Figure 2.5: The reactor cell used for in-situ Raman studies

Activation of catalyst under air

N_2 and synthetic air could be delivered to the in-situ reactor. Both gases were dried by passing them through a bed of molecular sieves (UNITEK, Batch no 31918) and a bed of neutral alumina (Activated aluminum oxide, Brockman I, STD grade, approximately. 150mesh, 58 Å, catalog nr 19,997-4).

The catalyst was activated in air. Prior to the activation, nitrogen was allowed to flow through the inlet over the sample 55 ml/min. The catalyst sample was heated up in nitrogen with 20 °C/min up to the activation temperature (550 °C). Once the activation temperature was reached, the inert gas flow was stopped and synthetic air was delivered to the reactor chamber for a period of 2 h at 55 ml/min. Spectrums were recorded during this period. After 2 h the temperature was brought down to 80 °C and kept at 80 °C for 1 h. During this period spectrums were recorded as well.

Reduction of catalysts with H_2

The catalyst sample was heated up in nitrogen 55 ml/min at 20 °C/min up to the activation temperature (550 °C) in order to avoid creating an explosive atmosphere. The nitrogen flow was stopped this temperature had been reached. The reducing gas, H_2, was allowed to flow over the catalyst at a flow of 70 ml/min. The reducing gas was kept flowing over the sample for a period of 20 h. After 20 h a spectrum was recorded. The hydrogen flow was stopped and the temperature was brought down to room temperature.

Reaction with 1-butene

The catalyst sample was activated under air as described above. Once the temperature reached 80 °C, the dried 1-butene was passed over the catalyst sample and spectrums were recorded every 2 min for a total of 15 min.

Mapping experiments

This multiple type scanning is used to obtain data from any group of points on the sample. This may be used to collect data from a number of interesting features, such as map of peak area, position and intensity, which was focussed on during these experiments. The peak area mapping is the usual map to look at the relative amount of a material. The peak position is normally used to look at the material chemical environment and the peak intensity can be used for comparing amounts of material.

2.3 Reactor studies

The metathesis of 1-octene was investigated. Pure 1-octene (*98%,Aldrich, catalog no, 0480-6*) was dried through a column containing activated neutral alumina to remove oxygenates, which might be present and will poison the catalyst (Banks and Bailey, 1964). Figure 2.6 shows schematically the glass column set-up used for the olefin purification.

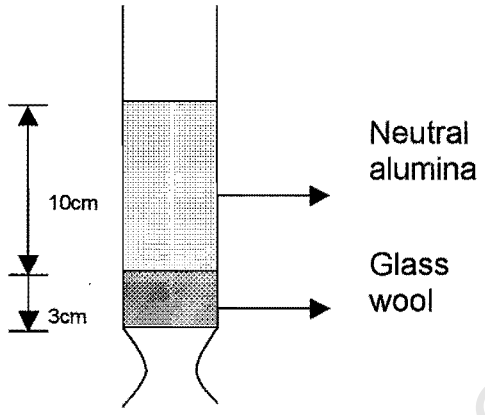

Figure 2.6: The column set-up to purify the 1-octene feed

All gas flow rates are reported at standard conditions (i.e. 0 °C and 1 bar)

2.3.1 Reactor Set-up

The reactor set-up (see Figure 2.7) can be divided into the feed section, the reactor, and the product recovery and analysis section.

The Feed Section

Feed pot – Contains the liquid feed (1-octene) which was pumped via the high-pressure pump (HPLC) into the reactor.

XCV 02-This non-return valve protects the pump from any liquid returning to the pump.

The Reactor Section

The temperature inside the fixed bed reactor was controlled with the following electrical elements:

TE 02A- This element is part of a duplex thermocouple, which is situated inside the reactor and is directly connected to a temperature indicator control (TIC 02). The temperature inside the reactor is controlled from this point (TIC 02).

TE 02B- This element is part of a duplex thermocouple, which is situated inside the reactor and is directly connected to the TSHH 02 (Trip amplifier). As soon as the temperature inside the reactor rises above the trip temperature (600 °C) this information relayed to the TSHH 02, which causes the power to be switched off.

TI 01- A thermocouple situated between the reactor and the reactor jacket. The design temperature for the thermocouple is set between 0-600 °C. As soon as the temperature on the outside of the reactor reaches 600 °C the power would then trip.

TSHH 02- This is the "Temperature Switch High High" and acts as a temperature trip.

I/E- Denotes a Current (4-20 mA) to Voltage converter. This is the instrumentation to the electrical interface and is used to show the instrument control of a heating element.

Any pressure increase inside the reactor system would be noticeable on the pressure indicator (PI & PI 02). The water seal acts as a safety precaution in case of a pressure build up. The excess pressure would be released into the water seal.

Product recovery and analysis

The gas and liquid product flowed directly from the reactor into a knockout pot. The liquid product was drained by opening the two hand valves (HV 02 & 03). An additional knockout pot was installed to accommodate excess amount of product that might form. This liquid product was weighed and injected into the GC (see section 2.3.2.1). The gas product flows to the gas sampling loop and a gas sample were taken with a syringe. This gas sample was injected into the GC for hydrocarbon analysis (see section 2.3.2.2). The gas could either flow directly into the glass gas bomb or it could by-pass the glass gas bomb by directing the valve (HV 05) away from the glass bomb. In the latter case, the valve (HV 06) has to be closed in order to avoid circular flow in the loop. The volume of gas formed was monitored via the wet gas flow meter.

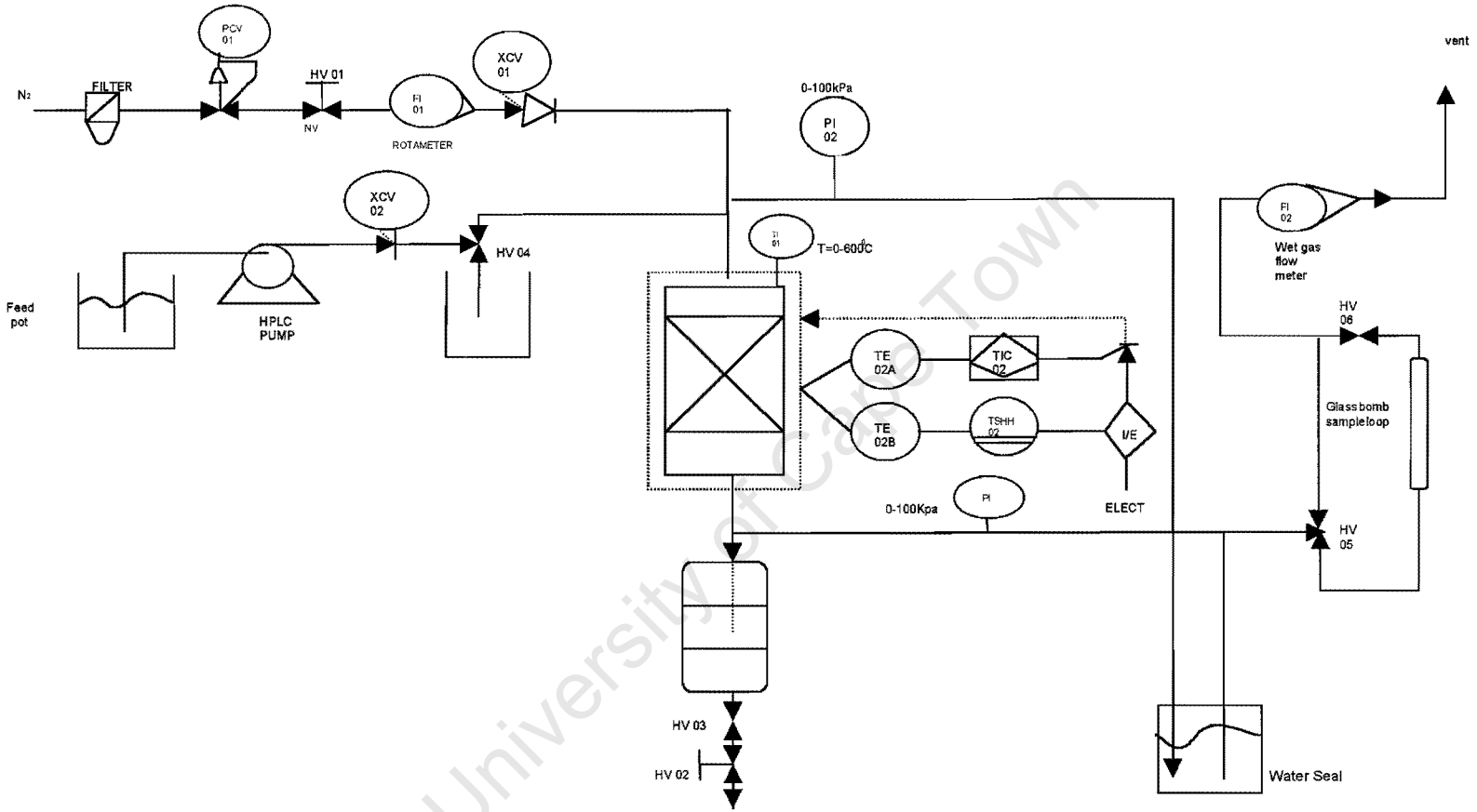

Figure 2.7: Schematic representation of the reactor set-up

2.3.1.1 Start-up Procedure for the Reactor

The plug flow reactor was loaded with 3 ml (2.8 g) of MoO_3/Al_2O_3 catalyst. Nitrogen was allowed to pass over the catalyst. The N_2 gas flow was set to 4 bar on the regulator and the flow was set to 25 ml/min on the Rotameter (FI 01). After 10 min, the temperature on the temperature control unit (TIC 02) was set to 550 °C with a heating rate of 4 °C/min. The system was left heating up and kept at 550 °C for 16 h. The system was left to cool down to operating temperature (80 °C). The N_2 was switched off before pumping the liquid to the reactor.

The appropriate liquid flow rate of 1-octene feed was set on the HPLC pump to 0.1 ml/min. This is equivalent with a LHSV of 2 h^{-1} or MHSV of 1.53 h^{-1}. Before the HPLC pump was started, the prime setting on the pump was switch on to remove any stagnant liquid in the lines. This was done for approximately 1 min. The hand valve (HV 04) was opened and the pump was started.

2.3.1.2 Sample Collection

Liquid samples

Liquid samples were taken at 30 min intervals. The liquid samples were collected by opening the hand valves HV 02 and HV 03. This product was then weighed. This sample was injected into a GC to monitor the product spectrum. The feed that was pumped into the system was also weighed on a balance placed on the HPLC pump, thus allowing a mass balance.

Gas samples

The product gas produced was constantly monitored using a wet gas flow meter and samples were taken at a central point using a glass gas bomb. A volume of 1ml gas sample was injected into the Gas Chromatogram for product analysis.

2.3.2 Product analysis using Gas Chromatography

2.3.2.1 Analysis of liquid product samples

The liquid samples were analysed using a gas chromatograph (GC) equipped with a flame ionisation detector (FID). The analysis conditions are given in Table 2.2. A typical GC-trace of a liquid product spectrum is given in Figure 2.8.

Table 2.2: Conditions for gas-chromatographic analysis of liquid samples

Injector	Split-injector
$T_{injector}$	250 °C
Head pressure	180 kPa(g)
Split ratio	1:100
Carrier gas	N_2 (80 ml/min)
Column	HP-PONA (l= 50 m; d= 0.2 mm; d_f= 0.5 μm)
Temperature program	Initial: 50 °C
	Hold: 2 min
	Heating rate: 12 °C/min
	Final: 270 °C
	Hold: 10 min
Detector	FID
$T_{detector}$	300 °C
Fuel gas	H_2: 40 ml/min
Air	400 ml/min
Make-up	N_2: 25 ml/min

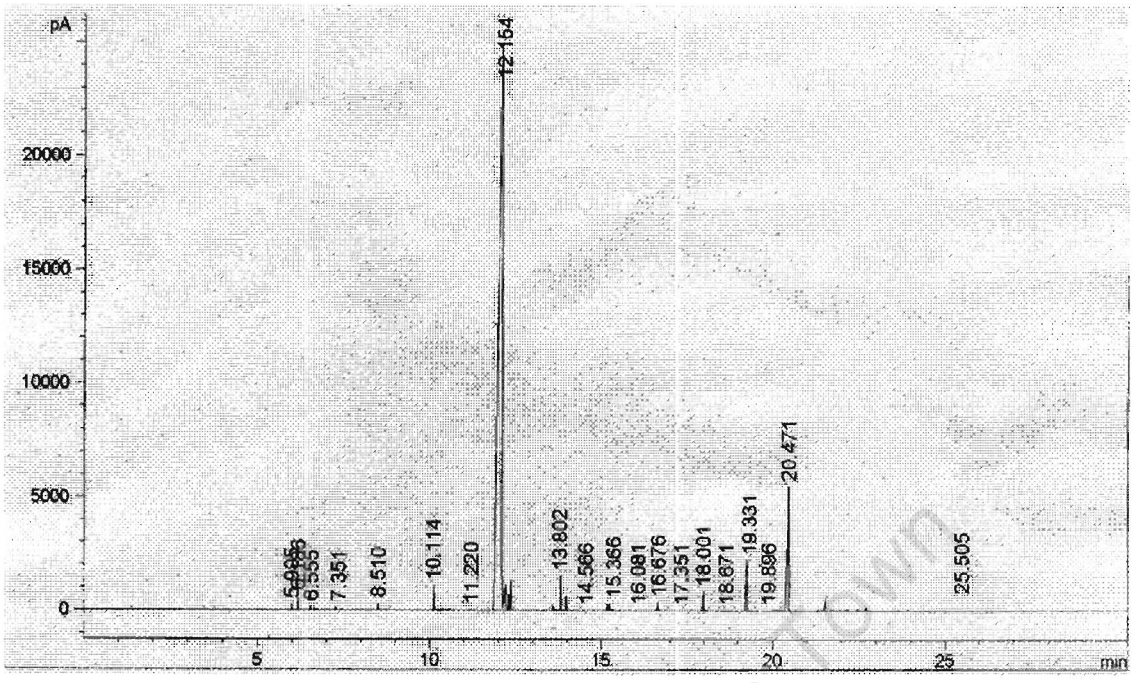

Figure 2.8: GC trace of the liquid product (Peak identification is given in Table 2.3)

Table 2.3: Retenticn times of compounds in the liquid product sample (analysis conditions are given in Table 2.2)

Product compound	Retention time (min)	Product compound	Retention time (min)
Ethylene	5.995	Linear C_{10}	15.366
Propylene	6.186	Branched C_{11}	16.081
C_4 isomers	6.555	Linear C_{11}	16.676
C_5 isomers	7.351	Branched C_{12}	17.351
Branched C_7	8.510	Linear C_{12}	18.001
Linear C_7	10.114	Branched C_{13}	18.671
Branched C_8	11.220	Linear C_{13}	19.331
Linear C_8	12.154	Branched C_{14}	19.896
Linear C_9	13.802	Linear C_{14}[1]	20.471

[1] primary metathesis product

2.3.2.2 Analysis of gaseous product samples

The gaseous samples were analysed using a gas chromatograph (GC) equipped with a flame ionisation detector (FID). The analysis conditions are given in Table 2.4. A typical GC-trace of a sample of the gaseous product stream is given in Figure 2.9.

Table 2.2: Conditions for gas-chromatographic analysis of liquid samples

Injector	Split-injector
$T_{injector}$	220 °C
Head pressure	30 kPa(g)
Split ratio	1:5
Carrier gas	N_2 (20 ml/min)
Column	HP-PLOT Al_2O_3 "S" deactivated, capillary column (l= 50 m; d= 0.53 mm; d_f= 15 μm)
Temperature program	Initial: 50 °C Hold: 2 min Heating rate: 10 °C/min Final: 180 °C Hold: 10 min
Detector	FID
$T_{detector}$	300 °C
Fuel gas	H_2: 40 ml/min
Air	400 ml/min
Make-up	N_2: 25 ml/min

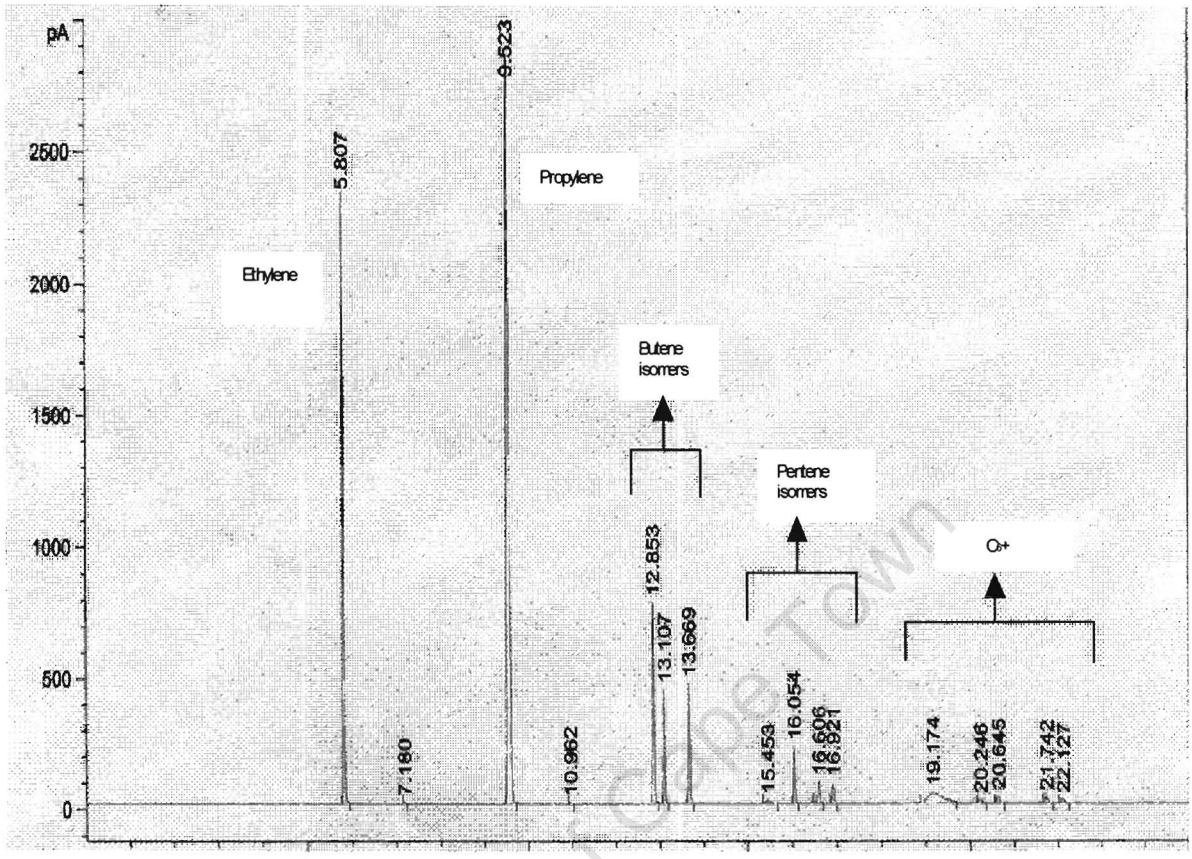

Figure 2.9: Typical GC trace of the gaseous product sample

2.3.3 Data evaluation

The amount of 1-octene converted was calculated on the basis of the mass of feed pumped ($\dot{m}_{feed}$) in and the mass of 1-octene collected as a liquid. The liquid was collected over a period of time hence the product mass flow rate ($\dot{m}_{product}$) can be determined. The mass fraction of 1-octene ($w_{1\text{-octene}}$) in these samples can be easily determined from the GC analysis.

$$w_{1-octene,\,liquid\,sample} = \left(\frac{A_{1-octene}}{\sum_i A_i} \right) \cdot 100\%\ \text{wt.-\%}$$

with $A_{1\text{-octene}}$: peak area of 1-octene in GC-trace of liquid sample

ΣA_i: sum of all peak areas in GC-trace of liquid sample

Thus, the conversion can be determined from:

$$X_{1-octene} = 100\left(1 - \frac{w_{1-octene} \cdot \dot{m}_{product}}{\dot{m}_{feed}}\right) wt.-\%$$

The yield of the various product compounds (or carbon number fraction) can be determined in a similar manner from the GC-trace of the liquid sample, since the weight fraction of a component in the liquid sample (w_i) is given by:

$$w_i = \left(\frac{A_i}{\sum_i A_i}\right) \cdot 100\%$$

Hence the yield for a given component (Y_i) is given by:

$$Y_i = 100\left(\frac{w_i \cdot \dot{m}_{product}}{\dot{m}_{feed}}\right) wt.-\%$$

The selectivity for a given component (S_i) is then defined as:

$$S_i = \frac{Y_i}{X_{1-octene}}$$

3 RESULTS

Supported molybdenum catalysts have been reported to be active catalysts for olefin metathesis. In this study a series of supported molybdenum on γ-Al_2O_3 catalysts were prepared, characterized, and tested as catalysts in 1-octene metathesis. The catalysts were differed with respect to molybdenum loading and the method of preparation (see Table 3.1).

3.1 Elemental analysis

The molybdenum content of the catalyst samples was determined using ICP-AAS (see Table 3.1). The catalyst prepared with the new slurry impregnation method (Zdrazil, 2001) shows within the error of analysis the correct amount of molybdenum. The catalysts prepared using the controlled adsorption technique all show a slightly lower amount of MoO_3 on the support, γ-Al_2O_3, than intended. It can be concluded that during the controlled adsorption not all molybdenum in the solution is taken up by the support.

Table 3.1: Method of preparation of MoO_3/γ-Al_2O_3-catalysts and the MoO_3-content in weight-% (in brackets the intended MoO_3-content)

Catalysts used	Preparation method	MoO_3-content (wt.-%)
0.1 g MoO_3/Al_2O_3 (NSI)	New slurry impregnation	9.6 (9.5)
0.1 g MoO_3/Al_2O_3 (CA)	Controlled adsorption	8.3 (9.1)
0.2 g MoO_3/Al_2O_3 (CA)	Controlled adsorption	16.5 (16.7)
0.3 g MoO_3/Al_2O_3 (CA)	Controlled adsorption	22.8 (23.1)
0.4 g MoO_3/Al_2O_3 (CA)	Controlled adsorption	27.2 (28.6)
0.5 g MoO_3/Al_2O_3 (CA)	Controlled adsorption	32.7 (33.3)

3.2 Structural analysis

3.2.1 XRD-analysis

The crystal phases present within the catalyst samples were analysed using X-ray diffraction (XRD). The XRD-spectrums are shown in Figure 3.1 and the detected crystal phases in the various catalysts are listed in Table 3.2.

The obtained XRD-patterns are similar to those reported by Okamoto et al. (1998). The catalysts with the lowest loading (0.1 g MoO_3/Al_2O_3 (CA)) (both the fresh and the spent catalyst) only show diffraction peaks attributable to γ-Al_2O_3. The catalyst prepared according to the new slurry impregnation method shows an additional diffraction peak at $2\Theta = 21^\circ$, which was initially believed to be that of MoO_3. Further investigation into the spectrum does not confirm the MoO_3 phase, due to superpositioning with the γ-Al_2O_3 diffraction peaks at $2\Theta = 23^\circ$. The catalysts with a higher molybdenum loading show the formation of $Al_2(MoO_4)_3$, although the amount of aluminium molybdate is rather small in the catalyst 0.2 g MoO_3/Al_2O_3 phases are present. The narrow shape of the diffraction peaks attributable to aluminium molybdate shows that large aluminium molybdate crystals are being formed.

Table 3.2: Crystal phases detected on the various catalysts by XRD

Catalyst sample	Phase detected
0.1 g MoO_3/Al_2O_3 (CA)	γ-Al_2O_3
0.1 g MoO_3/Al_2O_3 (CA) – spent	γ-Al_2O_3
0.1 g MoO_3/Al_2O_3 (NSI)	γ-Al_2O_3
0.2 g MoO_3/Al_2O_3 (CA)	γ-Al_2O_3 Aluminiummolybdate:$Al_2(MoO_4)_3$
0.3 g MoO_3/Al_2O_3 (CA)	γ-Al_2O_3 Aluminiummolybdate:$Al_2(MoO_4)_3$
0.4 g MoO_3/Al_2O_3 (CA)	γ-Al_2O_3 Aluminiummolybdate:$Al_2(MoO_4)_3$
0.5 g MoO_3/Al_2O_3 (CA)	γ-Al_2O_3 Aluminiummolybdate:$Al_2(MoO_4)_3$

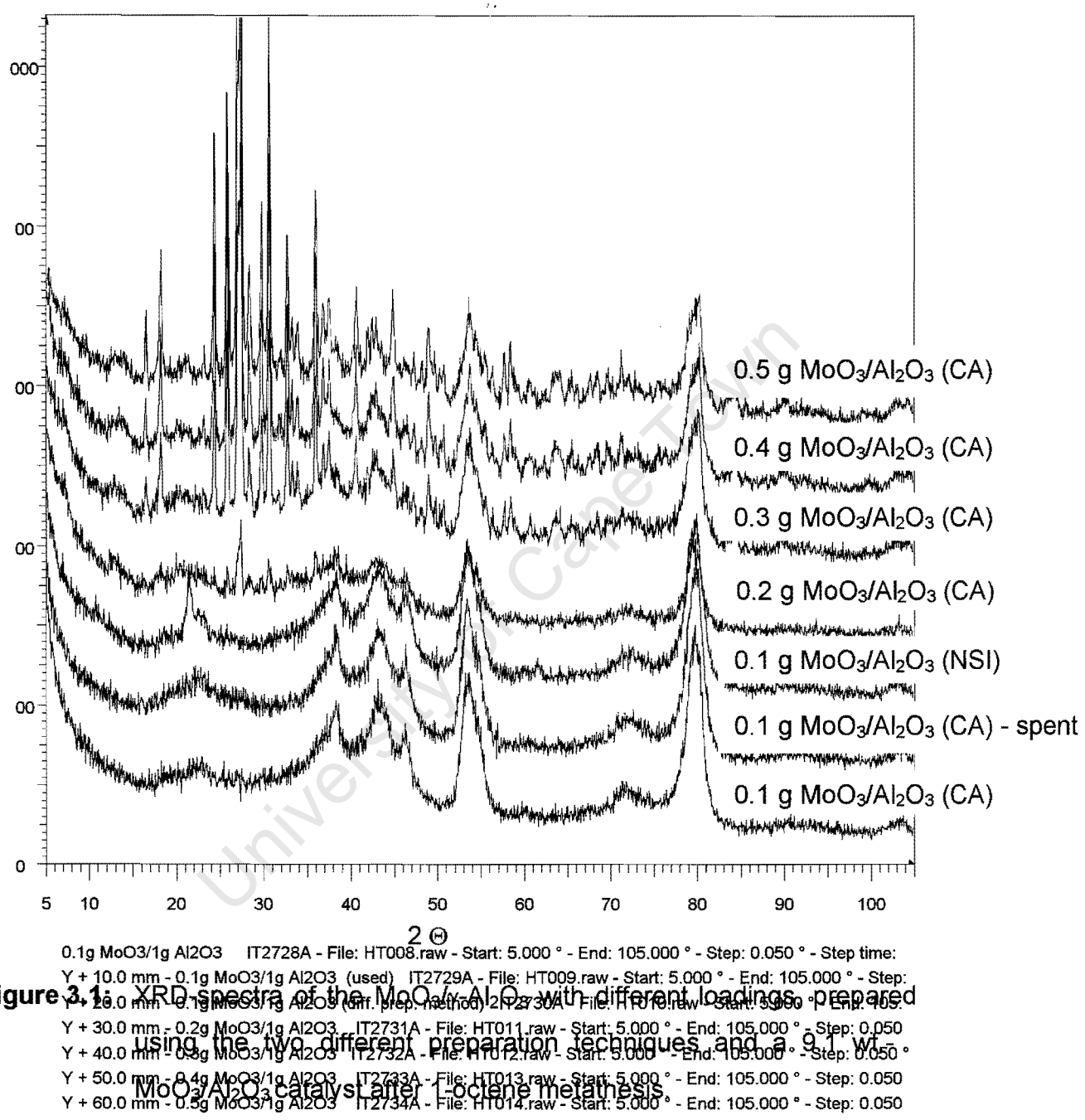

Figure 3.1: XRD spectra of the MoO_3/γ-Al_2O_3 with different loadings prepared using the two different preparation techniques and a 9:1 wt.- MoO_3/Al_2O_3 catalyst after 1-octene metathesis.

3.2.2 Transmission Electron Spectroscopy

Figure 3.2 shows the TEM-images of the catalysts prepared by the controlled adsorption technique. From the TEM images it can be seen that the big crystal-like structure becomes more prominent as the catalyst loading increases. The

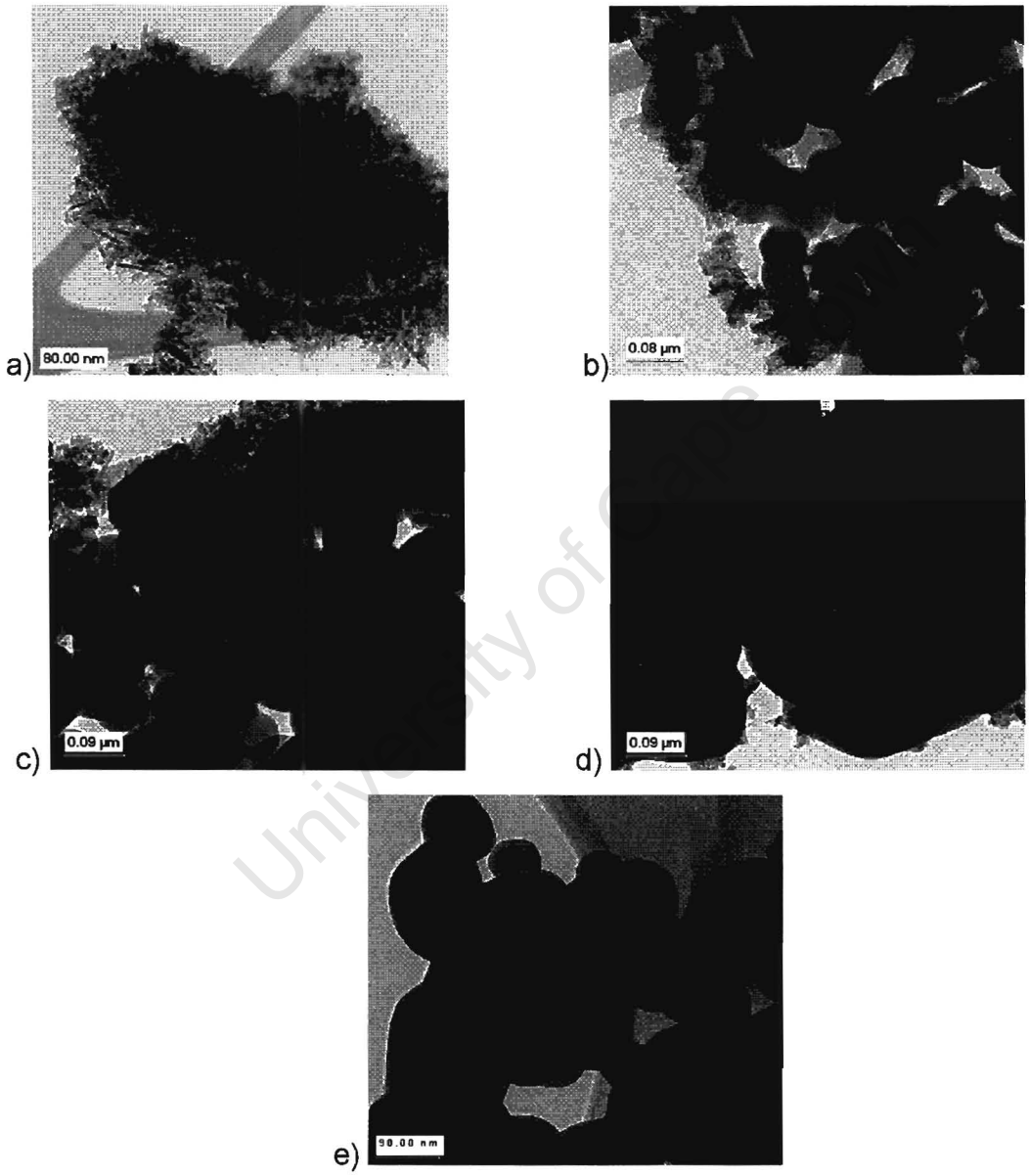

Figure 3.2: TEM micrographs of a) 0.1 g MoO_3/ Al_2O_3 (CA); b) 0.2 g MoO_3/ Al_2O_3 (CA); c) 0.3 g MoO_3/ Al_2O_3 (CA); d) 0.4 g MoO_3/ Al_2O_3 (CA); e) 0.5 g MoO_3/ Al_2O_3 (CA)

catalyst with the lowest loading, 9.1 wt.-%MoO_3/Al_2O_3, is the only catalyst where large crystallites are absent.

3.3 Surface area and metal dispersion

3.3.1 BET surface area

The BET-surface area of the freshly prepared MoO_3/g-Al_2O_3 catalysts was determined (see Table 3.3 and Figure 3.3). The support material has a surface area of 145 m^2/g and a pore volume of 0.47 cm^3/g. Thus, an average pore diameter of 12.9 nm can be deduced. The obtained surface area and pore volume are in close agreement with those supplied by producer of the support (150 m^2/g and 0.461 cm^3/g, respectively).

Table 3.3: BET-surface area, pore volume and average pore diameter of the support (γ-Al_2O_3) and the various MoO_3/Al_2O_3 catalysts

Catalyst	S_{BET} m^2/g	V_{Pore} cm^3/g	d_{pore} nm
γ-Al_2O_3	145	0.47	12.9
0.1 g MoO_3/Al_2O_3 (NSI)	152	0.39	10.5
0.1 g MoO_3/Al_2O_3 (CA)	143	0.42	11.8
0.2 g MoO_3/Al_2O_3 (CA)	128	0.37	11.5
0.3 g MoO_3/Al_2O_3 (CA)	116	0.33	11.6
0.4 g MoO_3/Al_2O_3 (CA)	97	0.29	12.1
0.5 g MoO_3/Al_2O_3 (CA)	87	0.26	12.2

At a loading of 0.1 g MoO_3 per gram of Al_2O_3, the BET-surface area is essentially the same with a small decrease in the pore volume. There appears to be a linear relationship between pore volume and the MoO_3-loading for catalyst prepared using the controlled adsorption method. This might be attributed to the formation of large aluminium molybdate crystals (see chapter 3.2).

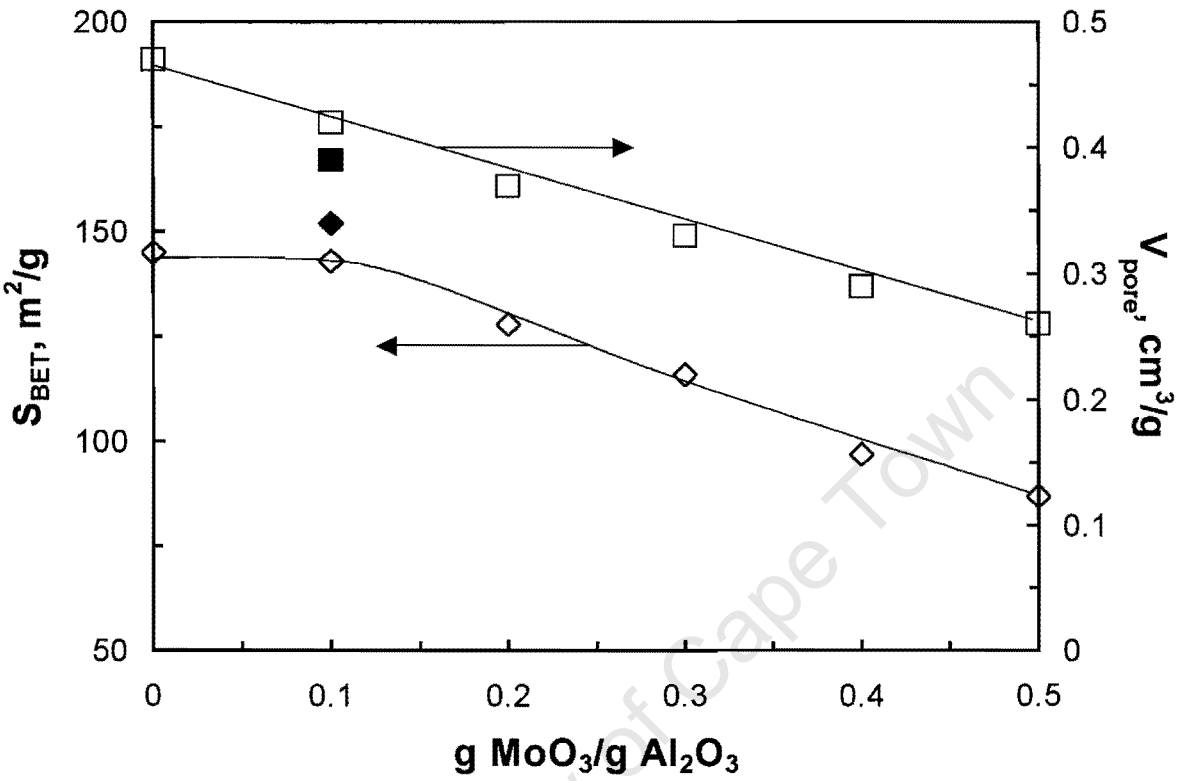

Figure 3.3: Relationship between BET-surface area, pore volume and MoO_3-loading (filled symbols: catalyst prepared using new slurry impregnation method; open symbols: catalyst prepared using controlled adsorption technique)

3.3.2 Metal dispersion by CO-chemisorption

CO can coordinate to surface-Mo-species. The CO-uptake is thus a measure for the number of molybdenum atoms at the surface (metal dispersion). The CO-uptake for the various freshly prepared catalysts is shown in Table 3.4. The CO consumption for the 0.1 g MoO_3/Al_2O_3 (CA) and 0.1 g MoO_3/Al_2O_3 (NSI) is comparable. With increasing Mo-loading, the CO-uptake increases. The CO-uptake per molybdenum atom present in the catalyst decreases, indicating a decrease in metal dispersion.

Table 3.4: Metal dispersion of the metathesis catalyst

CATALYST	CO-consumption(cm^3/g)
0.1 g MoO_3/Al_2O_3 (NSI)	2.0 / 9.6
0.1 g MoO_3/Al_2O_3 (CA)	1.9 / 8.3
0.2 g MoO_3/Al_2O_3 (CA)	2.3 / 16.5
0.3 g MoO_3/Al_2O_3 (CA)	3.4 / 22.8
0.4 g MoO_3/Al_2O_3 (CA)	3.8 / 27.2
0.5 g MoO_3/Al_2O_3 (CA)	4.3 / 32.7

3.4 Reducibility as determined by Temperature Programmed Reduction

The reducibility of two of the catalyst samples was investigated by means of temperature programmed reduction (TPR), viz. 0.1 g MoO_3/Al_2O_3 (CA) and 0.5 g MoO_3/Al_2O_3 (CA). The TPR-profiles are shown in Figure 3.4. The catalyst 0.1 g MoO_3/Al_2O_3 (CA) showed one region that is reduced at 420 °C. For the catalyst with the highest loading, 0.5 g MoO_3/Al_2O_3 (CA), there are two regions of reduction. The first reduction step appears at 400 °C. The second reduction step appears between 560 °C –570 °C. It appears that the H_2 consumption for the second reduction step is ca. 4-5 times greater than that for the first reduction step. The first reduction step might be attributed to a surface reduction of Mo^{6+} to Mo^{5+}. The second reduction step might be associated with a reductive decomposition of bulk aluminium molybdate.

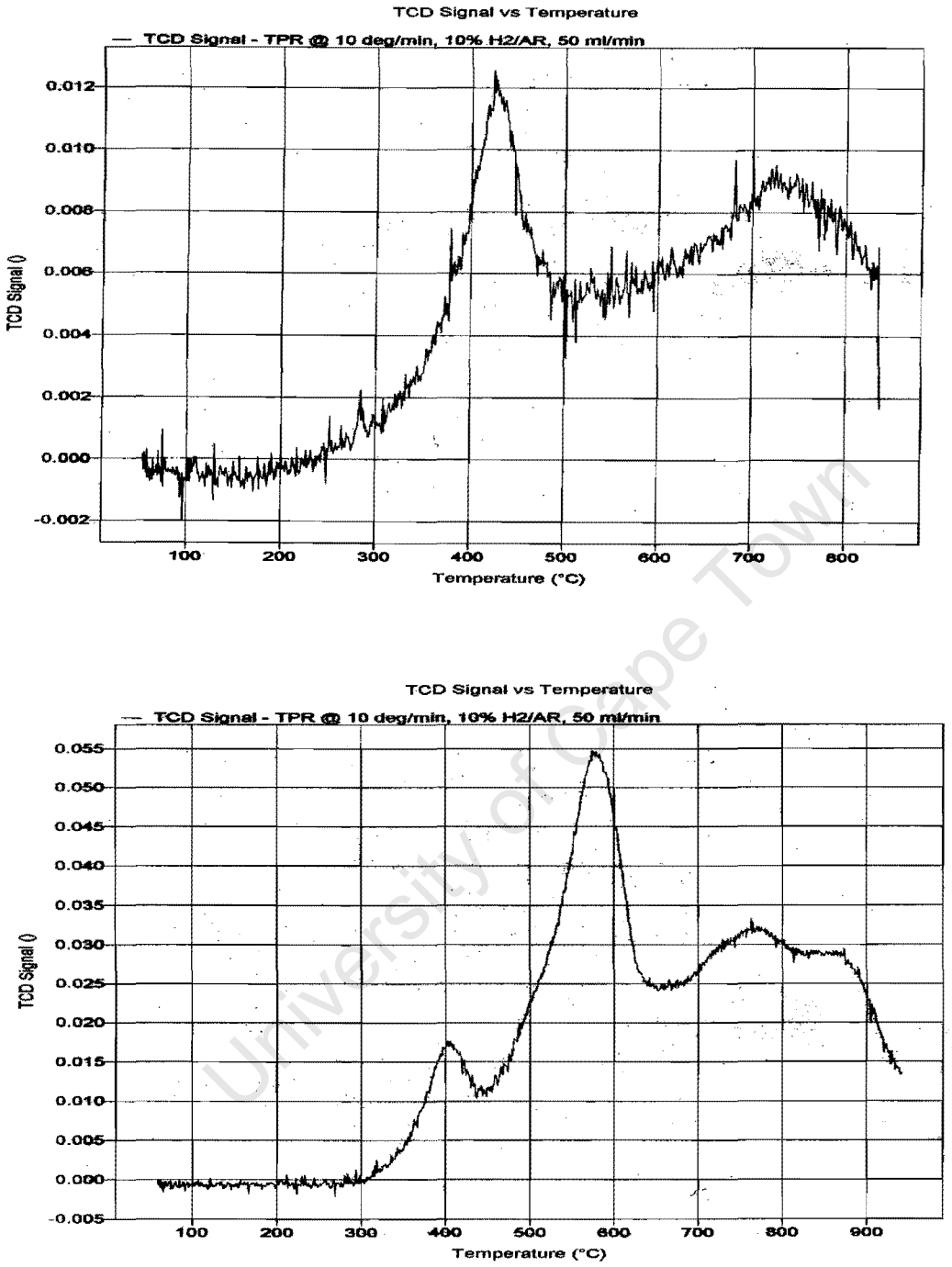

Figure 3.4: TPR profile of the MoO_3/Al_2O_3 catalysts prepared by controlled adsorption

Top: 0.1 g MoO_3/Al_2O_3 (CA)

Bottom: 0.5 g MoO_3/Al_2O_3 (CA)

3.5 Acidity determined by FTIR-Pyridine adsorption

The number of acid sites and the type of acid sites (Lewis or Brønsted acidity) were determined using pyridine adsorption. For these measurements, the same amount of catalyst (10 mg) was used each time. Hence, the intensity of the adsorption bands corresponds directly to the number of acid sites.

The results show that all the samples contain both the Lewis and the Brønsted acid sites with the Lewis acid site being predominant (see Figure 3.5). An increase in acidity was observed with an increase in the mass of MoO_3. This was observed up to a mass of 0.4 g MoO_3/Al_2O_3 thereafter, the Lewis acidity decreased. The observed increase in acidity with the increase in the MoO_3 loading is consistent with the literature observations (Rajagopal, 1995).

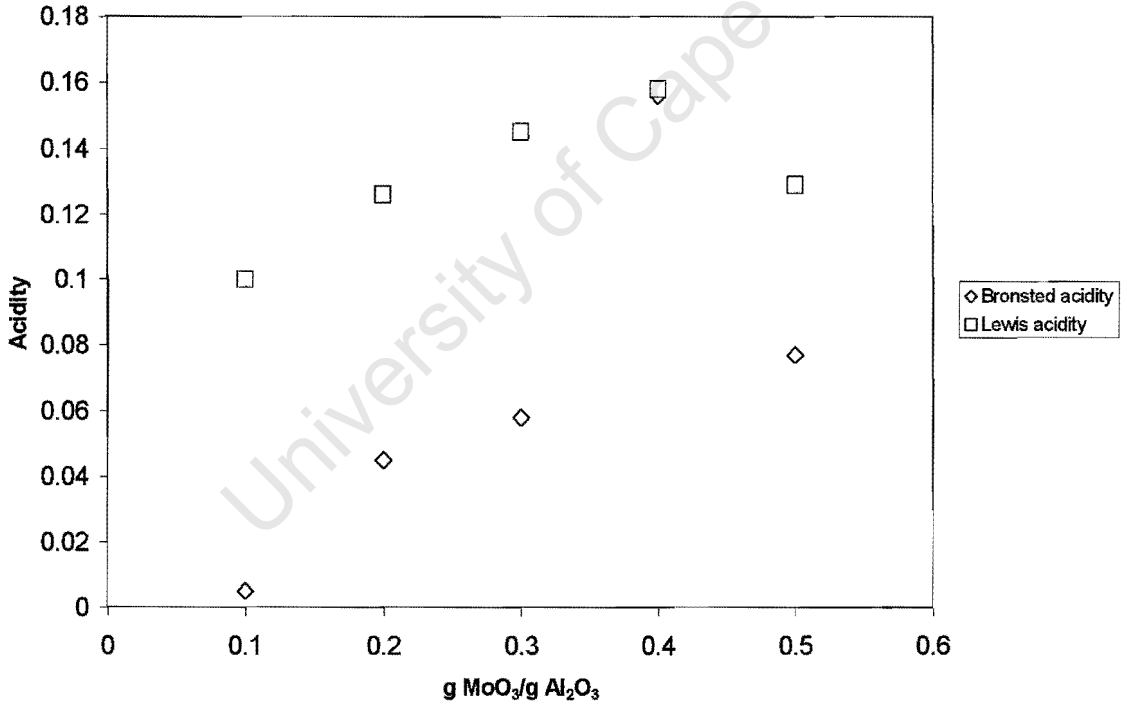

Figure 3.5: Lewis and Brønsted acidity as a function of the MoO_3-loading for the catalyst prepared by controlled adsorption.

3.6 Raman spectroscopy studies

3.6.1 Room temperature experiments

The room temperature Raman spectrums of the precursor (ammonium heptamolybdate) and the prepared catalysts are given in Figures 3.6 – 3.15.

In the spectrum of ammonium heptamolybdate (Wang and Hall, 1982) and (Kim et al., 1992) (see Figure 3.6) the following bands are observed: the symmetric Mo=O stretching frequency at 936 cm^{-1}, the asymmetric Mo=O stretching frequency at 880 cm^{-1}, the Mo=O bending mode at 363 cm^{-1} and the Mo-O-Mo bending mode at 220 cm^{-1} (Wang and Hall, 1982) and (Kim et al., 1992).

Figure 3.7 shows the Raman spectrum of the catalyst 0.1 g MoO_3/Al_2O_3 prepared using controlled adsorption technique. The peak appearing at 961 cm^{-1} in this spectrum is that of the symmetric Mo=O stretching vibration. The shoulder band appearing at 857 cm^{-1} is that of the asymmetric Mo=O stretching vibration. The stretching mode of the Mo-O-Mo bond at 557 cm^{-1} confirms the presence of a polymeric structure. The band appearing at 370 cm^{-1} and 219 cm^{-1} is that of the Mo=O bending mode and Mo-O-Mo bending mode, respectively.

The Raman spectrum of the catalyst 0.1 g MoO_3/Al_2O_3 prepared using the new slurry impregnation method (see Figure 3.8) compares well with corresponds well with the catalyst prepared via the controlled adsorption method. The only difference is the absence of the shoulder band at 857 cm^{-1}(asymmetric Mo=O stretching vibration) in the spectrum of the catalyst prepared using the new slurry impregnation technique.

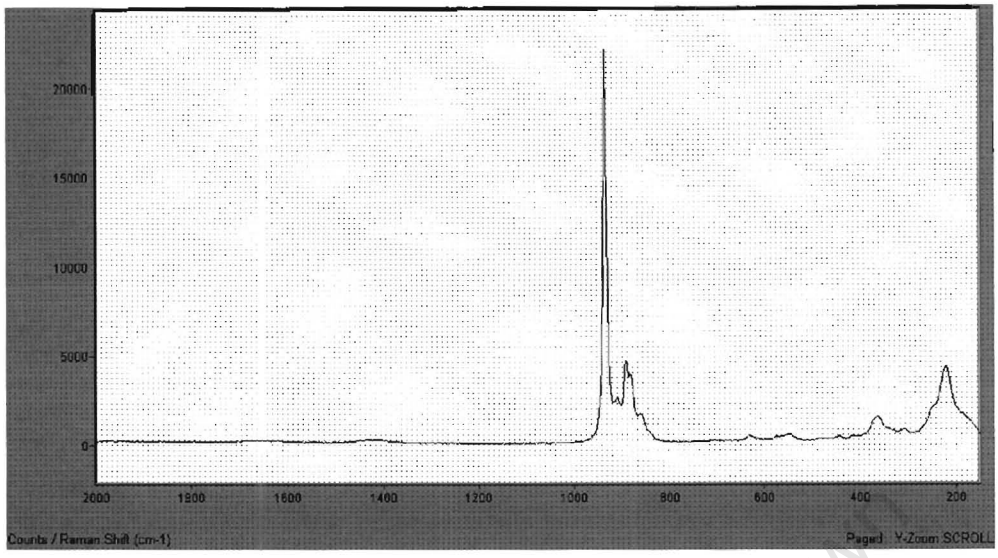

Figure 3.6: Room temperature Raman spectrum of ammonium heptamolybdate, which was used as a precursor for the catalysts prepared using controlled adsorption technique

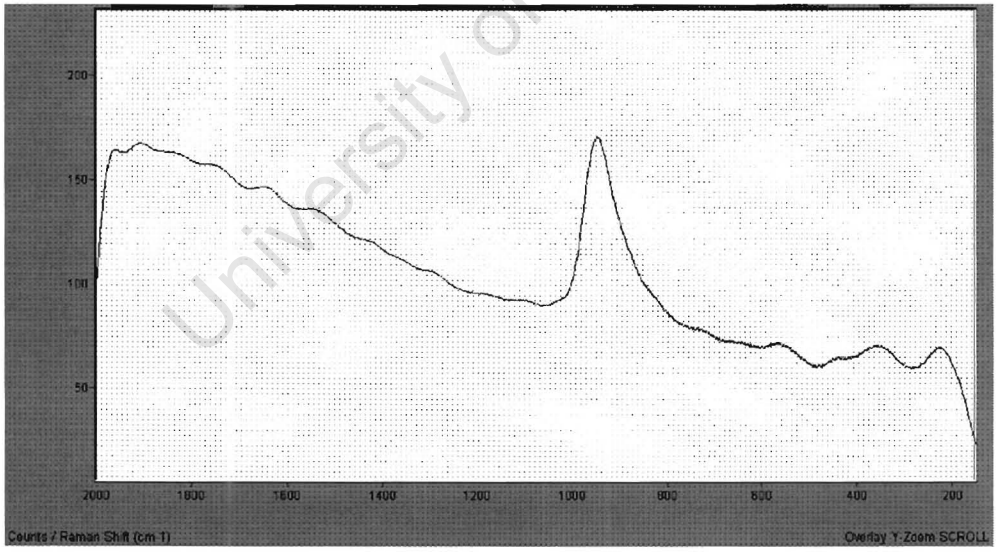

Figure 3.7: Room temperature Raman spectrum of the catalyst 0.1 g MoO_3/Al_2O_3 (CA) prepared using controlled adsorption technique

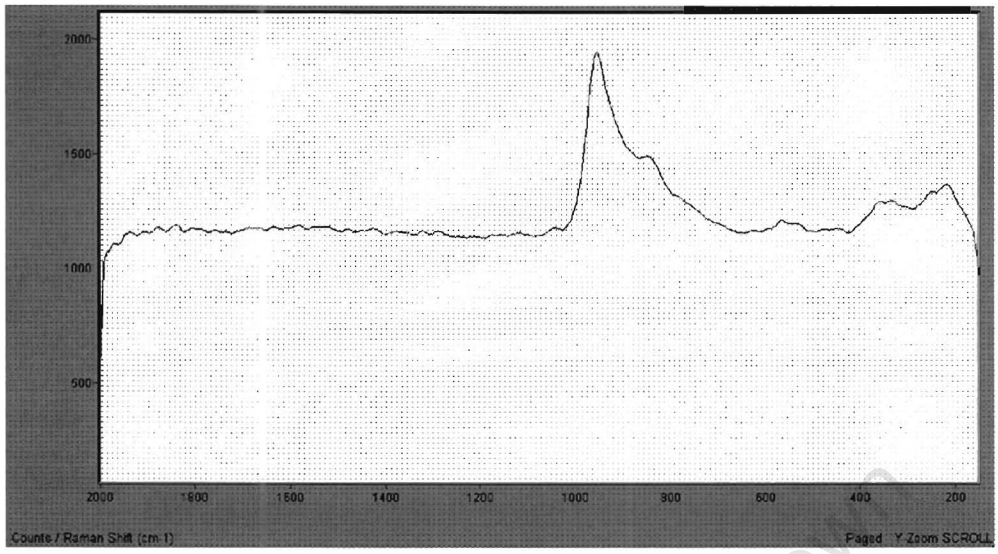

Figure 3.8: Room temperature Raman spectrum of the catalyst 0.1 g MoO_3/Al_2O_3 (NSI) prepared by the new slurry impregnation method

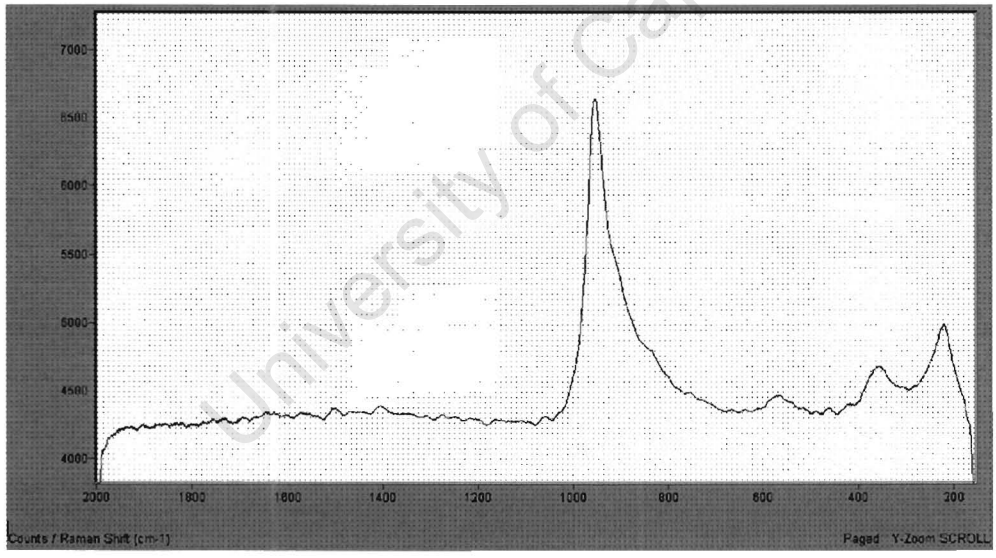

Figure 3.9: Room temperature Raman spectrum of the catalyst 0.2 g MoO_3/Al_2O_3 (CA) prepared using controlled adsorption technique

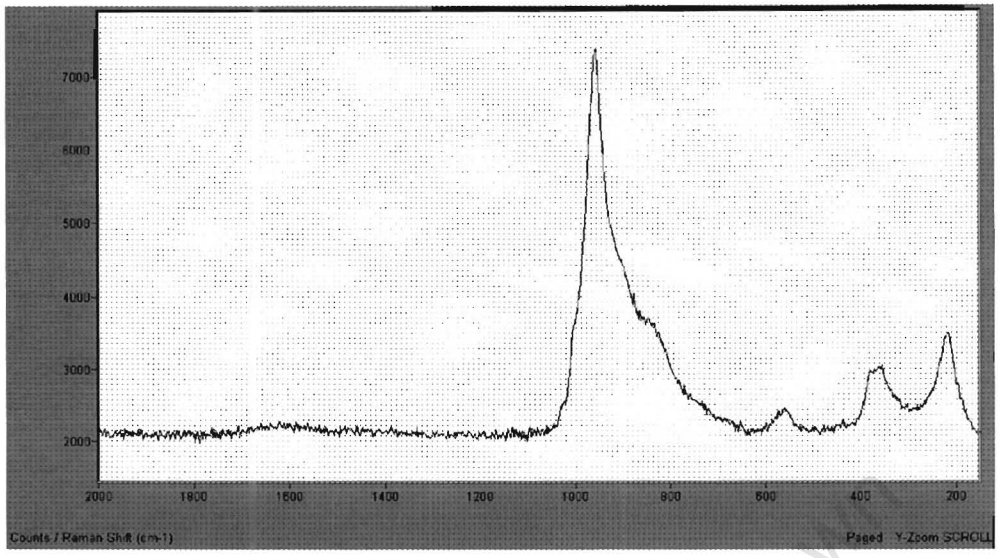

Figure 3.10: Room temperature Raman spectrum of the catalyst 0.3 g MoO_3/Ai_2O_3 (CA) prepared using controlled adsorption technique

In Raman spectrums of the catalysts 0.2 g MoO_3/Al_2O_3 (CA) (see Figure 3.9) and 0.3 g MoO_3/Al_2O_3 (CA) (see Figure 3.10) the following peaks (Wang and Hall, 1982) and (Kim et al., 1992) were observed: The symmetric Mo=O stretching frequency appearing at 954 cm^{-1}. The shoulder band at 841 cm^{-1} is that of the asymmetric Mo=O stretching frequency. The small band appearing at 557 cm^{-1} is attributed to the Mo-O-Mo stretching mode of the polymeric backbone. The bands appearing at 367 and 216 cm^{-1} are attributed to the Mo=O bending mode and Mo-O-Mo bending mode, respectively.

In the Raman spectrum of the catalyst 0.4 g MoO_3/Al_2O_3 (CA) (see Figure 3.11) shows a typical spectrum of the $Al_2(MoO_4)_3$ phase (Medema et al.,1978) that is present in the higher loading. This is also present in the Raman spectrum of the catalyst 0.5 g MoO_3/Al_2O_3 (CA) (see Figures 3.12 – 3.15). At this high molybdenum loading the catalyst is inhomogeneous. The vibrational modes of the crystalline phase present in the catalyst 0.5 g MoO_3/Al_2O_3 (CA) are given in Table 3.5.

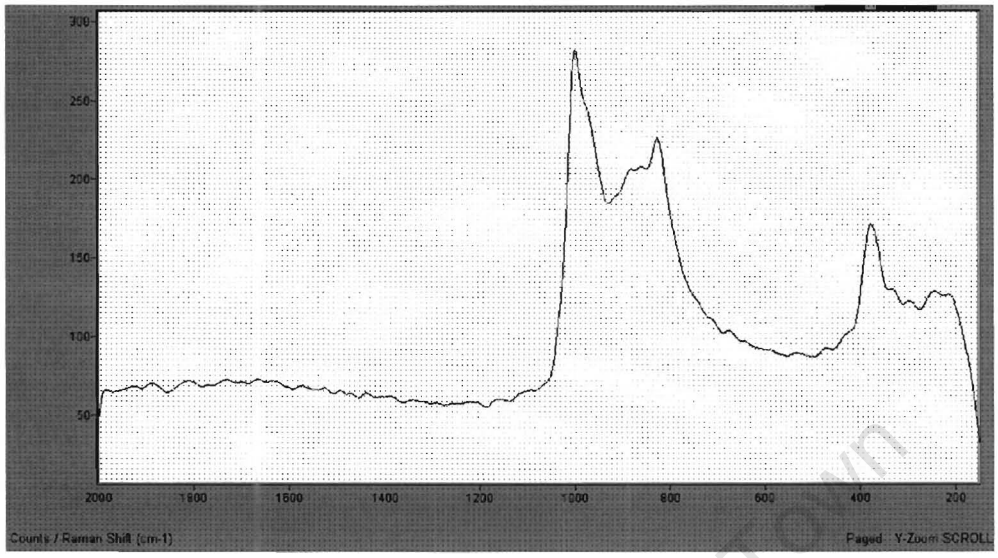

Figure 3.11: Room temperature Raman spectrum of the catalyst 0.4 g MoO_3/Al_2O_3 (CA) prepared using controlled adsorption technique

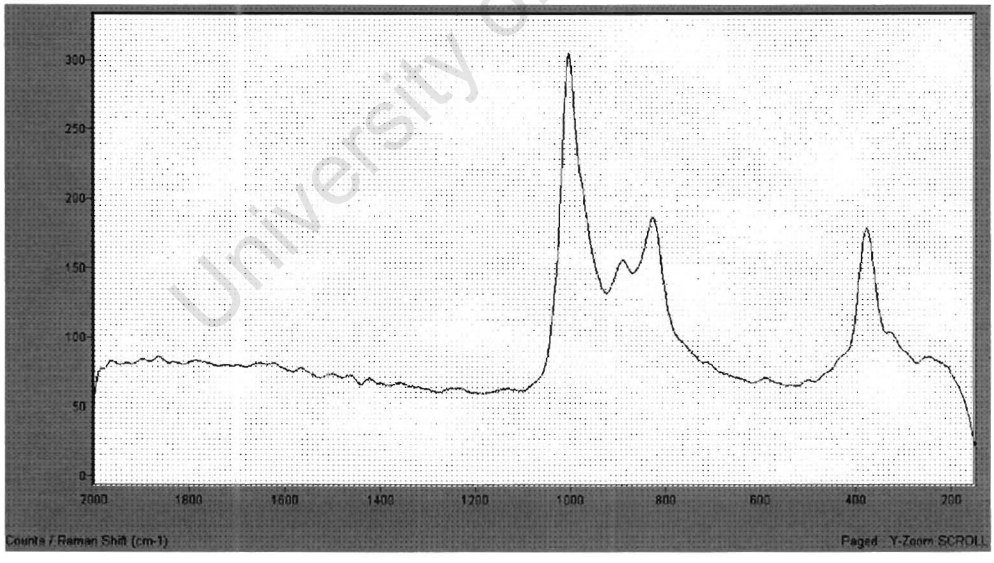

Figure 3.12: Room temperature Raman spectrum of the catalyst 0.5 g MoO_3/Al_2O_3 (CA) prepared using controlled adsorption technique

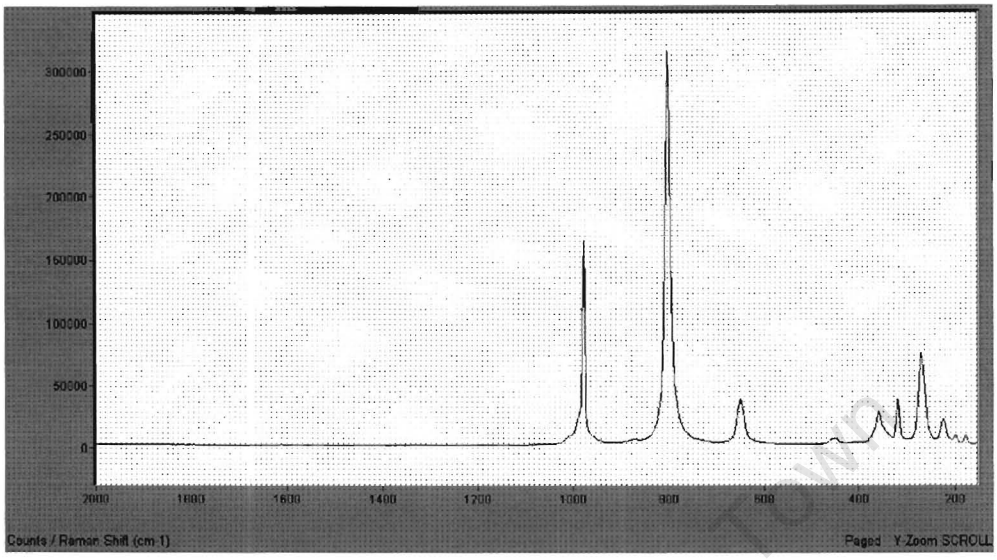

Figure 3.13: Room temperature Raman spectrum of the crystalline phase present in catalyst 0.5 g MoO_3/Al_2O_3 (CA) prepared using controlled adsorption technique

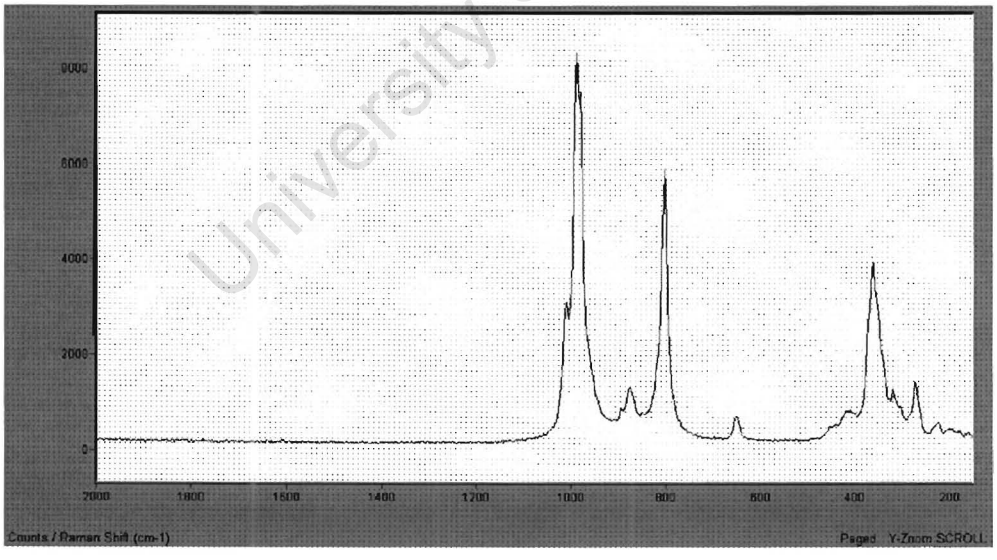

Figure 3.14: Room temperature Raman spectrum of a particle present in catalyst 0.5 g MoO_3/Al_2O_3 (CA) prepared using controlled adsorption technique

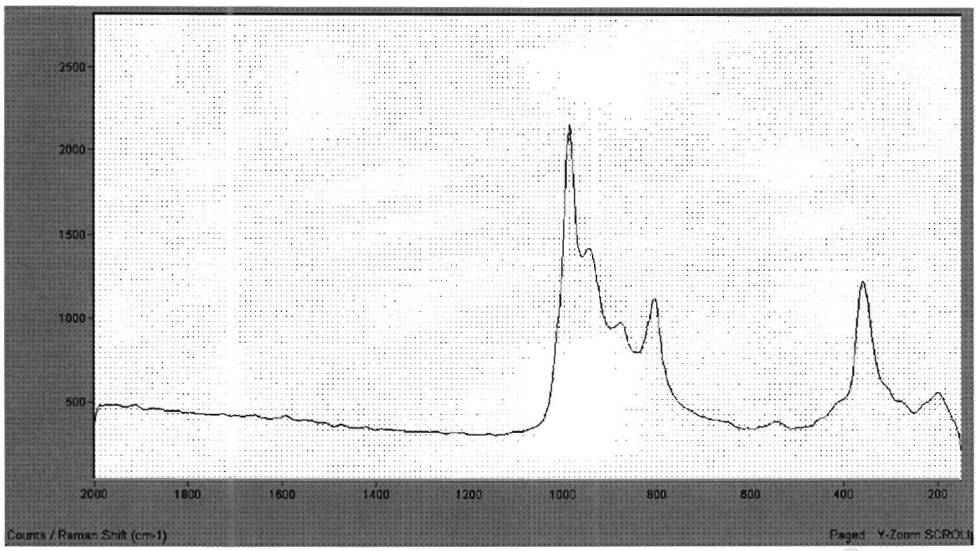

Figure 3.15: Room temperature Raman spectrum of a particle present in catalyst 0.5 g MoO_3/Al_2O_3 (CA) prepared using controlled adsorption technique

Table 3.5: Vibrational modes of the crystalline phase present in catalyst 0.5 g MoO_3/Al_2O_3 (CA) prepared using controlled adsorption technique

FREQUENCY (cm^{-1})	VIBRATION
996	ν_s Mo=O stretch
822	ν_{as} Mo=O stretch
667	ν_{as} Mo-O-Mo stretch
473	ν_{as} O-Mo-O stretch&bend
380	ν_{as} O-Mo-O scissor
366	δ O-Mo-O
334	δ O-Mo-O bending
293	δ O=Mo=O wagging
285	δ O=Mo=O wagging
247	τ O=Mo=O twist
216	Rotational MoO_4 chain mode

(Dieterle Martin, 2001)

3.6.2 Mapping Experiments

In order to have an idea of the different surface species that are present on the catalyst mapping experiments was performed on the catalysts calcined in air at 550 °C. Multiple points (8 pts) on each catalyst was selected and a spectrum taken at each point. A certain peak (vibrational mode) can then be mapped at each point chosen. With an increase in the MoO_3-loading the intensity and peak area are expected to increase. From Figure 3.16 it can be seen that an increase in the average peak intensity and area of $(M=O)\upsilon_s$ vibration is indeed observed up to 0.3 g MoO_3/Al_2O_3. Increasing to MoO_3-loading further leads to a decrease in the average peak intensity and area of $(M=O)\upsilon_s$ vibration. This is attributed to the formation of large amounts of $Al_2(MoO_4)_3$ and crystalline MoO_3 with the increase in MoO_3-loading. (The spectrums and the Tables showing the results of the mapping experiments are given in Appendix B)

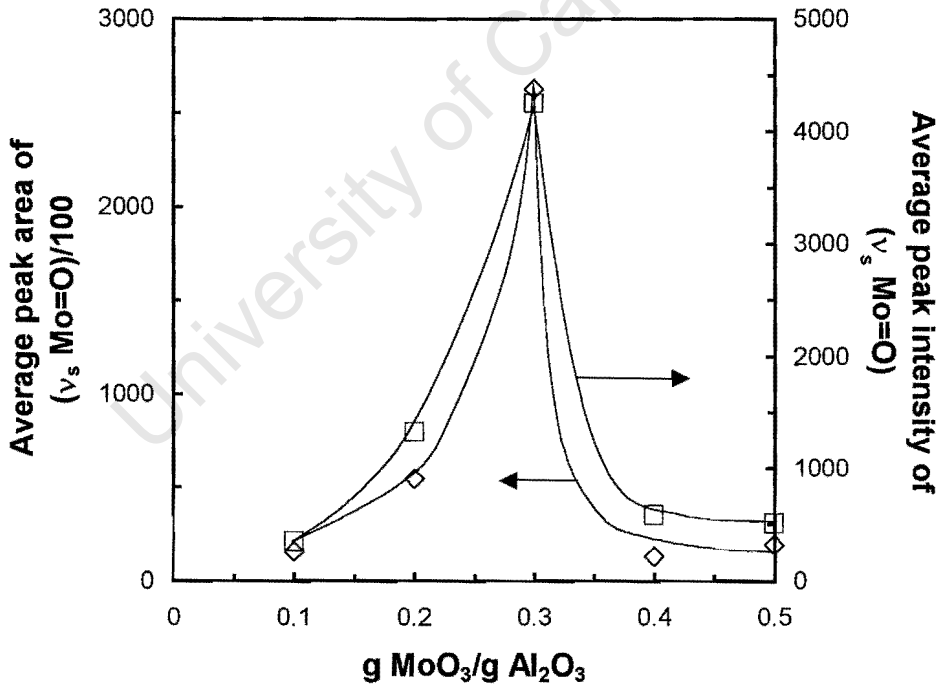

Figure 3.16: Average peak area and peak intensity of ν_s Mo=O vibrational band for the catalysts prepared by controlled adsorption after calcination in air at 550 °C.

3.6.3 In-situ reaction with 1-butene

Prior to the reaction with 1-butene, the catalyst was calcined in air at 550°C. Figure 3.17 shows the Raman spectrum of the calcined catalyst 0.1 g MoO_3/Al_2O_3 (CA). When the calcined catalyst is compared to the fresh 9.1 wt.-%MoO_3/Al_2O_3 (see Figure 3.7) it can be seen that there is a shift to a higher frequency (961→999 cm^{-1}) in the Mo=O stretching vibration. There is also a separation of the shoulder peak (Mo-O-Mo stretching vibration) in the fresh, uncalcined catalyst 0.1 g MoO_3/Al_2O_3 (CA). This shoulder band (864 cm^{-1}) becomes more pronounced in the calcined catalyst.

After the calcination step, the temperature was reduced to 80 °C before the 1-butene was brought into contact with the catalyst. The catalyst was in contact with the 1-butene for 20 min. Within a period of 5 min the formation of carbon peaks (1589 cm^{-1} and 1369 cm^{-1}) appeared, which is attributed to carbonaceous species (see Figure 3.18).

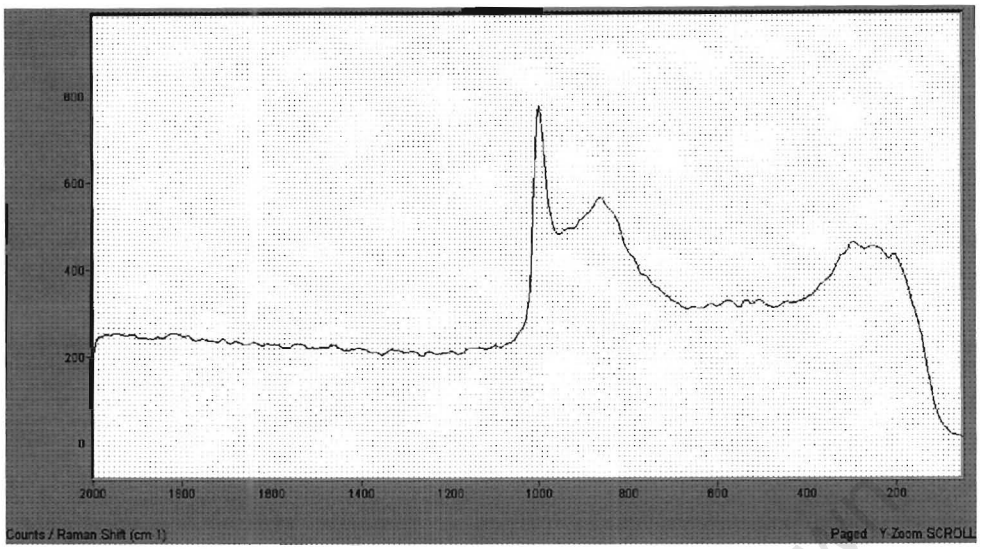

Figure 3.17: Raman spectrum of the calcined catalyst 0.1 g MoO_3/Al_2O_3 (CA) prepared using controlled adsorption technique (calcination in air at 550 °C; spectrum recorded at 550 °C) (Mestl., 2000)

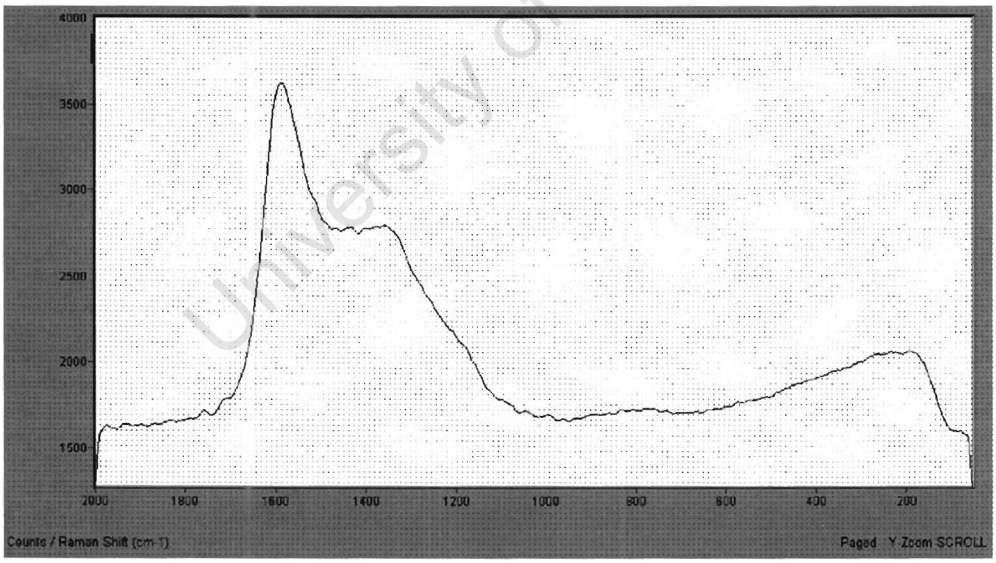

Figure 3.18: Raman spectrum of the calcined catalyst 0.1 g MoO_3/Al_2O_3 (CA) prepared using controlled adsorption technique after being brought into contact with 1-butene (calcination in air at 550 °C; contacting with 1-butene at 80 °C; spectrum recorded at 80 °C)

After regenerating the catalyst at 550 °C under air for 20 min, the catalyst returned to its initial composition (see Figure 3.19).

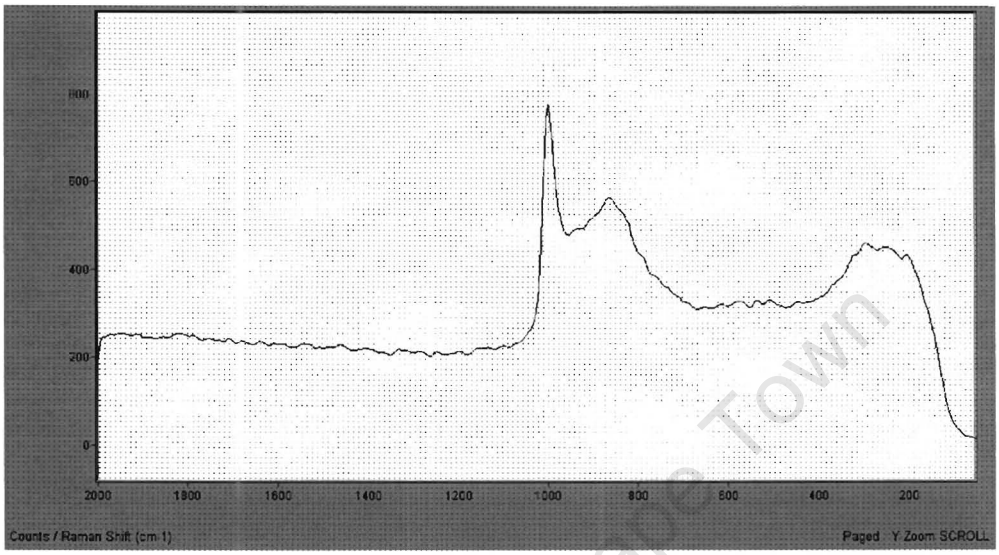

Figure 3.19: Raman spectrum of the calcined catalyst 0.1 g MoO_3/Al_2O_3 (CA) prepared using controlled adsorption technique after being brought into contact with 1-butene and regenerated in air at 550 °C (calcination in air at 550 °C; spectrum recorded at 550 °C)

3.6.4 Reduction experiment with H_2

The Raman spectrum of he catalyst 0.5 g MoO_3/Al_2O_3 (CA) after reduction in H_2 at 550 °C for 20 h is given in Figure 3.20. In the spectrum there are four broad bands appearing at 1003 cm^{-1}, 768 cm^{-1}, 523 cm^{-1} and 279 cm^{-1}. From the intensities in figure 3.20 there tends to be an indication that hydrogenation took place preferentially at the M=O bonds than the M-O-M bond, which is the weaker bond.

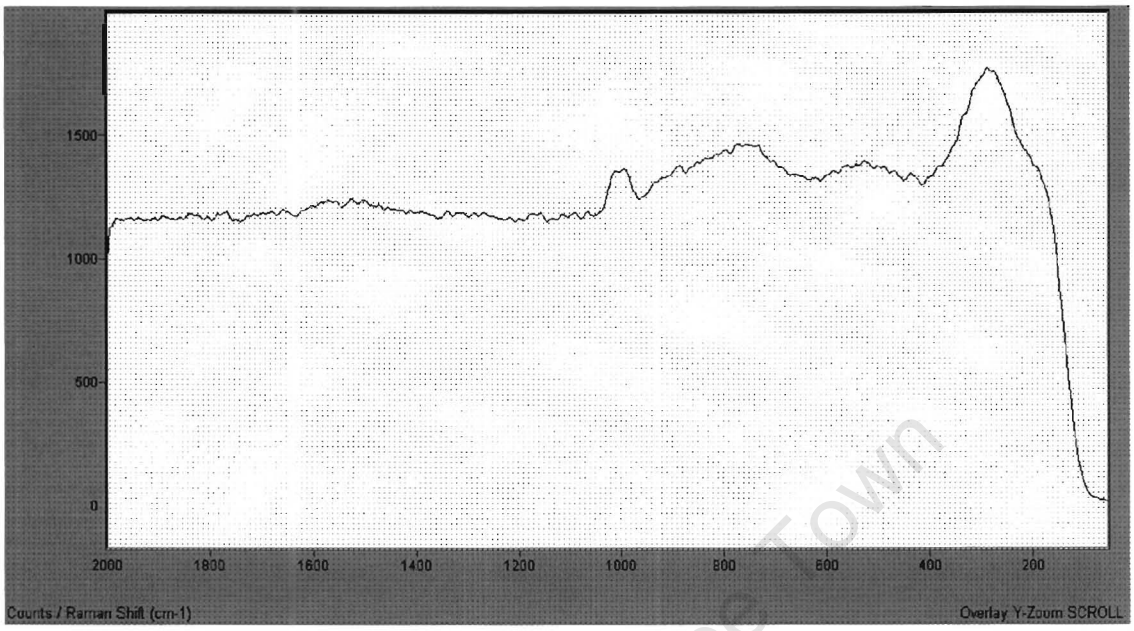

Figure 3.20: Raman spectrum of the reduced catalyst 0.5 g MoO_3/Al_2O_3 (CA) prepared using controlled adsorption technique after being reduced in hydrogen for 20 h at 550 °C (spectrum recorded at 550 °C).

3.7 Metathesis activity and selectivity of 1-octene

The metathesis activity of the prepared catalysts was measured as a function of time in a fixed bed reactor. The momentary mass balance was for all reported experiments between 97 and 99.5%.

The conversion of 1-octene was determined from the amount of liquid sample collected over a period of time, the amount of 1-octene in these samples and the feed rate of 1-octene. The reported conversions are thus over an average time period of collection of the liquid sample (the time-on-stream was taken to be the arithmetic mean between the two times of sampling). Similarly, the reported

yields and selectivities are also an average over the time period of sample collection.

3.7.1 Catalyst activity

Figure 3.21 shows the time-on-stream behaviour of the catalysts prepared using the controlled adsorption technique. Up to a loading of 0.3 g MoO_3 per g Al_2O_3 the initial conversion increases more than proportional to the MoO_3-loading. The catalysts with a MoO_3-loading higher than 0.3 g MoO_3 per gram Al_2O_3 show initially a lower activity, i.e. the activity per molybdenum atom in the catalyst decreases.

With increasing time-on-stream the activity of the catalysts declines. The decline is stronger with the catalysts with a higher initial activity.

The catalyst 0.1 g MoO_3 per gram Al_2O_3 was regenerated for 6 h at 550 °C under air (55 ml/min) after being tested in metathesis of 1-octene at 80 °C for 24 h. After the regeneration 1-octene metathesis was resumed at 80 °C. The activity of the regenerated catalyst is much higher than that of the freshly prepared catalyst (see Figure 3.22)

The activity of the catalyst prepared using the new slurry impregnation technique is comparable to the activity of the catalyst with the same MoO_3-loading prepared using the controlled adsorption method (see Figure 3.22).

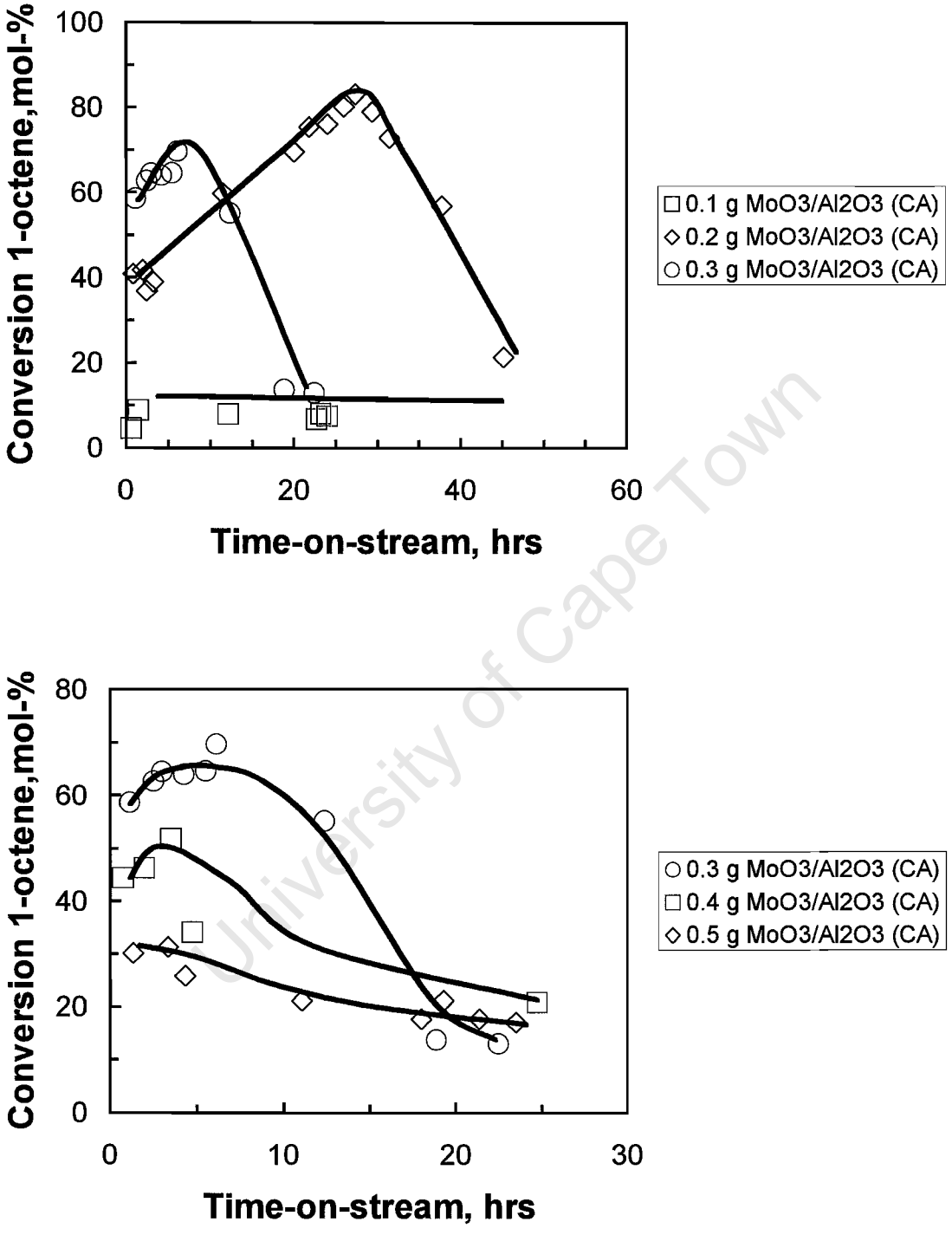

Figure 3.21: Activity of MoO_3/Al_2O_3 catalysts prepared by controlled adsorption (CA) in 1-octene metathesis as a function of time-on-stream (T^{rxn} = 80 °C, WHSV = 1.53 h^{-1})

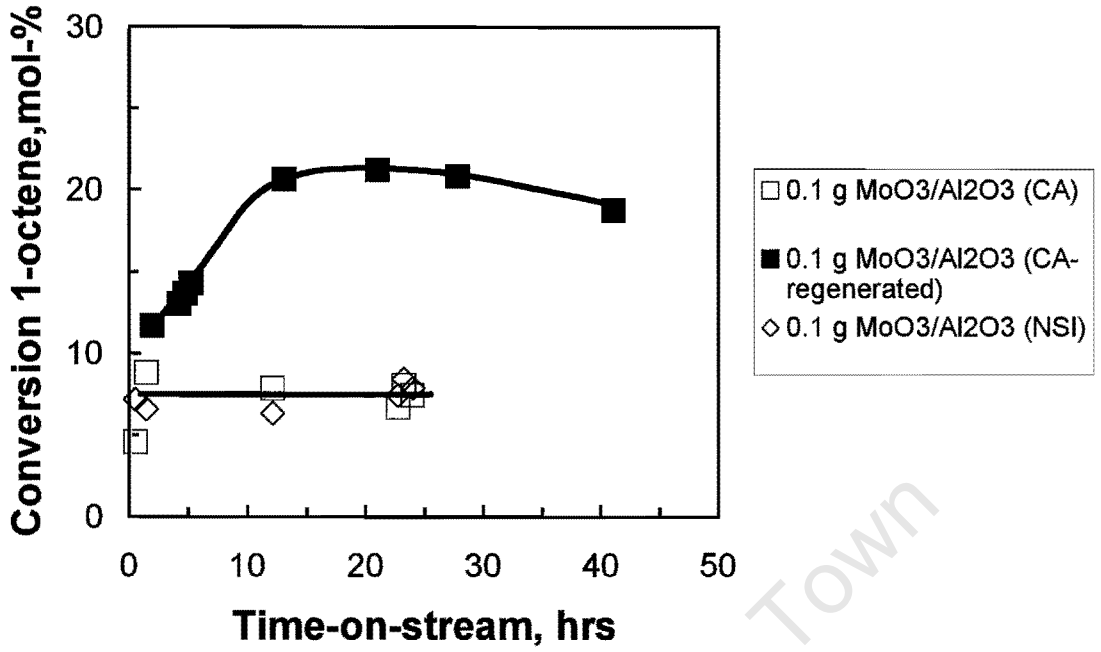

Figure 3.22: Activity of 0.1 g MoO_3/Al_2O_3 catalysts prepared using either the controlled adsorption (freshly prepared and regenerated) or the new slurry impregnation technique (NSI), in 1-octene metathesis as a function of time-on-stream (T^{rxn} = 80 °C, WHSV = 1.53 h^{-1})

3.7.2 Selectivity in 1-octene metathesis

The expected, primary products in 1-octene metathesis are ethene and 7-tetradecene. Figure 3.23 shows the selectivity of the expected primary products, ethene and 7-tetradecene, as a function of time-on-stream for the catalysts prepared using controlled adsorption. The selectivity for the primary products is high for the catalyst 0.1 g MoO_3 per g Al_2O_3 and seems to pass a maximum. The selectivity for these primary products is much lower for the catalysts with a higher MoO_3-loading. This might be partially attributed to the different level of conversion, since at high conversion secondary reactions become noticeable. The catalysts with a high MoO_3-loading seem to have similar selectivity to the primary products, which does not change significantly with time-on-stream, despite the largely different levels of conversion.

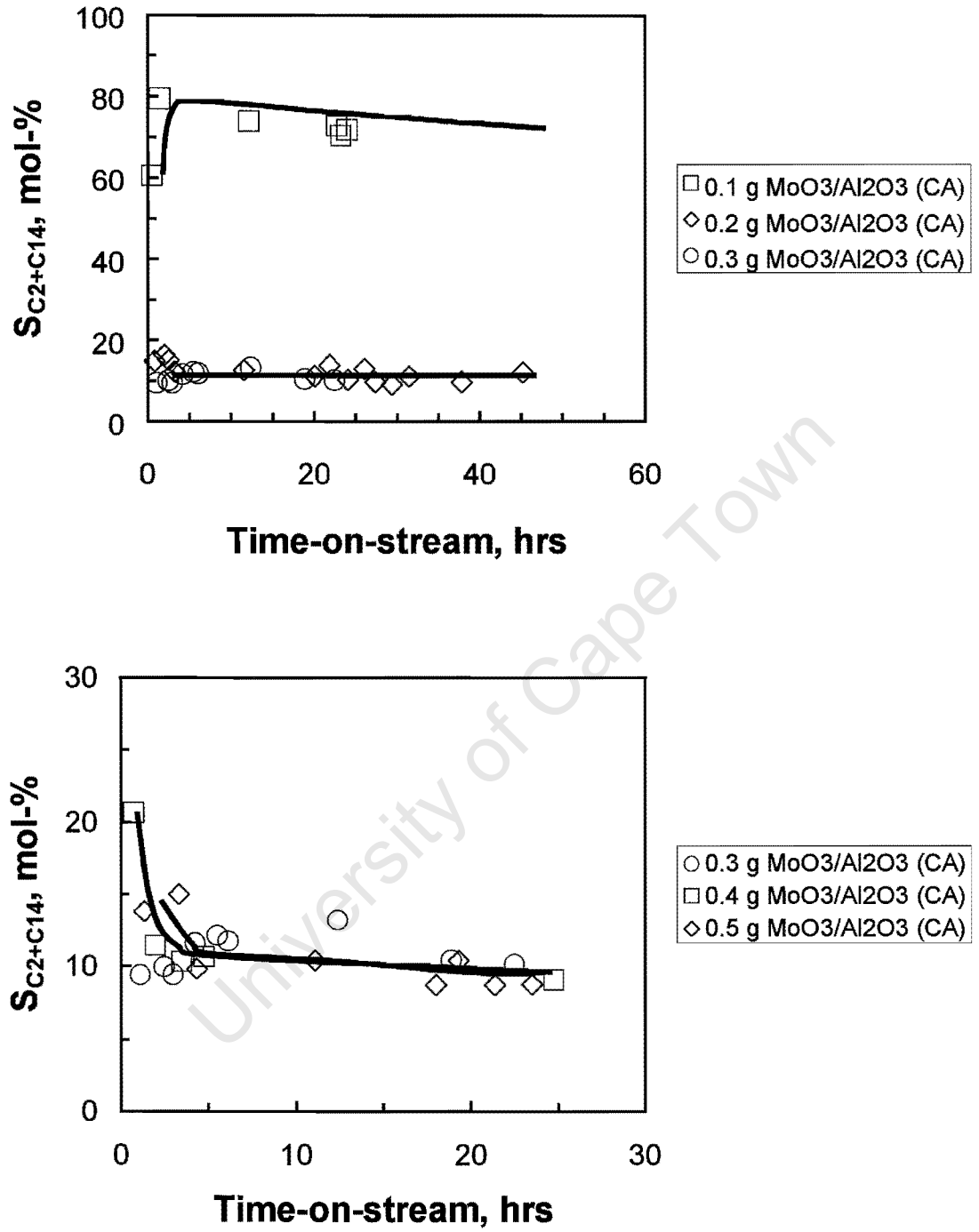

Figure 3.23: Selectivity of MoO_3/Al_2O_3 catalysts prepared by controlled adsorption (CA) in 1-octene metathesis for the formation of the primary metathesis products, ethene and 7-tetradecene, as a function of time-on-stream (T^{rxn} = 80 °C, WHSV = 1.53 h^{-1})

Figure 3.24 shows the effect of regeneration on the obtained selectivity for the primary metathesis products, ethene and 7-tetradecene. Upon regeneration the conversion of 1-octene goes up to 20 mol-%. Hence, the obtained selectivity for the primary products is much lower. However, it must be noted here that at similar conversion levels of ca. 20 mol-%, the regenerated catalyst 0.1 g MoO_3/Al_2O_3 (CA) is much more selective for the formation of primary products than catalysts prepared with a higher MoO_3-loading using controlled adsorption.

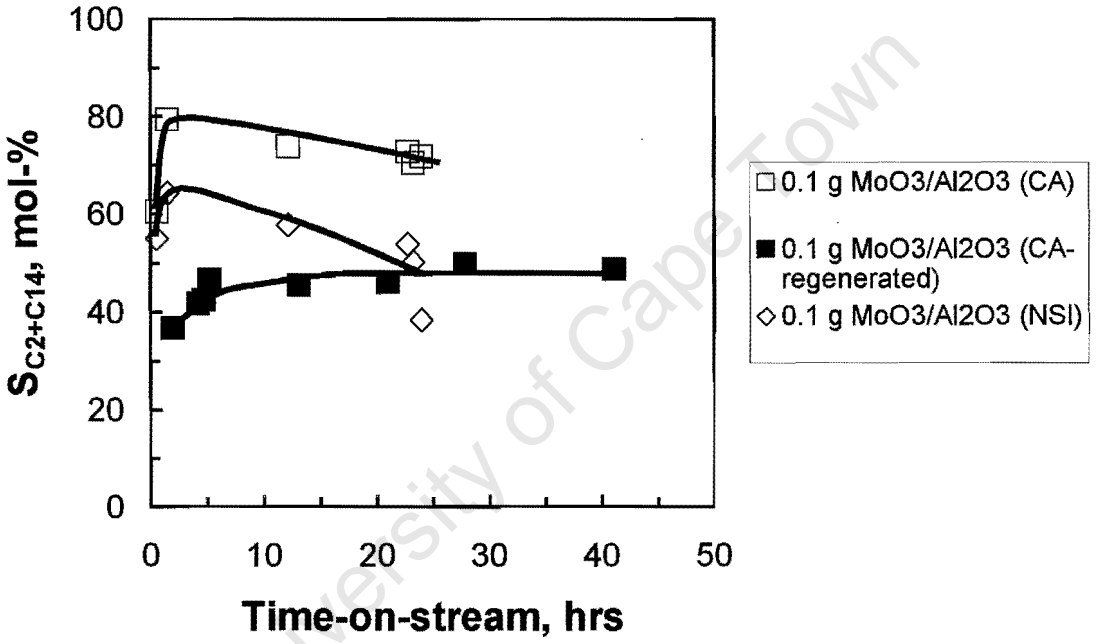

Figure 3.24: Selectivity of 0.1 g MoO_3/Al_2O_3 catalysts prepared using either the controlled adsorption (freshly prepared and regenerated) or the new slurry impregnation technique (NSI), in 1-octene metathesis for the formation of the primary metathesis products, ethene and 7-tetradecene, as a function of time-on-stream (T^{rxn} = 80 °C, WHSV = 1.53 h^{-1})

The selectivity for the primary metathesis products with the catalyst prepared using the new slurry impregnation is lower than that of the catalyst prepared using controlled adsorption technique.

Figure 3.25 shows the molar product distribution after ca. 24 h on stream for the various catalysts. The product distributions obtained with catalyst with a loading of 0.1 g MoO_3/gAl_2O_3 are characterised by a high molar selectivity for C_{14}. The selectivity for ethene is however markedly lower than the selectivity for C_{14}. In an ideal metathesis reaction the molar ratio of ethene to C_{14} should be equal to 1. The product distribution after ca. 24 h on stream for the catalysts with a MoO_3-loading higher than 0.1 g MoO_3/g Al_2O_3 is characterised by a relatively high selectivity for C_9. It is remarkable that the product distribution does not change significantly with the various catalysts.

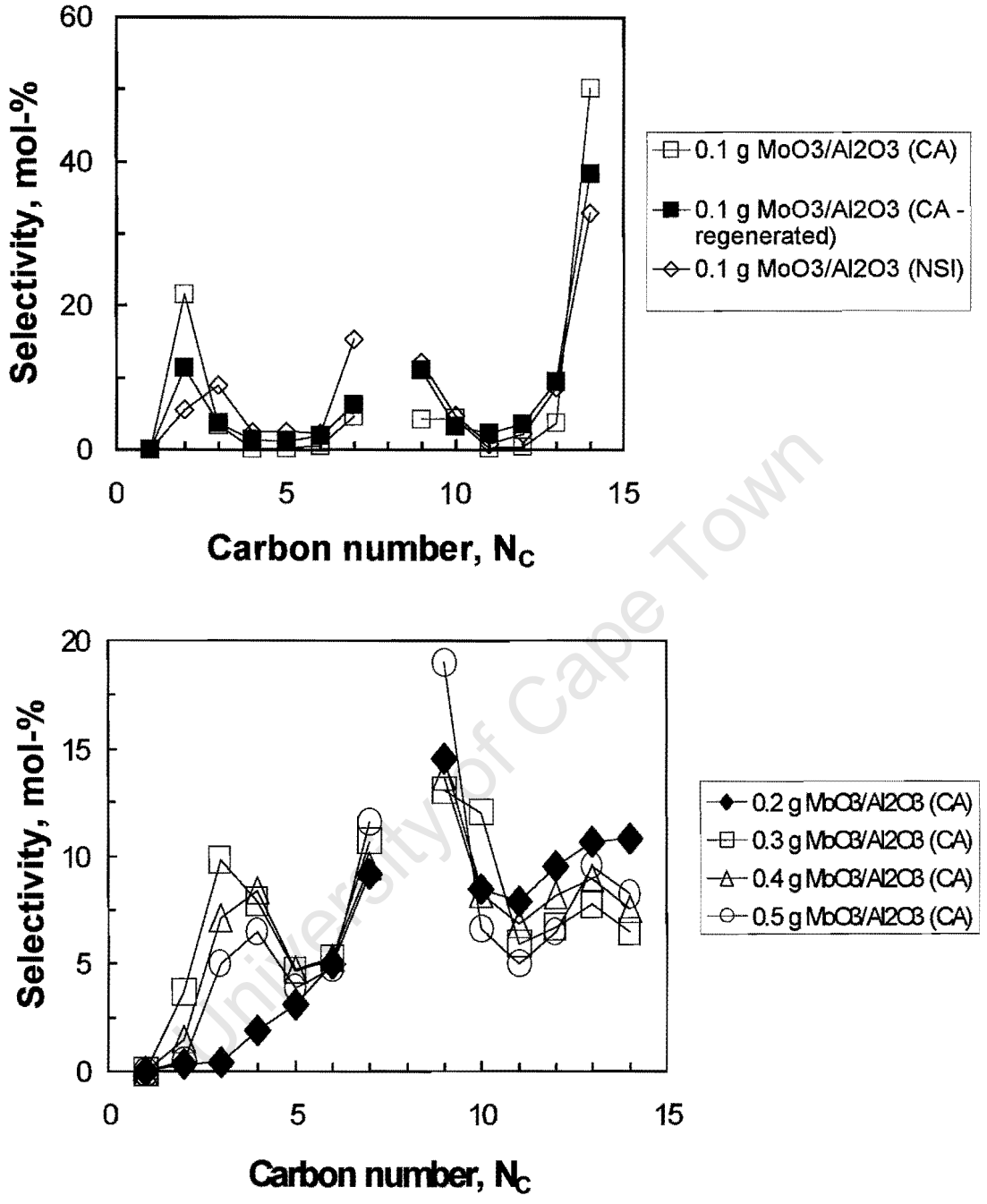

Figure 3.25: Molar product distribution obtained in 1-octene metathesis after ca. 24 h on stream (T^{rxn} = 80 °C, WHSV = 1.53 h^{-1})

4 DISCUSSION

4.1 Catalysts

4.1.1 Catalyst preparation

The catalysts were prepared using two different methods, viz. controlled adsorption of ammonium heptamolybdate on alumina and the new slurry impregnation, in which MoO_3 is brought into contact with the support Al_2O_3 (New Slurry Impregnation – NSI).

The actual Mo-metal obtained with the controlled adsorption technique is typically slightly less than the intended loading. This becomes more pronounced for catalysts with a higher Mo-loading. This could be due the impregnation time (24 h) that was too short for a higher loading.

The New Slurry Impregnated (NSI) catalyst (0.1 g MoO_3/gAl_2O_3) showed comparable activity after 24 h online to that of the catalyst (0.1 g MoO_3/gAl_2O_3) prepared via controlled adsorption. The amount of CO adsorbed for the 0.1 g MoO_3/gAl_2O_3 prepared via the New slurry impregnation and Controlled adsorption method correspond very well. The values obtained were 2.0 and 1.9 cm^3/g, respectively. This is an indication that a comparable number of active sites are available for the metathesis reaction.

The selectivity, however, towards the C_{14} olefin was 10-20% less than the catalyst prepared via the control adsorption method. This might be related to the extent of the acid catalysed double bond isomerization, and thus the amount of acid sites present on the catalyst. The New Slurry Impregnation method does not require calcination of the catalyst, because MoO_3 is already present as an oxide. During the calcination the ammonium ion from the precursor poisons some of the acid sites, thus retarding the double bond isomerization.

4.1.2 Crystal structure present in the catalysts

With an increase in the Mo-loading on the catalyst, sharper diffraction peaks become evident in the region of $2\theta=20^{o}$-50^{o} for the high loading (0.3 g MoO_3/gAl_2O_3 - 0.5 g MoO_3/gAl_2O_3). This occurs to a lesser extend in the 0.2 g MoO_3/gAl_2O_3 catalyst. These sharp diffraction peaks are indicative of large crystallites that are present. During the calcination step the catalyst undergoes phase changes, making it easier for the Al to diffuse into the molybdate layers, forming $Al_2(MoO_4)_3$. The presence of large crystallites in the catalysts with a high Mo-loading was confirmed by TEM. It is also clear from the TEM images that there are very fine particles present between the clusters. These fine particles are attributed to the Al_2O_3 (Xie and Tang, 1990). It should be noted that the formation of crystalline MoO_3 is not excluded owing to the critical superpositions of the diffraction peaks with those of $Al_2(MoO_4)_3$.

4.1.3 BET-surface area and Pore volume analyses

It is expected that with an increase in the catalyst loading that the pore volume of the catalyst would start to decrease, because more metal is deposited. This is indeed what was observed. The decrease in the pore volume is larger for the catalyst prepared with the new slurry method than for the catalyst prepared using the controlled adsorption technique. With increasing MoO_3-loading the BET-surface area decreases rapidly. The likely cause for this loss is the formation of multilayers of octahedrally coordinated Mo, which could lead to the restriction of the smallest micropores (Rajagopal, 1994). This can be expected due to the larger crystallites that were formed.

The average pore diameter for all the catalysts remains fairly constant. This implies that there is no preferential deposition of catalyst in neither the micropores nor macropores. This result tends to indicate a fairly homogeneous dispersion of the metal.

4.2 Catalytic activity

The activity of the molybdenum catalyst is clearly dependent on the metal content. It has been reported that the activity of supported MoO_3-catalysts increases up to monolayer coverage (Russell and Stokes, 1946). The catalyst with the lowest loading, 0.1 g MoO_3/gAl_2O_3, showed the lowest activity. The catalyst with 0.3 g MoO_3/gAl_2O_3, which is slightly above the theoretical monolayer capacity (19.4 wt.-%) had the highest initial activity.

The activity for all the catalyst with a MoO_3-loading larger than 0.1 g MoO_3/g Al_2O_3 passes through a maximum. The 0.2 g MoO_3/gAl_2O_3 showed a steep increase with time on line and reaches a maximum after 30 h. The maximum becomes less pronounced as the loading increases. This indicates that the catalyst system develops in the reaction medium. It might be speculated that partially reduced Mo-species are more active for the metathesis reaction than the Mo-species with an oxidation state of +6.

The activity of the catalyst prepared via control adsorption increases drastically when the catalyst is regenerated under air. This could be due to the structural changes taking place as the carbonaceous deposits are burned off.

The selectivity for the primary metathesis products, ethene and 7-tetradecene, is thought to be governed by the acidic properties of the catalyst, which catalyse double bond isomerization. The catalyst with the lowest loading, 0.1 g MoO_3/gAl_2O_3, showed the highest selectivity for the primary metathesis products, ethene and 7-tetradecene. This is attributed to the lowest Lewis/Brønsted acidity ratio (see Table 4.1).

The catalyst prepared via the new slurry impregnation (NSI) method had a lower primary metathesis selectivity than the catalyst prepared via the controlled adsorption (CA) method. The activity of these catalysts is comparable. Hence, the observed difference in the selectivity for the primary products cannot be

attributed to the difference in catalytic activity. The new slurry impregnated catalyst had a Lewis/Brønsted ratio of 0.321, which is higher than the value obtained for the controlled adsorption catalyst, 0.054. Consequently, less double bond isomerization would take place over the catalyst prepared via the controlled adsorption method. Hence, the selectivity for the primary metathesis products should be higher for the catalyst prepared using the controlled adsorption method.

Table 4.1: Acidity and C_{14} selectivity values obtained for the various catalysts.

Catalyst (wt%)	Brønsted acidity	Lewis acidity	B/L ratio	C_{14} selectivity
9.1(NSI)	0.061	0.191	0.321	36.0
9.1	0.005	0.100	0.054	46.5
16.7	0.045	0.126	0.376	11.9
23.1	0.058	0.145	0.411	9.70
28.6	0.156	0.158	0.988	9.30
33.3	0.077	0.129	0.598	11.26

NSI= New slurry impregnation

In order to elucidate the effect of conversion on the selectivity for the formation of the primary metathesis products, ethene and 7-tetradecene, the selectivity of all catalysts was plotted as a function of conversion (see Figure 4.1). Although a general trend of a increase in the selectivity of the primarily formed products as a function of 1-octene conversion can be observed, in the range of conversion between 10 and 30 mol-% differences in the selectivity of the various catalysts can be observed, which cannot be attributed to the change in conversion. For the new slurry impregnated catalyst a decrease in selectivity is observed in the same range of conversion.

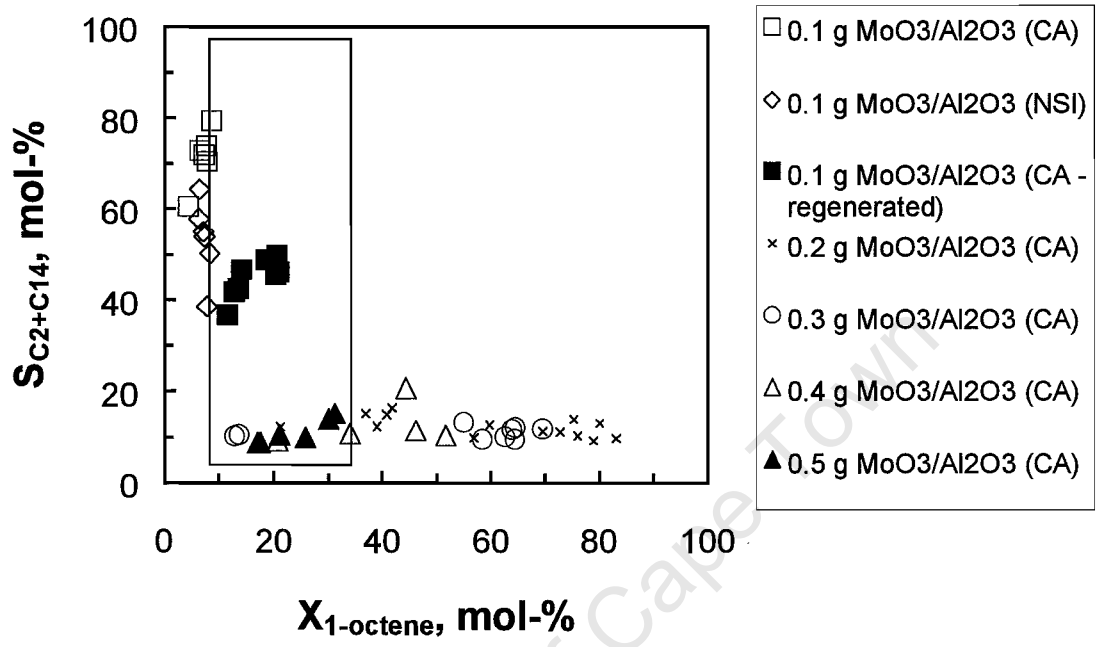

Figure 4.1: Selectivity for the formation of the primary metathesis products, ethene and 7-tetradecene, as a function of 1-octene conversion (T^{rxn} = 80 °C, WHSV = 1.53 h^{-1}; set-in: conversion range, in which different selectivities are observed for the different catalysts)

For an ideal metathesis reaction it is expected that 2 mol of alpha-olefin (C_8) reactant would yield 1 mol of ethene and 1 mol internal olefin. This was however not the case during these experiments. The carbon number range (C_2-C_{15}) in the product stream is evidence that it is possible not only to have self-metathesis of the reactant (C_8) but also cross metathesis with products, hence the wide product range. In general the molar selectivity for the products with less than 8 carbon atoms is less than the selectivity for the products with more than 8 carbon atoms. This might be indicative for secondary reactions of the light olefins (e.g. oligomerization).

For the lowest loading, 0.1 g MoO_3/Al_2O_3, there is a preference for ethene formation with the regenerated catalyst and the catalyst prepared via the controlled adsorption method. In the case of the new slurry impregnated catalyst, propene is preferentially formed. This is attributed to the higher Lewis/Brønsted ratio obtained for the new slurry impregnated catalyst, which leads to secondary metathesis products such as propene. This also applies for the higher loading where the degree of isomerization is also evident by the preference in the formation of secondary metathesis products, such as C_3 and C_{13}.

4.3 Raman Spectroscopy

During the catalyst preparation it would be ideal to obtain a catalyst containing tetrahedrally coordinated MoO_3. However, from the room temperature experiments (section 3.6.1) it becomes clear that mainly octahedrally coordinated polymolybdate species are present. Table 4.2 shows the vibrational modes of the various molybdate species (Wang and Hall, 1982)

Table 4.2: Raman vibrational modes of the different molybdate species.

Mode	$(NH_4)_6\ Mo_7O_{24}.H_2O$	$Mo_7O_{24}^{6-}$	$Mo_8O_{26}^{4-}$	MoO_4^{2-}
ν_s (Mo=O)	931	943	965	897
ν_{as} (Mo=O)	879	903	925	837
δ (Mo=O)	354	362	370	317
ν (Mo-O-Mo)		564	860	
δ (Mo-O-Mo)	217	219	230	

The two preparation methods, viz. controlled adsorption and new slurry impregnated method produce similar molybdenum coordinated species. These two spectrums reveal polymeric linkage present (ν Mo-O-Mo) at 557 cm^{-1}. The intense band appearing at 961 cm^{-1} is that of the symmetric vibration of M=O. The slight difference between the two catalysts appears to be the band appearing at 857 cm^{-1}, which is slightly obscured in the new slurry impregnated

catalyst. This band is attributed to the ν(Mo-O-Mo) mode of the heptamolybdate species (table 4.2). Good correlation was found to that in Figure 4.2.

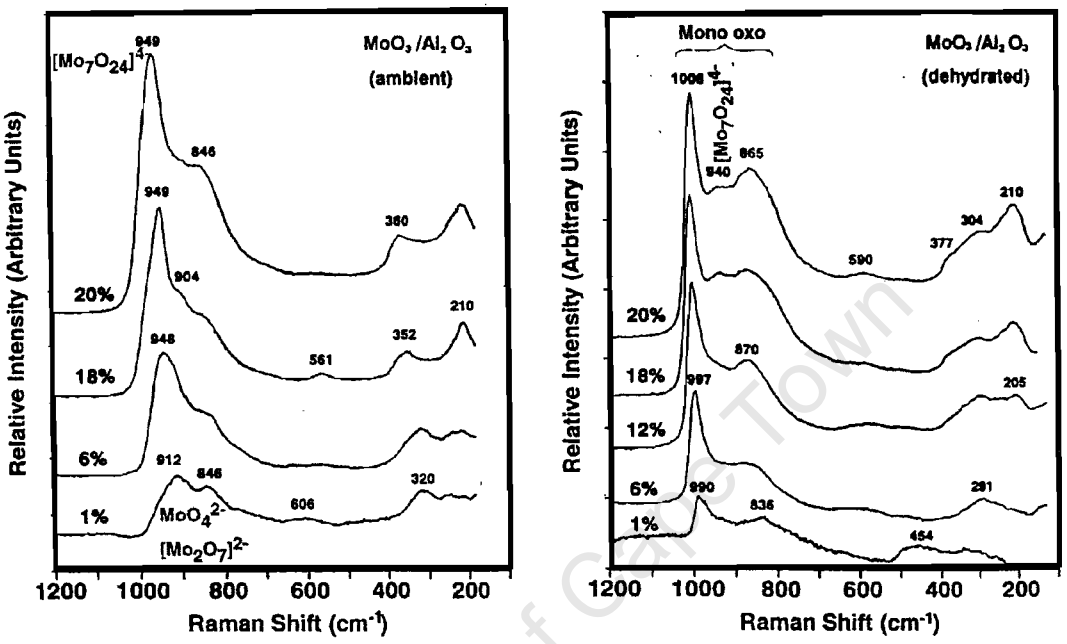

Figure 4.2: Molybdenum on alumina catalyst taken at ambient temperature and elevated temperature (360^0C) under dry air (Mestle, 2000).

The ν_s (Mo=O) appears at 954 cm^{-1}, the ν_{as} (Mo=O) at 841 cm^{-1} which could either be from the ammonium heptamolybdate or the MoO_4^{2-}. It is less likely that this band belongs to the tetrahedrally coordinated molybdenum, due to the absence of the ν_s(Mo=O) at 897 cm^{-1}, according to table 4.2. These two spectrums more likely suggest that there is heptamolybdate species present. The other difference between these two spectra is the intensity. It is expected to have a higher intensity for a higher loading, as is the case for the 0.3 g MoO_3/gAl_2O_3 catalyst.

It was shown in the XRD spectrum that the $Al_2(MoO_4)_3$ phase is predominantly in catalysts with a higher MoO_3-loading. The presence of crystalline material can

also be noted in the Raman spectrum (e.g. see Figure 3.13). Certain vibrational modes can be assigned to the crystalline material.

The catalyst definitely undergoes some change after calcination, which can be seen by the separation of the symmetric and anti-symmetric M=O vibration in the region of 800-1000 cm^{-1}. The 0.1 g MoO_3/gAl_2O_3 catalyst at room temperature does not exhibit the same resolution between these two peaks. The other observation is that the peak that appeared at 961 cm^{-1} shifts to a higher frequency of 999 cm^{-1}. This phenomenon could be due to the incorporation of oxygen into the catalyst structure bringing about a more defined structure in addition to the dehydration of the species at elevated temperatures (see Figure 4.2).

After the catalyst temperature was brought down to reaction temperature (80 °C), the in-situ reaction with 1-butene was started. The mechanism for the metathesis reaction involves the olefin (1-butene) coordinating to the M=O, consequently forming the metal carbene (M=CH-) specie. It was expected to see a shift or disappearance of the M=O vibrational mode in the spectrum. It was thus attempted to capture this carbene species using Raman spectroscopy, once the olefin has passed over the catalyst. Due to the intensity of the laser, decomposition of the olefin on the catalyst occurred. In the spectrum obtained minutes after the 1-butene was introduced into the system peaks appearing at 1589 cm^{-1} and 1369 cm^{-1} are attributed to the carbonaceous species.

This catalyst was subsequently heated up to 550 °C under a flow of air to remove the carbon deposits. It is interesting to note that the catalyst returned to its initial form.

The mapping experiments revealed that as the catalyst loading increases there tends to be different molybdate phases present on the surface of the catalyst, especially with the 0.4 g MoO_3/gAl_2O_3 and 0.5 g MoO_3/gAl_2O_3 catalysts. Eight

points on each of the catalyst were monitored and the main vibrational mode that was focussed on was the M=O vibration. It was observed that with an increase in catalyst loading, there was also an increase in intensity and area of the specific M=O vibrational mode. However, with the high loading of 0.4 g MoO_3/gAl_2O_3 and 0.5 g MoO_3/gAl_2O_3 there is a drop in both the area and intensity. This can be explained in the following manner. It was shown with the TEM, XRD and TPR analyses that the catalysts with the highest loading has a more complex phase, such as crystalline material and different molybdate species present. It is remarkable to note that the catalyst with the highest initial metathesis activity, 0.3 g MoO_3/gAl_2O_3, is also the catalyst with the highest M=O intensity and peak area in the mapping experiments.

The reducibility of the metathesis catalysts was investigated using temperature programmed reduction. The TPR profile of the 0.5 g MoO_3/gAl_2O_3 catalyst revealed two reduction steps, viz. the first peak being at 420 °C and the second at approximately 560 °C. In an attempt to simulate these results using Raman spectroscopy, the catalyst was heated up to 420 °C under inert nitrogen before introducing the H_2. No change was observed at 420 °C. The temperature was then increased to 550 °C and left at this temperature for a period of 20 h. Four distinct and broad bands appeared in the region of 1003 cm^{-1}, 768 cm^{-1}, 523 cm^{-1} and 279 cm^{-1}. The interesting observation is the intense and broad band at 279 cm^{-1}. It is expected that this band would be the smallest relative to the M=O band appearing at 960 cm^{-1}, due to the preferential attack by the H_2 on single bonded M-O-M rather than the strongly bonded M=O. This was, however not the case.

5 Conclusions

The metathesis reaction is a well-established reaction in the petrochemistry and organic synthesis. This reaction can be catalysed using a heterogeneous MoO_3/Al_2O_3 catalyst. In this study supported MoO_3 catalysts were prepared either using controlled adsorption or slurry impregnation.

When using the MoO_3/Al_2O_3 catalyst that was prepared via the new slurry impregnated and controlled adsorption, comparable results can be obtained. Even though there was comparable activity for the catalyst prepared via the two different methods, the selectivity was adversely affected in the case of the catalyst prepared via the new slurry impregnated catalyst. This is attributed to the absence of a precursor such as ammonium heptamolybdate. Upon calcination it is possible that the ammonium ion adsorbs onto the acids sites thereby diminishing the double bond isomerization activity. It was shown that the catalyst prepared via the new slurry method had a higher ratio of Lewis to Brønsted acid sites leading to secondary metathesis products such as propene.

The experimental results suggest that the activity of the MoO_3/Al_2O_3 catalyst is related to the metal content. Up to monolayer coverage the activity increases and then starts to decrease. This decrease could be due to the various phases such as the inactive crystalline MoO_3 and $Al_2(MoO_4)_3$ that are formed at high loading. The presence of these phases was confirmed by the various characterization techniques. A drop in the catalyst activity was observed for all the catalysts. This deactivation could be due to the oligomers that are formed on the catalyst surface at a temperature of 80 °C. Consequently, the active sites for metathesis are blocked. When these oligomers are burned off at 550 °C under air, the catalyst then has a higher activity than before. With the removal of the oligomers during the regeneration step, the catalyst is believed to undergo structural changes that enhance the initial activity of the catalyst.

Raman spectroscopy proves to be an effective tool in elucidating the structural information on the catalyst surface. From the room temperature experiments that was performed it can be seen that predominantly octahedrally coordinated polymolybdate species were formed and not the tetrahedrally coordinated species. These octahedral clusters could clearly be seen in the TEM images.

During the in situ Raman experiments with 1-butene it was shown that with the burning off of the carbonaceous species (oligomers) the structure appears to be similar to the initial structure. Although the activity was higher for the regenerated catalyst than the fresh catalyst during the experimental run, no definite correlation could be found in the Raman spectrums that relates to the activity of the fresh and regenerated catalyst.

From the mapping experiments that were performed it can be concluded that the peak area and intensity of the M=O band increases with increasing catalyst loading, but starts to decrease above 0.3 g MoO_3/gAl_2O_3, possibly due to multiphases forming above the monolayer capacity.

5 Conclusions

The metathesis reaction is a well-established reaction in the petrochemistry and organic synthesis. This reaction can be catalysed using a heterogeneous MoO_3/Al_2O_3 catalyst. In this study supported MoO_3 catalysts were prepared either using controlled adsorption or slurry impregnation.

When using the MoO_3/Al_2O_3 catalyst that was prepared via the new slurry impregnated and controlled adsorption, comparable results can be obtained. Even though there was comparable activity for the catalyst prepared via the two different methods, the selectivity was adversely affected in the case of the catalyst prepared via the new slurry impregnated catalyst. This is attributed to the absence of a precursor such as ammonium heptamolybdate. Upon calcination it is possible that the ammonium ion adsorbs onto the acids sites thereby diminishing the double bond isomerization activity. It was shown that the catalyst prepared via the new slurry method had a higher ratio of Lewis to Brønsted acid sites leading to secondary metathesis products such as propene.

The experimental results suggest that the activity of the MoO_3/Al_2O_3 catalyst is related to the metal content. Up to monolayer coverage the activity increases and then starts to decrease. This decrease could be due to the various phases such as the inactive crystalline MoO_3 and $Al_2(MoO_4)_3$ that are formed at high loading. The presence of these phases was confirmed by the various characterization techniques. A drop in the catalyst activity was observed for all the catalysts. This deactivation could be due to the oligomers that are formed on the catalyst surface at a temperature of 80°C. Consequently, the active sites for metathesis are blocked. When these oligomers are burned off at 550°C under air, the catalyst then has a higher activity than before. With the removal of the oligomers during the regeneration step, the catalyst is believed to undergo structural changes that enhance the initial activity of the catalyst.

Raman spectroscopy proves to be an effective tool in elucidating the structural information on the catalyst surface. From the room temperature experiments that was performed it can be seen that predominantly octahedrally coordinated polymolybdate species were formed and not the tetrahedrally coordinated species. These octahedral clusters could clearly be seen in the TEM images.

During the in situ Raman experiments with 1-butene it was shown that with the burning off of the carbonaceous species (oligomers) the structure appears to be similar to the initial structure. Although the activity was higher for the regenerated catalyst than the fresh catalyst during the experimental run, no definite correlation could be found in the Raman spectrums that relates to the activity of the fresh and regenerated catalyst.

From the mapping experiments that were performed it can be concluded that the peak area and intensity of the M=O band increases with increasing catalyst loading, but starts to decrease above 0.3g MoO_3/gAl_2O_3, possibly due to multiphases forming above the monolayer capacity.

6 Recommendations

The selectivity towards the primary metathesis products can be drastically improved by co-feeding an alkali metal such as ammonium ion or potassium ion. This will diminish the effect of double bond isomerization. The low stability, in terms of activity, is a disadvantage with the MoO_3/Al_2O_3 catalyst. This can be improved by optimising the reaction conditions, such as space velocity and temperature in order to avoid the formation of oligomer from blocking the active sites. The catalyst activity can also be improved by obtaining suitable catalyst preparation and calcination conditions, which would avoid the formation of the inactive crystalline MoO_3 and $Al_2(MoO_4)_3$ phases that are present at high loading.

REFERENCES

Banks, R.L., and Bailey, G.C.
Industrial Engineering Chemistry, Product Research Development **3** (1964), 170.

Banks, R.L., Banasiak, D.S., Hudson, P.S., and Norell, J.R.
Journal of Molecular Catalysis **15** (1982), 21.

Bradshaw, C.P.C., Howman, E.J., and Turner, L.
Journal of Catalysis **7** (1967), 269.

Dieterle Martin
http://edocs.tu-berlin.de/diss/2001/dieterle-martin.pdf

Daubert, T.E., and Danner, R.P
Physical and Thermodynamic properties of pure chemicals (1987)

Del Arco, M., Carrazán, S.R.G., Rives, V., Gil-Llambias, F.J. and Malet, P.
Journal of Catalysis, **141** (1993), 56.

Engelhardt, J.
Journal of Molecular Catalysis **8** (1980), 119.

Engelhardt, J.
Reaction Kinetics Catalysis Letters **21** (1982), 7.

Engelhardt, J., Goldwasser, J., and Hall, W.K.
Journal of Catalysis **76** (1982), 48.

Fransen, T. Van Berge, P.C., and Mars, P.
in *"Preparation of Catalysts"*(Belmont, P.A.Jacobs, and G.Poncelet, Eds.), Vol 1, p405, Elsevier,Amsterdam, (1976).

Fransen.T., van der Meer, O., and Mars, P.,
Journal of Catalysis **42** (1976), 79.

Giordano, N., Padovan, M., Vaghi, A., Bart, J.C., and Castellan, A.
Journal of Catalysis **38** (1973), 1.

Goldwasser, J., Engelhardt, J., and Hall, W.K.
Journal of Catalysis **70** (1981), 275.

Grange, P
Catal. Rev.-Sci. Eng. **21(1)** (1980), 143.

Grubbs R.H., and Swetnick, S.J.
Journal of Molecular Catalysis **8**(1980), 25.

Grünert, W., Feldhaus, R., Anders, K., Shpiro, E.S., and Minachev, Kh.M.
Journal of Catalysis **120** (1989), 444.

Grünert, W.
Indian Journal of Technology **30** (1992a), 113.

Grünert, W., Stakheev, A.Y., Feldhaus, R., Anders, K., Shpiro, E.S, and Minachev, K.M
Journal of Catalysis **135** (1992b), 289.

Haber, J.
"Molybdenum compounds in heterogeneous catalysis"
in "Molybdenum, An Outline of its chemistry and uses" (E.R Braithwaite, J.Haber, Eds.), Studies in chemistry, **Vol.19**, chapter 10, page 477, Elsevier, Amsterdam (1994).

Herisson J.C., and Chauvin Y.
Makromolecular Chemistry **141** (1971), 161.

Howard, T.R., Lee, J.B., and Grubbs, R.H.
Journal of American Chemical Society **102**(1980), 6876.

Ismayel-Milanovic, A., Basset, J.M., Praliaud, H., Dufaux, M., and de Mourgues, L.
Journal of Catalysis **31** (1973), 417.

Iwasawa, Y, Kubo. H., and Hamamura,H.
Journal of Molecular Catalysis **28** (1985), 191.

Ivin, K.J., and Mol, J.C.
Olefin Metathesis and Metathesis Polymerization
Academic Press, New York (1997)

Katz, T.J., and Hersch, W.H.
Tetrahedron Letters (1977), 585.

Kim, D.S., Segawa,K., Soeya, T., and Wachs, I.E.
Journal of Catalysis **136** (1992) 539

Knözinger, H.
Materials Science Forum **25/26** (1988), 233.
Koranyi, T.I., Paal, Z., Leyer, J., and Knözinger,H.
Applied Catalysis **64** (1990), L5.

Leyer, J., Zaki, M.I., and Knözinger,H.
Journal of Physical Chemistry **90** (1986), 4775.

Leyer, J., Margraf, M., Taglauer, E., and Knözinger,H.
Surface Science **201** (1988), 603.

Leyer, J., Mey, D., and Knözinger,H.
Journal of Catalysis **124** (1990), 349.

Lombardo, E.A., LoJacono, M., and Hall, W.K.
Journal of Molecular Catalysis **64** (1980), 150.

Maitra, A.M., Cant, N.W., and Trimm, D.L.
Applied Catalysis **27** (1986), 9.

Mestl.G
Journal of Molecular Catalysis A: Chemical **158** (2000) 54.

Medema, J., van Stam, C., de Beer, V.H.J., Konings, A.J.A., and Koningsberger, D.C.
Journal of Catalysis ***53*** (1978), 386.

Miyahara, K.
Journal of Research Institute Catalysis Hokkaido University **28** (1980), 279.

Mol, J.C., and Moulijn, J.A
"Catalysis Science and Technology" (Anderson, J.R., and Boudart, M, Eds.), Vol. **8**, p. 69., Springer Verlag, Berlin., Publisher (1987)

N.N.
European Chemical News, pg21, 25-31 March 2002.

Okamoto, Y., Arima, Y., Nakai, K., Umeno, S., Katada,N., Yoshida, H., Tanaka, T., Yamada, M., Akai, Y., Segawa, K., Nishijima, A., Matsumoto, H., Niwa, M., and Uchijima, T.
Applied Catalysis A: General **170**(1998), 316.

Pott, G.T., and Stork, W.H.J.,
in "Preparation of Catalysts" (B. Delmon, P.A. Jacobs, and G. Poncelet, Eds.), p.537. Elsevier, Amsterdam (1976).

Russell, A.S., and Stokes jr., J.J.,
Industrial Engineering Chemistry **38** (1946), 1071.

Startsev, A.N., Kutznetsov, B.N., and Yermakov, Y.I.
Reaction Kinetics Catalysis Letters **4** (1976), 321.

Shelimov, B.N., Elev, I.V., and Kazansky,V,B.
Journal of Catalysis **98** (1986), 70.

Shelimov, B.N., Elev, I.V., and Kazansky, V.B.
Journal of Molecular Catalysis **46** (1988), 187.

Taube, R., and Seyferth, K.
Rev.Inorg.Chem **8** (1986) 31.

Thomas, R., Moulijn, J.A., de Beer, V.H.J and Medema, J.
Journal of Molecular Catalysis **8** (1980), 161.

Thomas, R., and Moulijn, J.A.
Journal of Molecular Catalysis **15** (1982), 157.

Wang, L. and Hall, W.K.
Journal of Catalysis **77**(1982), 232.

Xie,Y., Gui, L., Liu,Y., Zhao, B., Yang, N., Zhang, Y., Guo, Q., Duan,L., Huang, H., Gai, X., and Tong, Y.
in "Proceedings, 8th International Congress on Catalysis, Berlin, 1984," Vol.**5**, p147. Dechema, Frankfurt-am-Main (1984).

Xie, Y.-C., and Tang, Y.-Q.
Advances In Catalysis **37** (1990), 1.

M. Zdrazil
Catalysis Today **65** (2001), 301-306.

APPENDICES

A. Analysis of results from gas chromatographs

Catalyst : 0.1gMoO_3/gAl_2O_3 prepared via controlled adsorption

Conditions : 80°C; WHSV=1.53h^{-1}; atmospheric pressure

Catalyst weight : 2.8g

PRODUCT GAS GC analysis						
Time (hours)	1.167	1.833	22.500	23.000	23.500	24.500
Product Gas (Volume l/h)	0.015	0.015	0.000	0.000	0.000	0.000
C1 Par	0.081	0.006	0.007	0.008	0.008	0.007
C2 Par	0.023	0.006	0.007	0.007	0.007	0.006
C2=	46.885	92.234	91.172	92.318	92.313	90.127
C3 Par	0.017	0.003	0.003	0.003	0.003	0.003
C3=	34.416	6.867	6.573	6.693	6.707	6.624
Butane	0.000	0.007	0.000	0.011	0.009	0.011
1-Butene + iso-butene	3.047	0.270	0.268	0.269	0.251	0.243
2-Butenes	1.540	0.225	0.216	0.221	0.213	0.242
C4	4.587	0.501	0.484	0.500	0.474	0.496
1-Pentene	1.530	0.138	0.133	0.127	0.128	1.208
Other C5	0.000	0.000	0.000	0.000	0.000	0.000
C5	1.530	0.138	0.133	0.127	0.128	1.208
C6 + Higher	12.460	0.245	1.622	0.345	0.361	1.531
Mass Gas/h (g/h)	0.019	0.015	0.000	0.000	0.000	0.000
Ethylene Purity (%)	99.779	99.986	99.985	99.984	99.984	99.986
Propylene Purity (%)	99.951	99.962	99.961	99.960	99.960	99.961
Total mol GC:	2.746	3.471	3.443	3.471	3.471	3.421
Total mol Gas/h:	0.001	0.001	0.000	0.000	0.000	0.000

LIQUID GC analysis						
Time (hours)	1.17	1.83	22.50	23	23.5	24.50
Mass (g/hr)	1.29	3.67	5.44	4.42	3.50	4.20
C2	0.000	0.082	0.036	0.112	0.147	0.218
C3	0.006	0.028	0.018	0.041	0.044	0.052
C4	0.002	0.002	0.006	0.004	0.005	0.002
C5	0.002	0.006	0.009	0.005	0.005	0.004
C6	0.013	0.013	0.014	0.019	0.021	0.016
C7-Par+Branched	0.001	0.000	0.001	0.001	0.002	0.000
C7-alpha	0.006	0.155	0.161	0.168	0.172	0.163
C8-Branched	0.086	0.077	0.086	0.079	0.079	0.075
C8	97.255	94.406	94.780	94.941	94.449	94.738
C9-Branched	0.022	0.015	0.023	0.000	0.004	0.014
C9	0.073	0.165	0.189	0.190	0.001	0.177
C10-Branched	0.016	0.011	0.013	0.012	0.191	0.011
C10	0.198	0.210	0.209	0.210	0.208	0.208
C11-Branched	0.004	0.002	0.001	0.002	0.001	0.002
C11	0.007	0.010	0.010	0.010	0.010	0.010
C12-Branched	0.004	0.002	0.001	0.001	0.001	0.001
C12	0.013	0.021	0.023	0.022	0.023	0.021
C13-Branched	0.001	0.001	0.002	0.002	0.002	0.002
C13	0.034	0.194	0.246	0.243	0.212	0.239
C14-Branched	0.001	0.001	0.004	0.001	0.001	0.001
C14	1.671	4.118	4.065	3.741	3.814	3.541
C15+	0.586	0.482	0.102	0.196	0.611	0.507

Catalyst : 0.1gMoO_3/gAl_2O_3 prepared via New slurry impregnation

Conditions : 80°C; WHSV=1.53h^{-1}; atmospheric pressure

Catalyst weight : 2.8g

PRODUCT GAS GC analysis								
Time (hours)	4	4.5	5	5.5	20.75	21.25	34.5	47.75
Product Gas (Volume l/h)	0.02	0.02	0.02	0.02	0.02	0.02	0.02	0.02
C1 Par	0.005	0.014	0.014	0.014	0.014	0.015	0.015	0.015
C2 Par	0.000	0.000	0.000	0.000	0.000	0.000	0.000	0.000
C2=	63.743	71.125	71.125	71.125	71.125	72.627	72.368	72.368
C3 Par	0.007	0.006	0.006	0.006	0.006	0.006	0.006	0.006
C3=	29.354	24.270	24.270	24.270	24.270	23.796	24.141	24.141
Butane	0.002	0.004	0.004	0.004	0.004	0.004	0.004	0.004
1-Butene + iso-butene	3.148	0.665	0.665	0.665	0.665	0.633	0.648	0.648
2-Butenes	0.679	1.601	1.601	1.601	1.601	1.533	1.584	1.584
C4	3.829	2.270	2.270	2.270	2.270	2.170	2.236	2.236
1-Pentene	0.021	0.012	0.012	0.012	0.012	0.320	0.330	0.330
Other C5	1.292	0.643	0.643	0.643	0.643	0.481	0.515	0.515
C5	1.313	0.655	0.655	0.655	0.655	0.801	0.845	0.845
C6 + Higher	1.749	1.659	1.659	1.659	1.659	0.587	0.389	0.389
Mass Gas/h (g/h)	0.022	0.022	0.022	0.022	0.022	0.021	0.021	0.021
Ethylene Purity (%)	99.992	99.980	99.980	99.980	99.980	99.980	99.980	99.980
Propylene Purity (%)	99.976	99.976	99.976	99.976	99.976	99.975	99.975	99.975
Total mol GC:	3.083	3.188	3.188	3.188	3.188	3.218	3.216	3.216
Total mol Gas/h:	0.001	0.001	0.001	0.001	0.001	0.001	0.001	0.001

LIQUID GC analysis								
Time (hours)	4	4.5	5	5.5	20.75	21.25	34.5	47.75
Mass (g/hr)	8.14	4.24	3.80	3.14	3.56	4.80	3.60	3.60
C2	0.005	0.003	0.010	0.005	0.189	0.042	0.007	0.163
C3	0.064	0.048	0.096	0.062	0.425	0.178	0.071	0.362
C4	0.119	0.110	0.145	0.125	0.224	0.151	0.090	0.171
C5	0.113	0.111	0.125	0.121	0.168	0.139	0.103	0.134
C6	0.183	0.198	0.209	0.211	0.290	0.263	0.221	0.244
C7-Par+Branched	0.000	0.000	0.000	0.000	0.000	0.000	0.000	0.000
C7-alpha	0.460	0.536	0.574	0.605	0.958	0.909	0.838	0.820
C8-Branched	0.083	0.079	0.076	0.077	0.079	0.073	0.072	0.072
C8	89.949	88.055	87.413	87.286	80.257	80.370	80.230	82.290
C9-Branched	0.000	0.000	0.000	0.000	0.000	0.000	0.000	0.000
C9	0.985	1.110	1.168	1.197	1.884	1.868	1.914	1.749
C10-Branched	0.008	0.009	0.009	0.009	0.011	0.010	0.009	0.012
C10	0.516	0.531	0.540	0.544	0.632	0.618	0.613	0.587
C11-Branched	0.024	0.022	0.023	0.027	0.035	0.035	0.033	0.023
C11	0.338	0.355	0.364	0.362	0.468	0.454	0.444	0.396
C12-Branched	0.037	0.025	0.028	0.037	0.031	0.027	0.028	0.035
C12	0.583	0.612	0.621	0.623	0.821	0.803	0.795	0.698
C13-Branched	0.016	0.025	0.025	0.015	0.023	0.020	0.023	0.025
C13	1.213	1.327	1.372	1.447	2.231	2.281	2.352	2.054
C14-Branched	0.077	0.022	0.021	0.077	0.068	0.046	0.038	0.097
C14	3.812	4.735	5.128	5.650	9.235	9.727	10.304	8.923
C15+	1.415	2.086	2.053	1.520	1.973	1.985	1.815	1.145

Catalyst : 0.1gMoO_3/gAl_2O_3 (regenerated)

Conditions : 80°C; WHSV=1.53h^{-1}; atmospheric pressure

Regeneration : 550°C under air

Catalyst weight : 2.8g

PRODUCT GAS GC analysis						
Time (hours)	1.17	1.83	22.50	23	23.5	24.50
Product Gas (Volume l/h)	0.01	0.03	0.01	0.01	0.01	0.00
C1 Par	0.036	0.056	0.044	0.019	0.022	0.018
C2 Par	0.011	0.011	0.017	0.013	0.013	0.013
C2=	34.013	74.411	82.979	82.303	81.231	80.922
C3 Par	0.003	0.005	0.004	0.002	0.002	0.002
C3=	3.998	8.554	10.153	14.714	14.645	14.618
Butane	0.037	0.002	0.003	0.001	0.023	0.012
1-Butene + iso-butene	0.001	0.000	0.002	0.000	0.000	0.001
2-Butenes	0.000	0.000	0.000	0.000	0.000	0.000
C4	0.038	0.002	0.005	0.001	0.023	0.013
1-Pentene	0.227	0.392	0.370	0.291	0.354	0.280
Other C5	1.871	5.719	2.593	1.211	1.390	0.790
C5	2.098	6.111	2.963	1.502	1.744	1.070
C6 + Higher	59.803	10.851	3.835	1.445	2.319	3.343
Mass Gas/h (g/h)	0.017	0.030	0.011	0.015	0.016	0.000
Ethylene Purity (%)	99.863	99.910	99.926	99.961	99.957	99.961
Propylene Purity (%)	99.933	99.947	99.965	99.986	99.986	99.986
Total mol GC:	2.053	3.078	3.293	3.328	3.303	3.293
Total mol Gas/h:	0.000	0.001	0.000	0.001	0.001	0.000

LIQUID GC analysis						
Time (hours)	1.17	1.83	22.50	23	23.5	24.50
Mass (g/hr)	1.44	4.03	3.05	3.75	4.17	3.47
C2	0.011	0.038	0.048	0.083	0.068	0.065
C3	0.035	0.064	0.091	0.155	0.148	0.156
C4	0.017	0.027	0.034	0.062	0.067	0.057
C5	0.001	0.012	0.011	0.056	0.065	0.074
C6	0.027	0.032	0.048	0.016	0.022	0.080
C7-Par+Branched	0.005	0.008	0.001	0.001	0.001	0.001
C7-alpha	0.363	0.428	0.454	0.521	0.612	0.627
C8-Branched	0.074	0.075	0.075	0.075	0.001	0.001
C8	95.204	95.057	94.969	94.454	94.418	94.329
C9-Branched	0.012	0.010	0.003	0.010	0.010	0.006
C9	0.354	0.415	0.449	0.546	0.595	0.632
C10-Branched	0.022	0.020	0.020	0.020	0.018	0.018
C10	0.232	0.235	0.241	0.253	0.256	0.261
C11-Branched	0.001	0.000	0.002	0.001	0.000	0.001
C11	0.015	0.019	0.022	0.034	0.042	0.048
C12-Branched	0.002	0.002	0.002	0.001	0.003	0.003
C12	0.045	0.059	0.074	0.108	0.132	0.149
C13-Branched	0.001	0.001	0.007	0.003	0.002	0.001
C13	0.334	0.389	0.424	0.547	0.605	0.654
C14-Branched	0.000	0.000	0.022	0.003	0.001	0.001
C14	2.849	2.771	2.675	2.695	2.618	2.693
C15+	0.397	0.338	0.326	0.356	0.318	0.141

Catalyst : 0.2gMoO_3/gAl_2O_3 prepared via controlled adsorption

Conditions : 80°C; WHSV=1.53h^{-1}; atmospheric pressure

Catalyst weight : 2.8g

PRODUCT GAS

GC analysis

Time (hours)	1.75	2.25	2.75	3.75	19.42	20.75	22.92	25.17	26.92	27.92	30.92	32.08	43.58	46.92
Product Gas (Volume l/h)	0.04	0.04	0.04	0.02	0.02	0.00	0.00	0.00	0.02	0.01	0.01	0.01	0.00	0.00
C1 Par	0.007	0.005	0.002	0.002	0.001	0.001	0.001	0.001	0.001	0.001	0.001	0.001	0.001	0.002
C2 Par	0.007	0.006	0.006	0.006	0.007	0.007	0.008	0.013	0.008	0.008	0.009	0.009	0.010	0.010
C2=	51.322	47.536	44.426	43.026	38.323	40.330	39.785	68.351	38.071	36.627	34.923	34.852	39.025	42.056
C3 Par	0.019	0.018	0.017	0.017	0.047	0.019	0.020	0.034	0.023	0.024	0.026	0.026	0.026	0.026
C3=	43.373	45.577	47.102	47.688	47.470	49.770	50.771	16.596	51.517	52.059	53.006	53.264	51.816	49.789
Butane	0.018	0.020	0.019	0.021	0.277	0.020	0.021	0.036	0.025	0.028	0.030	0.029	0.045	0.034
1-Butene + iso-butene	3.412	4.525	5.575	6.060	3.655	5.934	6.335	10.227	7.017	7.591	8.034	7.934	6.136	5.457
2-Butenes	0.004	0.003	0.003	0.003	0.003	0.004	0.004	0.006	0.005	0.006	0.007	0.007	0.033	0.006
C4	3.434	4.548	5.596	6.084	3.935	5.958	6.360	10.270	7.047	7.624	8.071	7.970	6.214	5.497
1-Pentene	0.977	1.336	1.687	1.841	1.523	1.759	1.875	3.019	2.107	2.299	2.437	2.409	1.848	1.607
Other C5	0.000	0.000	0.001	0.004	0.001	0.002	0.000	0.001	0.001	0.001	0.001	0.001	0.001	0.001
C5	0.977	1.336	1.688	1.845	1.524	1.761	1.875	3.020	2.107	2.300	2.439	2.410	1.849	1.607
C6 + Higher	0.861	0.975	1.162	1.332	8.693	2.154	1.181	1.713	1.225	1.357	1.528	1.469	1.058	1.014
Mass Gas/h (g/h)	0.047	0.047	0.048	0.024	0.023	0.000	0.006	0.000	0.021	0.013	0.008	0.011	0.000	0.000
Ethylene Purity (%)	99.974	99.977	99.981	99.981	99.979	99.979	99.979	99.978	99.976	99.974	99.973	99.973	99.972	99.971
Propylene Purity (%)	99.956	99.961	99.964	99.964	99.901	99.962	99.960	99.794	99.956	99.954	99.952	99.951	99.949	99.948
Total mol GC:	2.951	2.895	2.846	2.823	2.694	2.783	2.784	3.083	2.757	2.733	2.706	2.707	2.777	2.821
Total mol Gas/h:	0.001	0.001	0.001	0.001	0.001	0.000	0.000	0.000	0.001	0.000	0.000	0.000	0.000	0.000

LIQUID GC analysis														
Time (hours)	1.75	2.25	2.75	3.75	19.42	20.75	22.92	25.17	26.92	27.92	30.92	32.08	43.58	46.92
Mass (g/hr)	5.30	3.64	4.04	3.77	1.65	1.05	0.37	0.29	0.90	1.79	1.35	1.06	2.27	5.18
C2	0.028	0.020	0.013	0.045	0.045	0.043	0.000	0.000	0.017	0.018	0.058	0.000	0.156	0.169
C3	0.456	0.445	0.462	0.840	0.995	0.074	0.035	0.018	0.558	0.577	1.091	0.291	1.614	0.940
C4	0.815	0.844	1.030	1.107	2.089	0.481	0.472	0.147	2.127	1.898	2.334	1.125	2.111	0.782
C5	0.623	0.677	0.754	0.173	1.528	0.988	1.026	0.606	2.102	1.938	0.394	0.273	1.432	0.511
C6	0.959	1.054	1.082	1.818	2.023	1.891	2.116	1.863	2.806	2.796	4.305	3.178	1.870	0.680
C7-Par+Branched	0.002	0.008	0.000	0.002	0.000	0.000	0.000	0.000	0.002	0.002	0.000	0.000	0.000	0.001
C7-alpha	2.945	3.101	2.838	2.776	4.175	4.065	4.259	4.502	4.644	4.570	4.737	4.469	3.626	1.382
C8-Branched	0.040	0.119	0.030	0.054	0.119	0.121	0.125	0.138	0.140	0.154	0.171	0.149	0.114	0.048
C8	61.349	60.615	63.976	62.986	41.251	30.558	25.199	24.833	20.210	17.273	21.126	27.951	43.448	80.528
C9-Branched	0.015	0.023	0.020	0.028	0.037	0.047	0.053	0.057	0.060	0.076	0.108	0.077	0.060	0.023
C9	4.875	5.414	4.866	4.771	7.316	8.208	8.868	9.520	8.972	9.004	9.030	9.224	7.036	2.581
C10-Branched	0.012	0.078	0.008	0.015	0.014	0.017	0.018	0.013	0.013	0.022	0.089	0.031	0.052	0.024
C10	2.247	2.705	2.544	2.679	4.194	5.355	6.005	6.329	6.207	6.536	6.485	6.089	4.243	1.462
C11-Branched	0.095	0.169	0.880	0.005	0.124	0.222	0.197	0.267	0.265	0.286	0.170	0.180	0.135	0.021
C11	2.070	2.557	2.350	2.432	3.974	5.300	5.857	6.143	6.112	6.379	6.077	5.670	3.969	1.213
C12-Branched	0.187	0.186	0.209	0.216	0.315	0.410	0.526	0.589	0.616	0.644	0.643	0.584	0.309	0.088
C12	3.192	3.580	3.352	3.302	5.198	6.804	7.441	7.509	7.498	7.485	7.199	6.864	5.010	1.601
C13-Branched	0.001	0.029	0.018	0.047	0.043	0.016	0.027	0.197	0.190	0.281	0.145	0.077	0.031	0.005
C13	4.497	5.078	4.595	4.437	7.048	8.744	9.331	9.153	9.011	9.168	8.586	8.490	6.570	2.289
C14-Branched	0.082	0.050	0.036	0.015	0.018	0.174	0.184	0.197	0.068	0.114	0.075	0.068	0.077	0.001
C14	5.075	5.505	4.875	4.690	7.609	9.401	9.799	9.467	9.304	9.154	8.295	8.566	7.104	2.667
C15+	10.434	7.745	6.060	7.561	11.886	17.082	18.464	18.452	19.080	21.625	18.882	16.645	11.032	2.983

Catalyst : 0.3gMoO_3/gAl_2O_3 prepared via controlled adsorption

Conditions : 80°C; WHSV=1.53h^{-1}; atmospheric pressure

Catalyst weight : 2.8g

PRODUCT GAS GC analysis									
Time (hours)	2.25	2.75	3.25	5.25	5.75	6.5	18.25	19.5	25.5
Product Gas (Volume l/h)	0.06	0.06	0.04	0.04	0.02	0.02	0.01	0.01	0.00
C1 Par	0.000	0.000	0.000	0.000	0.000	0.000	0.002	0.003	0.001
C2 Par	0.000	0.000	0.000	0.000	0.000	0.005	0.005	0.005	0.006
C2=	15.410	16.118	15.410	22.109	22.619	24.739	29.419	30.012	32.750
C3 Par	0.000	0.041	0.000	0.035	0.035	0.034	0.036	0.036	0.035
C3=	40.715	42.868	40.715	49.198	50.351	49.114	52.847	52.401	48.146
Butane	0.000	0.000	0.000	0.016	0.016	0.017	0.000	0.000	0.571
1-Butene + iso-butene	13.364	12.718	13.364	8.873	8.451	6.775	4.864	4.705	3.325
2-Butenes	14.373	12.620	14.373	9.676	9.157	7.338	5.832	5.704	4.580
C4	27.737	25.338	27.737	18.566	17.624	14.130	10.696	10.409	8.476
1-Pentene	6.817	4.811	6.817	2.536	2.143	1.254	0.000	0.067	0.262
Other C5	4.805	4.334	4.805	2.469	1.633	0.569	0.000	0.045	0.480
C5	11.623	9.145	11.623	5.006	3.776	1.823	0.000	0.112	0.742
C6 + Higher	4.515	6.491	4.515	5.086	5.594	10.155	6.994	7.022	9.844
Mass Gas/h (g/h)	0.092	0.091	0.062	0.064	0.028	0.028	0.007	0.011	0.002
Ethylene Purity (%)	100.000	100.000	100.000	100.000	100.000	99.981	99.975	99.971	99.978
Propylene Purity (%)	100.000	99.905	100.000	99.929	99.930	99.931	99.932	99.932	99.928
Total mol GC:	2.235	2.257	2.235	2.425	2.442	2.452	2.583	2.591	2.595
Total mol Gas/h:	0.002	0.002	0.001	0.002	0.001	0.001	0.000	0.000	0.000

LIQUID GC analysis									
Time (hours)	2.25	2.75	3.25	5.25	5.75	6.5	18.25	19.5	25.5
Mass (g/hr)	2.20	3.20	4.60	3.08	1.34	1.27	0.34	5.18	3.60
C2	0.000	0.000	0.018	0.046	0.000	0.014	0.126	0.061	0.079
C3	0.196	0.373	0.532	0.867	0.362	0.452	1.276	0.457	0.374
C4	1.168	1.268	1.444	1.641	1.083	2.129	1.454	0.512	0.426
C5	1.319	1.106	1.131	1.173	0.920	0.004	0.970	0.362	0.317
C6	1.979	1.575	1.587	1.668	1.460	1.419	1.351	0.477	0.423
C7-Par+Branched	0.016	0.013	0.013	0.013	0.013	0.000	0.013	0.006	0.007
C7-alpha	5.208	4.552	4.804	4.697	4.329	3.974	3.344	0.970	1.013
C8-Branched	0.191	0.166	0.000	0.158	0.152	0.000	0.000	0.123	0.000
C8	43.131	39.539	37.099	37.308	36.895	31.150	45.820	86.449	88.269
C9-Branched	3.445	0.000	0.000	0.000	0.000	0.000	0.000	0.000	0.000
C9	6.256	7.220	7.748	8.125	8.046	7.265	6.438	1.744	1.609
C10-Branched	0.078	0.101	0.080	0.082	0.084	0.006	0.080	0.037	0.034
C10	2.564	3.061	3.296	3.660	3.722	3.504	3.508	1.736	1.604
C11-Branched	0.225	0.306	0.321	0.333	0.324	0.376	0.272	0.079	0.073
C11	2.350	2.906	3.151	3.533	3.616	4.039	3.647	0.926	0.821
C12-Branched	0.191	0.314	0.338	0.342	0.326	0.061	0.047	0.053	0.065
C12	3.723	4.576	4.962	5.478	5.545	5.398	5.016	1.132	1.039
C13-Branched	0.099	0.174	0.150	0.186	0.244	0.452	0.156	0.000	0.000
C13	4.632	6.058	6.904	7.652	7.776	7.426	6.604	1.484	1.374
C14-Branched	0.347	0.425	0.422	0.353	0.428	0.646	0.323	0.039	0.000
C14	4.123	5.494	6.490	7.303	7.452	7.032	6.146	1.412	1.239
C15+	18.758	20.773	19.509	15.381	17.224	24.655	13.407	1.940	1.235

Catalyst : 0.4gMoO_3/gAl_2O_3 prepared via controlled adsorption

Conditions : 80°C; WHSV=1.53h^{-1}; atmospheric pressure

Catalyst weight : 2.8g

PRODUCT GAS GC analysis					
Time (hours)	1.5	2.5	4.5	5	44.5
Product Gas (Volume l/h)	0.08	0.04	0.02	0.02	0.00
C1 Par	0.004	0.003	0.001	0.001	0.007
C2 Par	0.005	0.004	0.004	0.004	0.007
C2=	29.646	27.157	28.058	28.500	52.701
C3 Par	0.021	0.023	0.025	0.025	0.021
C3=	49.263	50.593	53.352	53.522	39.810
Butane	0.000	0.000	0.000	0.000	0.000
1-Butene + iso-butene	5.925	6.972	7.344	7.145	3.280
2-Butenes	7.670	8.101	8.000	7.769	0.978
C4	13.595	15.073	15.344	14.914	4.258
1-Pentene	0.099	0.036	0.032	0.080	0.000
Other C5	7.367	7.110	3.185	2.955	1.186
C5	7.466	7.146	3.217	3.034	1.186
C6 + Higher	0.000	0.000	0.000	0.000	2.010
Mass Gas/h (g/h)	0.107	0.054	0.033	0.026	0.004
Ethylene Purity (%)	99.970	99.976	99.984	99.983	99.974
Propylene Purity (%)	99.958	99.954	99.954	99.954	99.947
Total mol GC:	2.581	2.546	2.592	2.602	2.947
Total mol Gas/h:	0.003	0.001	0.001	0.001	0.000

LIQUID GC analysis					
Time (hours)	1.5	2.5	4.5	5	44.5
Mass (g/hr)	1.40	2.64	4.13	4.26	4.65
C2	0.000	0.000	0.043	0.000	0.023
C3	0.258	0.320	0.682	0.489	0.429
C4	1.067	1.227	1.164	1.011	0.719
C5	0.793	0.980	0.826	0.729	0.506
C6	0.882	1.275	1.196	1.027	0.684
C7-Par+Branched	0.005	0.000	0.000	0.012	0.000
C7-alpha	2.677	3.366	3.016	2.520	1.431
C8-Branched	0.121	0.000	0.118	0.129	0.000
C8	63.467	54.995	49.015	66.418	80.077
C9-Branched	6.153	2.766	0.000	0.051	0.043
C9	3.407	5.119	5.728	4.685	2.612
C10-Branched	0.085	0.066	0.065	0.052	0.037
C10	1.321	2.575	3.290	2.407	1.737
C11-Branched	0.102	0.186	0.259	0.103	0.072
C11	1.177	2.466	3.639	2.597	1.543
C12-Branched	0.062	0.175	0.044	0.467	0.031
C12	1.966	3.463	4.543	3.562	2.084
C13-Branched	0.000	0.000	0.308	0.075	0.000
C13	2.824	4.498	5.715	4.594	2.506
C14-Branched	0.007	0.174	0.421	0.143	0.000
C14	2.750	4.212	5.168	4.064	2.268
C15+	10.876	12.139	14.760	4.865	3.197

Catalyst : 0.5gMoO_3/gAl_2O_3 prepared via controlled adsorption

Conditions : 80°C; WHSV=1.53h^{-1}; atmospheric pressure

Catalyst weight : 2.8g

PRODUCT GAS GC analysis								
Time (hours)	2.67	4	4.67	17.5	18.5	20.08	22.67	24.33
Product Gas (Volume l/h)	0.02	0.02	0.00	0.01	0.00	0.00	0.00	0.00
C1 Par	0.007	0.004	0.006	0.005	0.009	0.005	0.007	0.007
C2 Par	0.006	0.006	0.006	0.006	0.006	0.006	0.006	0.006
C2=	52.831	49.288	48.650	48.144	49.183	49.330	50.343	51.250
C3 Par	0.021	0.023	0.024	0.025	0.026	0.025	0.024	0.024
C3=	38.878	42.152	42.755	44.557	45.142	44.148	43.233	43.335
Butane	0.000	0.000	0.000	0.000	0.000	0.001	0.000	0.000
1-Butene + iso-butene	2.049	2.695	2.849	2.351	2.361	2.236	2.057	2.046
2-Butenes	1.807	1.955	2.014	1.702	1.731	1.659	1.551	1.752
C4	3.857	4.651	4.863	4.053	4.092	3.895	3.608	3.798
1-Pentene	1.115	1.417	1.502	1.308	1.286	1.245	1.135	1.132
Other C5	0.000	0.000	0.000	0.000	0.000	0.000	0.000	0.000
C5	1.115	1.417	1.502	1.308	1.286	1.245	1.135	1.132
C8 + Higher	3.285	2.459	2.195	1.902	0.255	1.346	1.643	0.448
Mass Gas/h (g/h)	0.018	0.027	0.000	0.006	0.000	0.000	0.000	0.000
Ethylene Purity (%)	99.975	99.980	99.976	99.977	99.968	99.977	99.973	99.974
Propylene Purity (%)	99.946	99.945	99.944	99.943	99.943	99.943	99.944	99.946
Total mol GC:	2.936	2.896	2.890	2.894	2.926	2.916	2.928	2.951
Total mol Gas/h:	0.001	0.001	0.000	0.000	0.000	0.000	0.000	0.000

LIQUID GC analysis								
Time (hours)	2.67	4	4.67	17.5	18.5	20.08	22.67	24.33
Mass (g/hr)	3.96	3.83	4.58	4.82	3.66	4.21	3.85	4.20
C2	0.012	0.026	0.028	0.076	0.016	0.015	0.035	0.030
C3	0.248	0.379	0.387	0.584	0.244	0.238	0.343	0.317
C4	0.531	0.681	0.663	0.649	0.417	0.410	0.428	0.412
C5	0.449	0.511	0.479	0.424	0.315	0.309	0.288	0.285
C6	0.702	0.763	0.716	0.589	0.468	0.454	0.430	0.416
C7-Par+Branched	0.006	0.007	0.006	0.004	0.004	0.004	0.003	0.003
C7-alpha	2.146	2.258	2.112	1.626	1.323	1.278	1.217	1.174
C8-Branched	0.123	0.122	0.121	0.109	0.102	0.100	0.099	0.096
C8	72.163	71.665	74.317	80.082	83.154	84.545	85.187	85.749
C9-Branched	0.000	0.088	0.419	0.406	0.514	0.539	0.237	0.437
C9	3.574	3.792	3.497	2.686	2.302	2.164	2.025	1.962
C10-Branched	0.047	0.000	0.073	0.059	0.063	0.063	0.036	0.053
C10	1.706	1.723	1.570	1.257	1.062	0.991	0.945	0.901
C11-Branched	0.132	0.136	0.125	0.098	0.066	0.061	0.056	0.053
C11	1.555	1.572	1.416	1.129	0.873	0.814	0.768	0.730
C12-Branched	0.112	0.119	0.106	0.016	0.070	0.040	0.049	0.039
C12	2.258	2.340	2.126	1.575	1.330	1.194	1.137	1.097
C13-Branched	0.044	0.050	0.045	0.063	0.055	0.048	0.026	0.038
C13	3.398	3.594	3.277	2.393	2.055	1.908	1.838	1.764
C14-Branched	0.035	0.036	0.027	0.005	0.009	0.001	0.047	0.004
C14	3.742	3.848	3.337	2.226	1.945	1.829	1.814	1.734
C15+	7.017	6.291	5.153	3.944	3.614	2.997	2.992	2.704

B. Raman mapping spectrums

Table 5.1: Raman data of mapping performed on 9.1wt%MoO_3/Al_2O_3 catalyst

Point Selected	Vibration	Peak Position (cm^{-1})	Peak intensity	Peak area
1	(υ_s M=O)	957.9	734.2	33492
2	(υ_s M=O)	955.7	306.3	13376
3	(υ_s M=O)	958.9	319.0	13484
4	(υ_s M=O)	956.1	318.6	15819
5	(υ_s M=O)	957.9	293.1	14070
6	(υ_s M=O)	955.9	301.4	13661
7	(υ_s M=O)	961.4	162.1	6074
8	(υ_s M=O)	956.2	346.3	15697

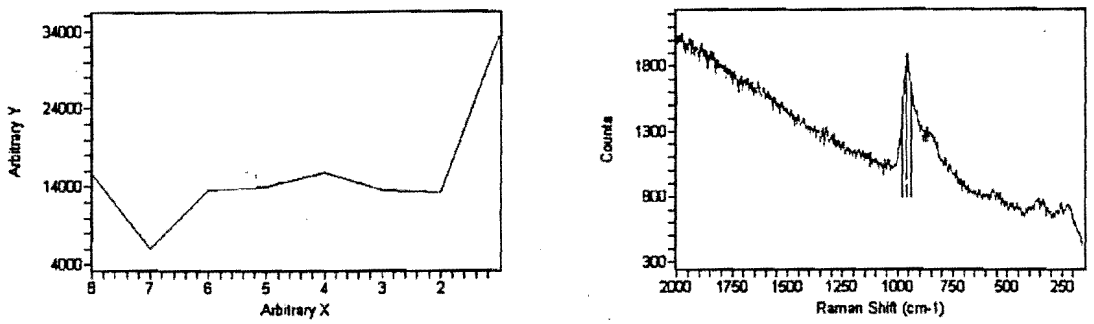

Spectrum 1: Mapping experiment performed on the 9.1wt%MoO_3/Al_2O_3. The peak area of the M=O symmetric stretching vibration were monitored.

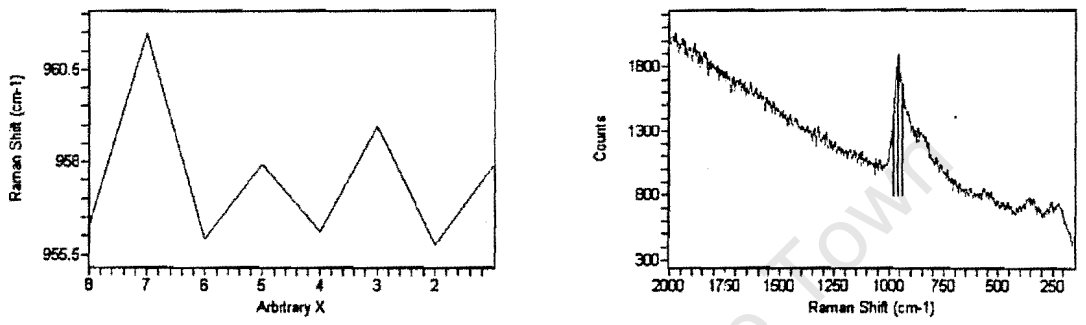

Spectrum 2: Mapping experiment performed on the 9.1wt%MoO_3/Al_2O_3. The peak position of the M=O symmetric stretching vibration were monitored.

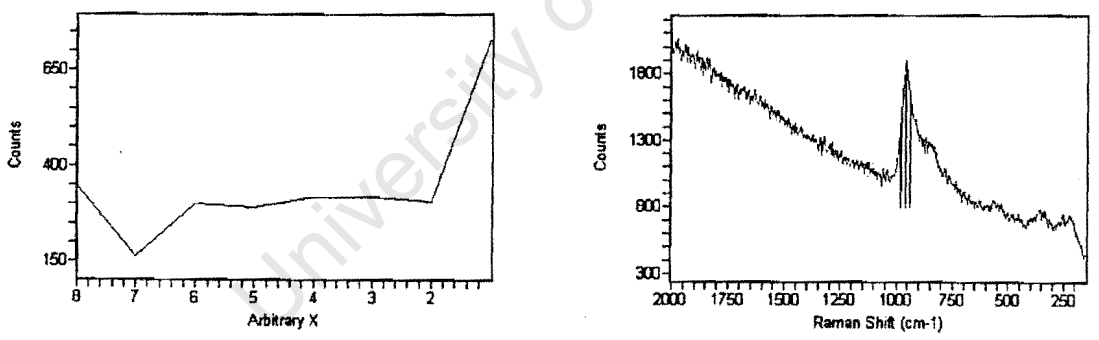

Spectrum 3: Mapping experiment performed on the 9.1wt%MoO_3/Al_2O_3. The peak intensity of the M=O symmetric stretching vibration were monitored.

Table 5.2: Raman data of mapping performed on 16.7wt%MoO_3/Al_2O_3 catalyst

Point Selected	Vibration	Peak Position (cm^{-1})	Peak intensity	Peak area
1	(υ_s M=O)	952.2	879.1	43255
2	(υ_s M=O)	954.4	1793.5	78872
3	(υ_s M=O)	954.0	1699	74687
4	(υ_s M=O)	951.1	363.2	87869
5	(υ_s M=O)	954.5	1554.9	55599
6	(υ_s M=O)	952.7	386.9	9442.5
7	(υ_s M=O)	954.7	2064.7	86198
8	(υ_s M=O)	954.2	1871.2	79017

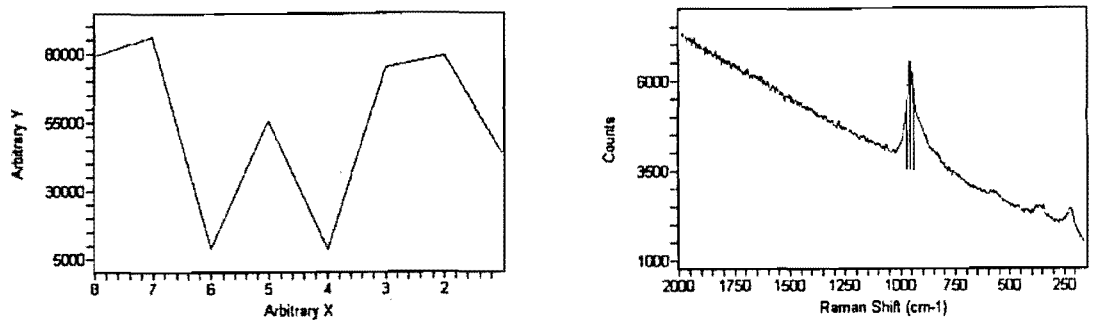

Spectrum 4: Mapping experiment performed on the 16.7wt%MoO_3/Al_2O_3. The peak area of the M=O symmetric stretching vibration were monitored.

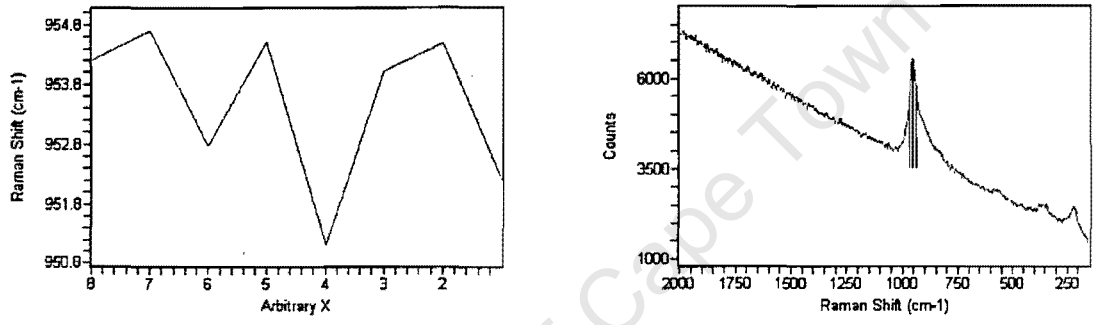

Spectrum 5: Mapping experiment performed on the 16.7wt%MoO_3/Al_2O_3. The peak position of the M=O symmetric stretching vibration were monitored.

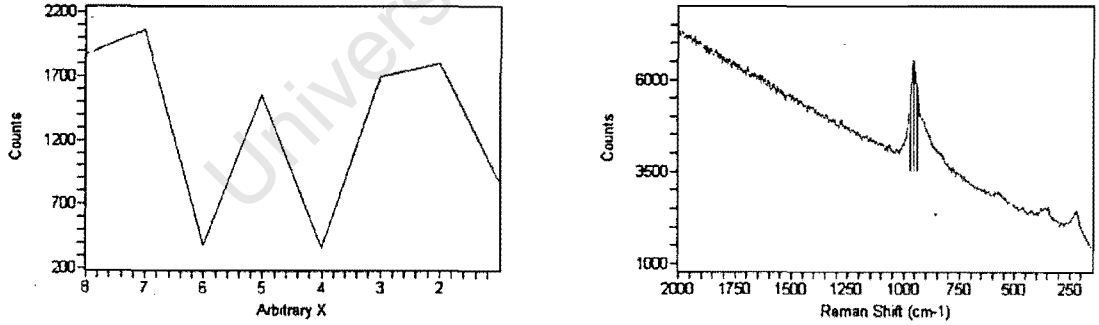

Spectrum 6: Mapping experiment performed on the 16.7wt%MoO_3/Al_2O_3. The peak intensity of the M=O symmetric stretching vibration were monitored.

Table 5.3: Raman data of mapping performed on 23.1wt%MoO_3/Al_2O_3 catalyst

Point Selected	Vibration	Peak Position (cm^{-1})	Peak Intensity	Peak area
1	(υ_s M=O)	957.7	4381.5	330402
2	(υ_s M=O)	958.3	3595.7	300290
3	(υ_s M=O)	1004.1	6071.8	218659
4	(υ_s M=O)	1005	3285.2	82850
5	(υ_s M=O)	975.8	4062.9	406006
6	(υ_s M=O)	971.7	1804.9	191048
7	(υ_s M=O)	1004	5914	213703
8	(υ_s M=O)	958.4	4870.6	359292

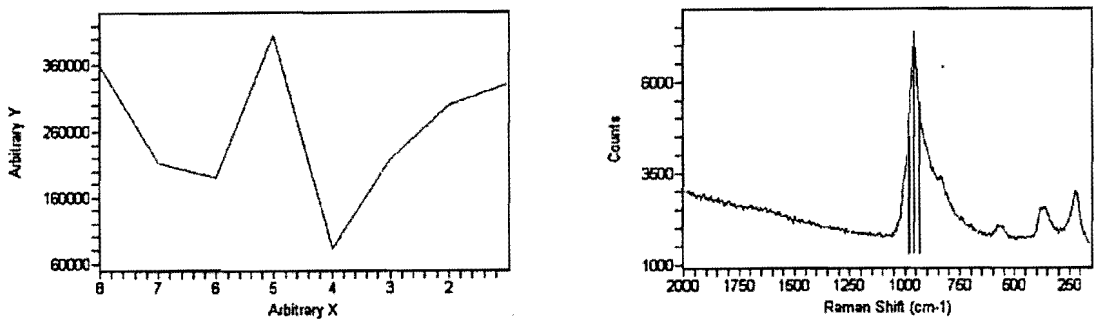

Spectrum 7: Mapping experiment performed on the 23.1wt%MoO_3/Al_2O_3. The peak area of the M=O symmetric stretching vibration were monitored.

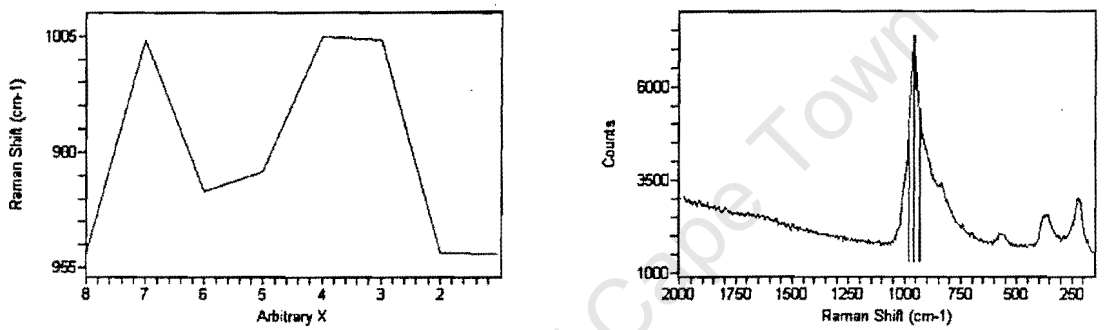

Spectrum 8: Mapping experiment performed on the 23.1wt%MoO_3/Al_2O_3. The peak position of the M=O symmetric stretching vibration were monitored.

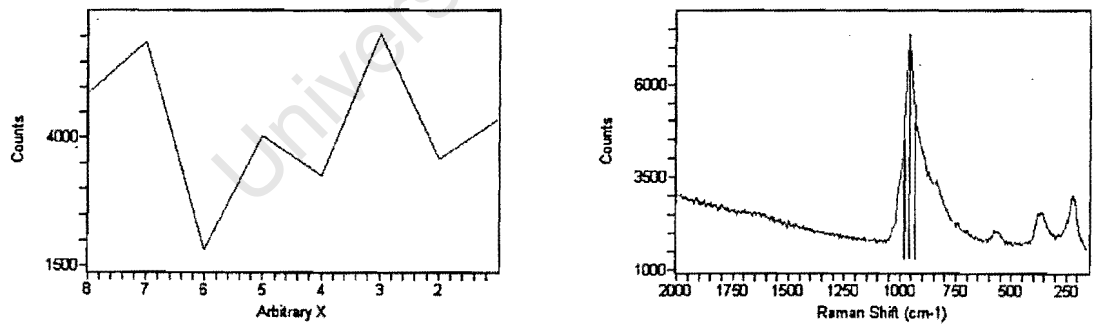

Spectrum 9: Mapping experiment performed on the 23.1wt%MoO_3/Al_2O_3. The peak intensity of the M=O symmetric stretching vibration were monitored.

Table 5.4: Raman data of mapping performed on 28.6wt%MoO_3/Al_2O_3 catalyst

Point Selected	Vibration	Peak Position (cm^{-1})	Peak Intensity	Peak Area
1	(υ_s M=O)	1006.3	1825.7	40580
2	(υ_s M=O)	1004.2	406.86	9463.5
3	(υ_s M=O)	1004.3	260.77	5967.7
4	(υ_s M=O)	1004.4	372.03	9330
5	(υ_s M=O)	1005.5	414.29	9172.2
6	(υ_s M=O)	1005.1	282.31	5307.6
7	(υ_s M=O)	1004.5	524.73	11922
8	(υ_s M=O)	1004.2	564.63	12623

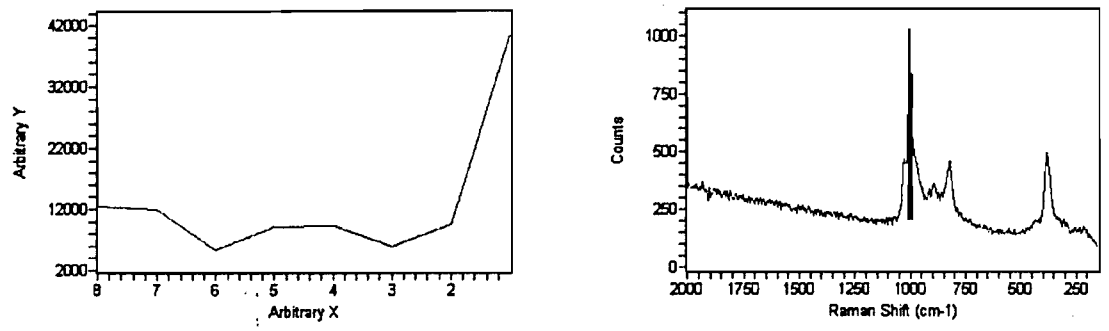

Spectrum 10: Mapping experiment performed on the 28.6wt%MoO_3/Al_2O_3. The peak area of the M=O symmetric stretching vibration were monitored.

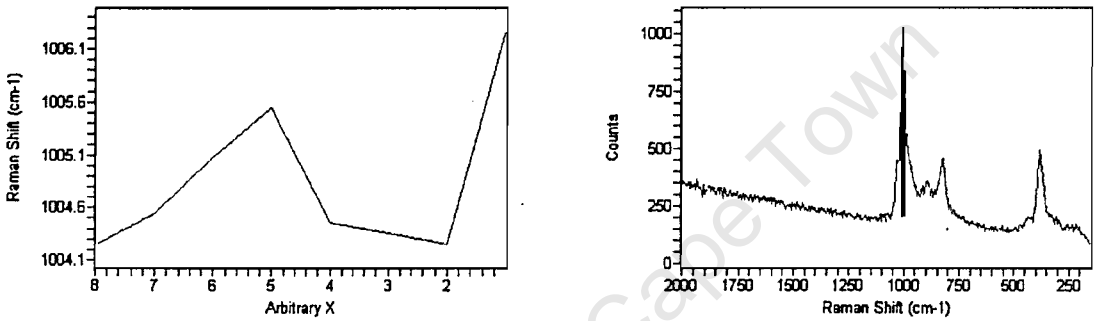

Spectrum 11: Mapping experiment performed on the 28.6wt%MoO_3/Al_2O_3. The peak position of the M=O symmetric stretching vibration were monitored.

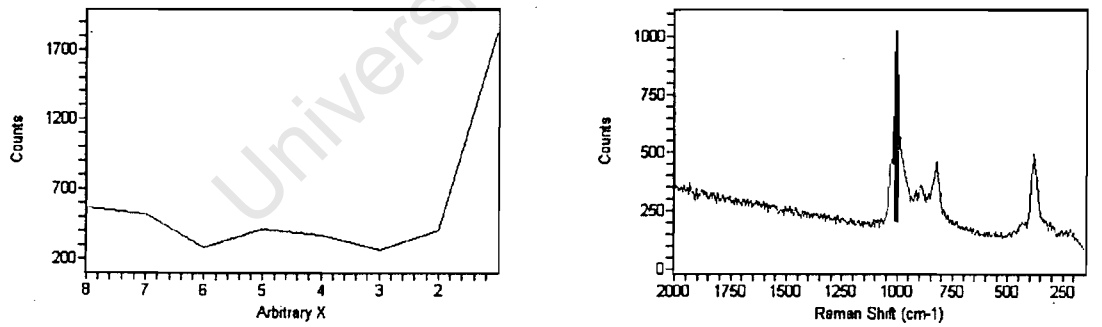

Spectrum 12: Mapping experiment performed on the 28.6wt%MoO_3/Al_2O_3. The peak intensity of the M=O symmetric stretching vibration were monitored.

Table 5.5: Raman data of mapping performed on 33.3wt%MoO_3/Al_2O_3 catalyst

Point Selected	Vibration	Peak Position (cm^{-1})	Peak Intensity	Peak Area
1	(υ_s M=O)	1003.4	294.36	10025
2	(υ_s M=O)	1004.5	317.49	7372.1
3	(υ_s M=O)	1004.1	292.87	9701.6
4	(υ_s M=O)	1004.3	643.39	25810
5	(υ_s M=O)	1004.5	172.6	5608.4
6	(υ_s M=O)	1004.0	739.73	30450
7	(υ_s M=O)	1002.7	796.74	31807
8	(υ_s M=O)	1002.6	789.06	31990

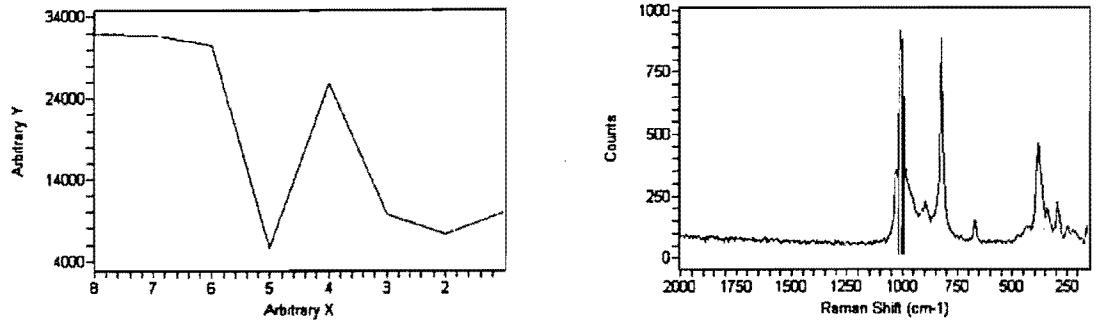

Spectrum 13: Mapping experiment performed on the 33.3wt%MoO_3/Al_2O_3. The peak area of the M=O symmetric stretching vibration were monitored.

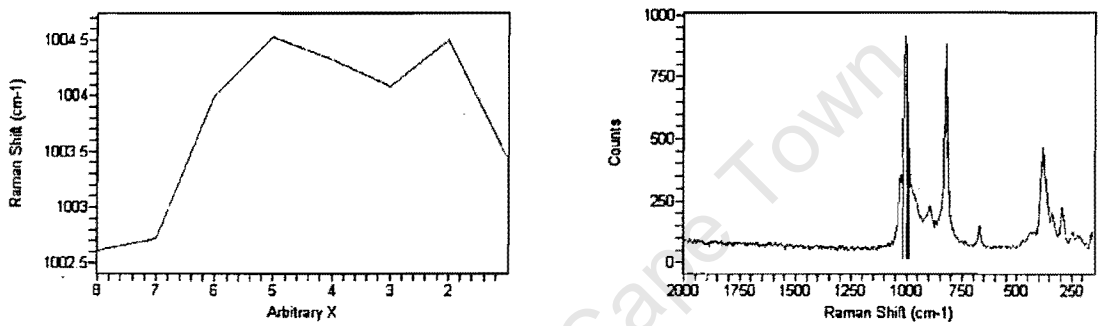

Spectrum 14: Mapping experiment performed on the 33.3wt%MoO_3/Al_2O_3. The peak position of the M=O symmetric stretching vibration were monitored.

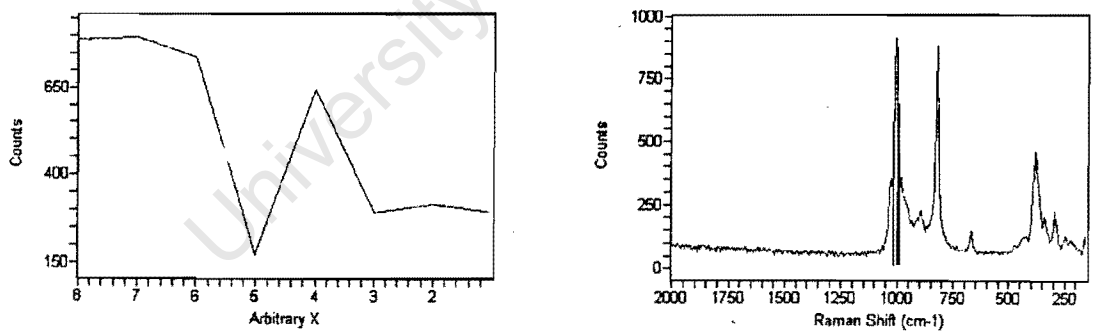

Spectrum 15: Mapping experiment performed on the 33.3wt%MoO_3/Al_2O_3. The peak intensity of the M=O symmetric stretching vibration were monitored.